



NTNU – Trondheim
Norwegian University of
Science and Technology

One-Dimensional Viscoelastic Simulation of Ice Behaviour in relation to Dynamic Ice Action

Maxim Yazarov

Coastal and Marine Civil Engineering

Submission date: June 2012

Supervisor: Knut Vilhelm Høyland, BAT

Norwegian University of Science and Technology
Department of Civil and Transport Engineering

Maxim Yazarov

**One-Dimensional Viscoelastic Simulation of Ice
Behaviour in Relation to Dynamic Ice Action**

Master Thesis

Trondheim, June 2012

Norwegian University of Science and Technology
Faculty of Engineering and Science and Technology
Department of Civil and Transport Engineering

ERASMUS MUNDUS MSc PROGRAMME

COASTAL AND MARINE ENGINEERING AND MANAGEMENT
CoMEM

ONE-DIMENSIONAL VISCOELASTIC SIMULATION OF ICE BEHAVIOUR IN RELATION TO DYNAMIC ICE ACTION

Norwegian University of Science and Technology
June 11, 2012

Maxim Yazarov
4128885

The Erasmus Mundus MSc Coastal and Marine Engineering and Management is an integrated programme organized by five European partner institutions, coordinated by Delft University of Technology (TU Delft). The joint study programme of 120 ECTS credits (two years full-time) has been obtained at three of the five CoMEM partner institutions:

- Norges Teknisk- Naturvitenskapelige Universitet (NTNU) Trondheim, Norway
- Technische Universiteit (TU) Delft, The Netherlands
- City University London, Great Britain
- Universitat Politècnica de Catalunya (UPC), Barcelona, Spain
- University of Southampton, Southampton, Great Britain

The first year consists of the first and second semesters of 30 ECTS each, spent at NTNU, Trondheim and Delft University of Technology respectively.

The second year allows for specialization in three subjects and during the third semester courses are taken with a focus on advanced topics in the selected area of specialization:

- Engineering
- Management
- Environment

In the fourth and final semester an MSc project and thesis have to be completed.

The two year CoMEM programme leads to three officially recognized MSc diploma certificates. These will be issued by the three universities which have been attended by the student. The transcripts issued with the MSc Diploma Certificate of each university include grades/marks for each subject. A complete overview of subjects and ECTS credits is included in the Diploma Supplement, as received from the CoMEM coordinating university, Delft University of Technology (TU Delft).

Information regarding the CoMEM programme can be obtained from the programme coordinator and director

Prof. Dr. Ir. Marcel J.F. Stive
Delft University of Technology
Faculty of Civil Engineering and geosciences
P.O. Box 5048
2600 GA Delft
The Netherlands



Report Title: One-Dimensional Viscoelastic Simulation of Ice Behaviour in relation to Dynamic Ice Action	Date: June 11, 2012		
	Number of pages :116		
	Master Thesis	X	Project Work
Name: Maxim Yazarov			
Professor in charge/supervisor: Prof. Knut V. Høyland			
Other external professional contacts/supervisors:			

<p>Abstract:</p> <p>When level ice is approaching the structure it exhibits the cyclic stress with in an increasing amplitude. The uniaxial compression cyclic tests of ice, performed at University Centre on Svalbard in 2007 (Sæbø, 2007), indicated an increase in the ice sample stiffness. The objective of this study was to verify whether this phenomenon can be explained by viscoelastic behaviour of ice.</p> <p>Linear viscoelastic Kelvin, Maxwell and Burgers models were implemented into Matlab by means of the Boltzmann principle of superposition in order to simulate the behaviour of ice under cyclic loading. The Burgers model was calibrated with the creep test, performed by Sinha (Sinha, 1978), in order to get the input parameters specific for simulation of ice behaviour.</p> <p>An extensive sensetivity analysis of the model were carried out and confirmed that the increase of the modulus of elasticity of ice under cyclic loading can be explained by concept of viscoelasticity. However, the degree of this increase is different from the one obtained in uniaxial compression cyclic test. A precise behaviour of ice in this experiment cannot be described by means of the linear viscoelastic model of ice.</p>

Keywords:

1. linear viscoelastic model
2. cyclic creep test
3. ice
4. dynamic ice action

MASTER DEGREE THESIS

Spring 2012

for

Student: Maxim Yazarov

One-Dimensional Viscoelastic Simulation of Ice Behaviour in relation to Dynamic Ice Action.

BACKGROUND

Ice action is one of the key issues when designing an Arctic offshore or coastal structure. Ice-structure interaction is a complicated dynamic process, affecting by many different processes. When ice is approaching the structure it exhibits the cyclic stress with in an increasing amplitude. This process may affect the properties of ice and therefore the ice action. None of the present dynamic ice-structure interaction models include is phenomenon.

TASK DESCRIPTION

In 2007 uniaxial cyclic compression tests of ice was performed at University Centre on Svalbard (Sæbø, 2007). these tests indicated an increase of the stiffness of ice under cyclic loading. The task of this work is to check weather this phenomenon might be explained by viscoelastic behaviour of ice. In order to do that the numerical linear viscoelastic model of ice should be developed. The case when the ice is subjected to cyclic loading should be analyzed by means of this numerical model.

General about content, work and presentation

The text for the master thesis is meant as a framework for the work of the candidate. Adjustments might be done as the work progresses. Tentative changes must be done in cooperation and agreement with the professor in charge at the Department.

In the evaluation thoroughness in the work will be emphasized, as will be documentation of independence in assessments and conclusions. Furthermore the presentation (report) should be well organized and edited; providing clear, precise and orderly descriptions without being unnecessary voluminous.

The report shall include:

- Standard report front page (from DAIM, <http://daim.idi.ntnu.no/>)
- Title page with abstract and keywords.(template on: <http://www.ntnu.no/bat/skjemabank>)
- Preface

- Summary and acknowledgement. The summary shall include the objectives of the work, explain how the work has been conducted, present the main results achieved and give the main conclusions of the work.
- Table of content including list of figures, tables, enclosures and appendices.
- If useful and applicable a list explaining important terms and abbreviations should be included.
- The main text.
- Clear and complete references to material used, both in text and figures/tables. This also applies for personal and/or oral communication and information.
- Text of the Thesis (these pages) signed by professor in charge as Attachment 1..
- The report must have a complete page numbering.

Advice and guidelines for writing of the report is given in: "Writing Reports" by Øivind Arntsen. Additional information on report writing is found in "Råd og retningslinjer for rapportskrivning ved prosjekt og masteroppgave ved Institutt for bygg, anlegg og transport" (In Norwegian). Both are posted on <http://www.ntnu.no/bat/skjemabank>

Submission procedure

Procedures relating to the submission of the thesis are described in DAIM (<http://daim.idi.ntnu.no/>). Printing of the thesis is ordered through DAIM directly to Skipnes Printing delivering the printed paper to the department office 2-4 days later. The department will pay for 3 copies, of which the institute retains two copies. Additional copies must be paid for by the candidate / external partner.

On submission of the thesis the candidate shall submit a CD with the paper in digital form in pdf and Word version, the underlying material (such as data collection) in digital form (eg. Excel). Students must submit the submission form (from DAIM) where both the Ark-Bibl in SBI and Public Services (Building Safety) of SB II has signed the form. The submission form including the appropriate signatures must be signed by the department office before the form is delivered Faculty Office.

Documentation collected during the work, with support from the Department, shall be handed in to the Department together with the report.

According to the current laws and regulations at NTNU, the report is the property of NTNU. The report and associated results can only be used following approval from NTNU (and external cooperation partner if applicable). The Department has the right to make use of the results from the work as if conducted by a Department employee, as long as other arrangements are not agreed upon beforehand.

Tentative agreement on external supervision, work outside NTNU, economic support etc.

Separate description to be developed, if and when applicable. See <http://www.ntnu.no/bat/skjemabank> for agreement forms.

Health, environment and safety (HSE) <http://www.ntnu.edu/hse>

NTNU emphasizes the safety for the individual employee and student. The individual safety shall be in the forefront and no one shall take unnecessary chances in carrying out the work. In particular, if the student is to participate in field work, visits, field courses, excursions etc. during the Master Thesis work, he/she shall make himself/herself familiar with "Fieldwork HSE Guidelines". The document is found on the NTNU HMS-pages at <http://www.ntnu.no/hms/retningslinjer/HMSR07E.pdf>

The students do not have a full insurance coverage as a student at NTNU. If you as a student want the same insurance coverage as the employees at the university, you must take out individual travel and personal injury insurance.

Start and submission deadlines

The work on the Master Thesis starts on January 16, 2012

The thesis report as described above shall be submitted digitally in DAIM at the latest at 3pm June 11, 2012

Professor in charge: Prof. Knut V. Høyland

Other supervisors:

Trondheim, January 16, 2012. (revised: dd.mm.yyyy)

Professor in charge (sign)

ACKNOWLEDGMENTS

The last two years spent in as a graduate student under the Erasmus Mundus Masters Programme: Coastal and Marine Engineering and Management (CoMEM) have been a great learning experience for me, not only academically but also personally. Exposure to different cultures, universities and way of life have helped me gain invaluable life experiences. I hereby thank the CoMEM board for having floated this wonderful programme and for the financial assistance.

This thesis work has been carried out under the supervision of Professor Knut Høyland at the Department of Civil and Transport Engineering, Norwegian University of Science and Technology (NTNU). I am wholeheartedly grateful to him for his meaningful insights, comments and guidance without which carrying out this work would not have been possible.

I would also like to express my gratitude to Professor Karl Scheinik of SPSPU for his useful insights and advice.

Professor Mauri Määttänen took time off his busy schedule to discuss concepts of dynamics ice action with me which helped me to better appreciate the topic. PhD Stipendiat Torodd Nord was very forthcoming with suggestions about the thesis and I am grateful to him.

I would like to thank the SAMCOT RCI as the opportunity to work on this topic appeared from the need for such a study to supplement a project funded by it and its partners.

CONTENTS

Abstract	v
Task description	vii
Acknowledgements.....	xi
Contents	xii
List of figures.....	xiv
List of tables.....	xviii
List of symbols.....	xix
1.INTRODUCTION	1
1.1. General	1
1.2. Ice action	2
1.2.1. Quasi-static load on vertical structures.	2
1.2.2. Ice crushing failure mode.	3
1.2.3. Dynamic ice action on vertical structures.	4
1.3. Ice properties and dynamic ice action	7
1.4. Objective of the thesis	9
2.THEORY AND METHODS	10
2.1. Concept of viscoelasticity	10
2.1.1. General viscoelasticity.	10
2.1.2. Linear viscoelasticity.....	13
2.1.2.1.Mechanical models.	13
2.2. The Boltzmann superposition principle	20
2.3. Validation of the Matlab code(numerical method)	22
2.4. Cyclic uniaxial compression test.....	26
2.5. System's modulus of elasticity	29
2.6. Non-linear viscoelastic model for polycrystalline ice.....	30
3.RESULTS	31
3.1. Sensitivity analysis	31

3.1.1. Kelvin model.....	31
3.1.2. Maxwell model.....	42
3.1.3. Burgers model.....	48
3.2. Sensitivity analysis of secant system's modulus of elasticity	57
3.2.1. Kelvin model.....	57
3.2.2. Maxwell model.....	61
3.2.3. Burgers model.....	64
3.3. Calibration of the model.....	70
3.4. Numerical simulation of cyclic uniaxial compression test.....	72
4.ANALYSIS AND DISCUSSION	74
4.1. Sensitivity analysis	74
4.2. Sensitivity analysis of the secant system's modulus of elasticity	75
4.2.1. Kelvin model.....	75
4.2.2. Maxwell model.....	78
4.2.3. Burgers model.....	78
4.3. Calibration of the model	79
4.4. Numerical simulation of cyclic uniaxial compression test.....	79
4.5. Summary	82
5.CONCLUSIONS	83
5.1. Conclusions	83
5.2. Recommendations for future work.....	83
REFERENCES.....	84
APPENDIX.....	86
A. Matlab code for linear viscoelastic models	A
B. Results of the numerically simulated creep tests for Kelvin model	B
C. Matlab code for non-linear viscoelastic model.....	C

LIST OF FIGURES

Figure 1.2.2.1. Schematic illustration of the main processes of spalling and high-pressure zones formation	4
Figure 1.2.3.1. Modes of time-varying action due to ice crushing and the corresponding dynamic component of structure response	5
Figure 1.2.3.2. Idealized time histories of the ice action due to intermittent crushing	6
Figure 1.2.3.3. Assumed ice load history for frequency lock-in conditions	7
Figure 2.1.1.1. Creep test of a viscoelastic material	11
Figure 2.1.1.3. Fluid and solid response in creep and relaxation test	12
Figure 2.1.2.1. Hookean model	14
Figure 2.1.2.2. Newtonian model	15
Figure 2.1.2.3. Maxwell model	17
Figure 2.1.2.4 Kelvin model	18
Figure 2.1.2.5. Burgers model	19
Figure 2.2.1. Superposition of strain increments	22
Figure 2.3.1. Stress history	22
Figure 2.3.2. Comparison of numerical and analytical strain response	24
Figure 2.3.3. Comparison of strain response calculated using 2 different methods ..	25
Figure 2.3.4. Stress history and corresponding numerically calculated strain response for 25s	25
Figure 2.3.5. Stress history and corresponding numerically calculated strain response for 10s	26
Figure 2.4.1. a) Kompis. b) Closer picture of a compressive unit	27
Figure 2.4.2. Stress plotted against time	27

Figure 2.4.3. Young's modulus found by the linear regression for the different cycle numbers	28
Figure 2.4.4. A stress-strain plot for cycle nr 3 and cycle nr 60.....	28
Figure 2.5.1. Tangent and secant system's modulus	29
Figure 3.1.1.1. Stress history and strain response of Kelvin model in a creep tests ..	33
Figure 3.1.1.2. Selecting of a critical value of λ in order to obtain elastic behavior of the Kelvin model	34
Figure 3.1.1.3. Viscous response of Kelvin model	35
Figure 3.1.1.4. Phase lag between harmonic stress and corresponding strain response	36
Figure 3.1.1.5. Elastic response of the Kelvin model under harmonic loading	38
Figure 3.1.1.6. Viscous response of the Kelvin model under harmonic loading	39
Figure 3.1.1.7. Strain responses of Kelvin model in case 1	40
Figure 3.1.1.8. Strain responses of Kelvin model in case 3.....	41
Figure 3.1.1.9. Strain responses of Kelvin model in case 4.....	41
Figure 3.1.2.1. Maxwell model. Creep test	43
Figure 3.1.2.2. Elastic behavior of Maxwell model in creep test	43
Figure 3.1.2.3. Viscous behavior of Maxwell model in creep test	44
Figure.3.1.2.4. Viscous response of the Maxwell model under harmonic loading ...	45
Figure.3.1.2.5. Elastic response of the Maxwell model under harmonic loading	45
Figure 3.1.2.6. Strain responses of Maxwell model in case 1	46
Figure 3.1.2.7. Strain responses of Maxwell model in case 3	47
Figure 3.1.2.8. Strain responses of Maxwell model in case 4	47
Figure 3.1.3.1. Burgers model. Creep test	48
Figure 3.1.3.2. Elastic response of Burgers model	50

Figure 3.1.3.3. Burgers model. Creep test	50
Figure 3.1.3.4. Burgers model. Creep test	51
Figure 3.1.3.5. Viscous response of Burgers model	52
Figure 3.1.3.6. Burgers model. Creep test	52
Figure 3.1.3.7. Burgers model. Creep test	53
Figure 3.1.3.8. Burgers model. Creep test	53
Figure 3.1.3.9. Strain responses of Burgers model in case 3 for first 20 cycles	55
Figure 3.1.3.10. Strain responses of Burgers model in case 4.....	55
Figure 3.1.3.11. Strain responses of Burgers model in case 3a during first 50 seconds	56
Figure 3.1.3.12. Strain responses of Burgers model in case 4a during first 20 cycles	56
Figure 3.2.1.1.a. Kelvin model response under cyclic loading	58
Figure 3.2.1.1.b. Secant system's modulus of elasticity estimated for each cycle in case 2 when material, represented by Kelvin model, exhibit cyclic loading	58
Figure 3.2.1.2.a. Kelvin model response under cyclic loading. Stress-strain curve in case 3.....	59
Figure 3.2.1.2.b. Secant system's modulus of elasticity estimated for each cycle in case 3 when material, represented by Kelvin model, exhibit cyclic loading	59
Figure 3.2.1.3.a. Kelvin model response under cyclic loading. Stress-strain curve in case 4.....	60
Figure 3.2.1.3.b. Secant system's modulus of elasticity estimated for each cycle in case 3 when material, represented by Kelvin model, exhibit cyclic loading	60
Figure 3.2.2.1.a. Maxwell model response under cyclic loading. Stress-strain curve in case 2 for first 20 cycles	61
Figure 3.2.2.1.b. Secant system's modulus of elasticity estimated for each cycle in case 2 when material, represented by Maxwell model, exhibit cyclic loading	62

Figure 3.2.2.2.a. Maxwell model response under cyclic loading. Stress-strain curve in case 3.....	62
Figure 3.2.2.2.b. Secant system's modulus of elasticity estimated for each cycle in case 3 when material, represented by Maxwell model, exhibit cyclic loading	63
Figure 3.2.2.3.a. Maxwell model response under cyclic loading. Stress-strain curve in case 4.....	63
Figure 3.2.2.3.b. Secant system's modulus of elasticity estimated for each cycle in case 4.....	64
Figure 3.2.3.1.a. Burgers model response under cyclic loading. Stress-strain curve for first 5 cycles in case 2	65
Figure 3.2.3.1.b. Secant system's modulus of elasticity estimated for each cycle in case 2 when material, represented by Burgers model, exhibit cyclic loading	65
Figure 3.2.3.2.a. Burgers model response under cyclic loading. Stress-strain curve in case 3.....	66
Figure 3.2.3.2.b. Secant system's modulus of elasticity estimated for each cycle in case 3 when material, represented by Burgers model, exhibit cyclic loading	66
Figure 3.2.3.3.a. Burgers model response under cyclic loading. Stress-strain curve for first 4 cycles in case 4	67
Figure 3.2.3.3.b. Secant system's modulus of elasticity estimated for each cycle in case 4 when material, represented by Burgers model, exhibit cyclic loading	67
Figure 3.2.3.4.a. Burgers model response under cyclic loading. Stress-strain curve in case 3a	68
Figure 3.2.3.4.b. Secant system's modulus of elasticity estimated for each cycle in case 3a when material, represented by Burgers model, exhibit cyclic loading	68
Figure 3.2.3.5.a. Burgers model response under cyclic loading. Stress-strain curve in for first 10 cycles in case 4a	69
Figure 3.2.3.5.b. Secant system's modulus of elasticity estimated for each cycle in case 4a when material, represented by Burgers model, exhibit cyclic loading	69
Figure 3.3.1. Creep and recovery of ice at -10°C	71

Figure 3.3.2. Creep and recovery of ice at -19.8°C	71
Figure 3.4.1. Stress history of uniaxial cyclic compression test	72
Figure 3.4.2. Comparison of strain response in uniaxial cyclic compression test with strain response simulated by linear viscoelastic model	73
Figure 4.2.1.4. Stress-strain curves for cycles 2 and 39 in case 2	77
Figure 4.4.1. Elastic-plastic material response	81
Figure 4.4.2. Ideal plastic unit	81

LIST OF TABLES

Table 3.1.1.1. Values of creep function multiplied with modulus of elasticity for certain values of t/λ ratio	32
Table 4.2.1.1. The values for secant system's modulus of elasticity E_s for case 2....	76

LIST OF SYMBOLS

a_T	inverse relaxation time
b, c, s	Constants of non-linear viscoelastic model
f	frequency
h	ice thickness
$n, \#$	number of cycles
p_G	ice pressure averaged over the nominal contact
p_n, q_n	model parameter
t	time
u	displacement of a structure at the waterline
v	ice velocity
w	width of the structure
A	amplitude of stress
C_R	coefficient that considers the ice strength in different ice regimes
E	Young's Modulus
E_1	Young's Modulus of Maxwell unit
E_2	Young's Modulus of Kelvin unit
E_t	tangent system's modulus of elasticity
E_s	secant system's modulus of elasticity
F	ice action
F_G	quasi-static global ice action normal to the surface
F_{\max}	maximal value of ice action
F_{\min}	minimal value of ice action
$H(t)$	Heaviside function
K, M	dimensionless coefficients used in sensitivity analysis
R	gas constant
T	period of ice action or duration of a cycle
Q	activation energy

α	creep function
α_1	storage compliance
α_2	loss compliance
α_e	equilibrium compliance
α_g	glass compliance
β	relaxation function
β_e	equilibrium modulus
β_g	glass modulus
γ_s	parameter that considers the magnifying influences on the external load
δ	loss angle
ε	strain
ε_t	total strain
ε_e	elastic strain
ε_d	delayed elastic strain
ε_v	viscous strain
η	viscosity
η_1	viscosity of Maxwell unit
η_2	Viscosity of Kelvin unit
λ	relaxation time
λ_1	relaxation time of Maxwell unit
λ_2	relaxation time of Kelvin unit
σ	stress
σ_0, A	amplitude of stress
ω	angular frequency

1.INTRODUCTION

1.1.General

Cold climate coastal and offshore engineering became an important issue with the onset of developments of oil and gas fields in arctic and subarctic regions in the late 1960s. Around 25% of world oil reserves and 75% of world gas reserves are concentrated in these regions, making them attractive for further oil and gas developments(Wikipedia). However, building of the offshore structures in severe arctic climate conditions is a challenging task. Construction and operation in cold climate implies working in ice-infested waters. Therefore, for an engineer it is important to determine the ice action that an offshore structure can withstand for a given structural form, the ice properties and environmental conditions.

There are many parameters that affect ice action. Mainly ice action depends on the real contact area and the local stresses, whereas the last two depends on the type of ice feature interacting with the structure, properties of the ice feature, scenario of interaction of the ice feature with the structure, geometry of the structure and the mode of ice failure against the structure.

The most vulnerable type of structure with respect to ice action is a vertical structure. Lighthouses, multi-legged offshore structure, bridge piers, etc can be regarded as vertical structures. A structure can be considered as vertical if its sloping angle is less than 10° .

The ice feature that is believed to create the maximum loads on the structure is ice ridge. Therefore this ice feature is considered in design calculations. The part of the ice ridge called consolidated layer constitutes to the major part of ice ridge action. At the same time the action of the consolidated layer can be seen as the action from level ice.

The mode of ice failure against the structure is an important parameter and have a strong influence on ice action. Different modes of ice failure my exist even for same structure type and they can replace each other during the same event, depending on the ice thickness, velocity, the ice feature size, etc (Løset et al, 2006). The classification of the failure modes based on observations during the laboratory experiments was proposed by Sanderson (1988). When ice interacts with the

structure the following failure mechanisms can take place: creep, radial cracking, buckling, circumferential cracking, spalling and crushing. From the engineering point of view crushing is considered as the most important failure mode for vertical structures, since is believed to cause the highest ice action and severe vibrations.

The phenomenon of ice induced vibrations is known since the 1960s. Peyton in 1968 and Blenkarn in 1970 reported about ice induced vibrations on the drilling platforms in Cook Intel, Alaska. Later this phenomenon was noticed when there was an interaction of ice with lighthouse (Engelbektson, 1977), bridge piers (Sodhi, 1988) and offshore jacket oil platforms (Yue et al., 2001). These observations show that ice action should be considered to be dynamic. A common understanding of any dynamic action is that external time-varying force can be magnified due to internal forces within the structure (Kärnä, 2007). Dynamic ice action can be significant and imply structure damages. Moreover, fatigue can occur. Ice induced vibrations can lead to unacceptable level of displacement and acceleration of the structure, making it uncomfortable and dangerous for crew to stay on the structure. It is clear that knowledge of dynamic ice action is essential for economically sound and safe design of an offshore structure. Nevertheless, the mechanism responsible for this phenomenon is still not fully understood.

1.2. Ice action

1.2.1. Quasi-static global ice action for vertical structures.

Classical procedure of dealing with this problem is to define an equivalent external quasi-static load (Kärnä, 2007).

According to ISO 19906 (2010) when the ice crushing occurs against a structure, the quasi-static global ice action normal to the surface, F_G , can be expressed as:

$$F_G = p_G A \quad (1.2.1.1)$$

where p_G is the ice pressure averaged over the nominal contact area associated with the global action and A is the nominal contact area, or projected area of the ice feature on the structure. When level ice, rafted ice or the consolidated layer of the ridge interacts with the structure the nominal contact area can be seen as a product of ice thickness h and the width of the structure w .

$$F_G = p_G h w \quad (1.2.1.2.)$$

The pressure p_G is a key parameter when designing the structure against the ice action. At the same time pressure p_G is a function of other parameters.

$$p_G = p_G [C_R, w, h, v, \gamma_S(K', u), T'] \quad (1.2.1.3)$$

where, v is ice velocity [m/s], C_R is a coefficient that considers the ice strength in different ice regimes, $\gamma_S(K, u)$ is a parameter that considers the magnifying influences on the external load, K' is stiffness of the structure at the waterline, u is peak value of the structural displacement at the waterline, T' is ice temperature.

It should be mentioned that the ice pressure varies in time.

1.2.2. Ice crushing failure mode

In crushing failure mode several failure mechanisms are considered, which are influenced by ice velocity, compliance of the structure and temperature. Ice crushing failure involves sequential development of horizontal splits, spalls, that cause ice pieces of various size to break off and flakes. During the process of ice compressive failure most of the force from the structure is transmitted to the ice through small areas termed high-pressure zones. During the ice crushing process, the number of high-pressure zones as well as their position change. When the ice velocity is high the fracturing of large pieces of ice results in the areas of little or no pressure with a narrow contact area. This leads to constant fluctuations in load and pressure. On the other hand, when ice velocity is little deformation of the ice leads to simultaneous contact between an advancing ice sheet and a structure. Figure 1.2.2.1. shows the process of compressive failure of ice in crushing.

For compliant structures the following failure modes depending on the ice velocity are proposed:

- ductile
- intermittent ductile-brittle crushing
- continuous brittle crushing

These ice failure modes are responsible for different types of dynamic response of the structure.

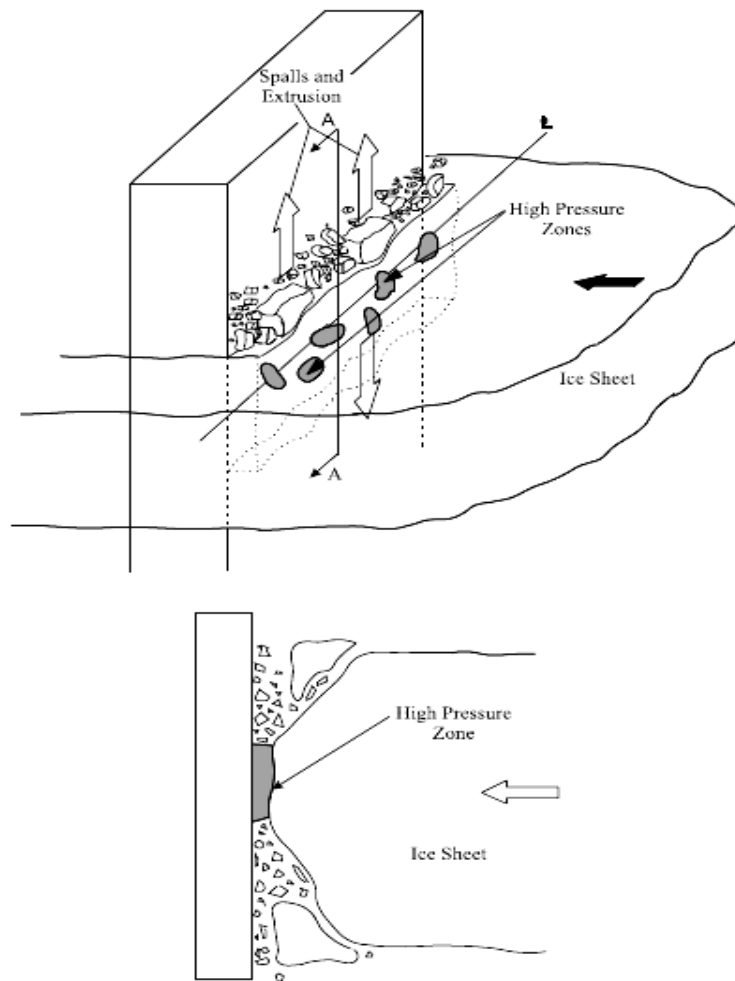


Figure 1.2.2.1. Schematic illustration of the main processes of spalling and high-pressure zones formation (Jordaan,2001).

1.2.3. Dynamic ice action on vertical structures

The process of dynamic ice-structure interaction process is controlled by the ice velocity and the waterline displacement of the structure. In case of continuous crushing of ice usually three different regimes modes of vibrations may occur:

- intermittent ice crushing
- frequency lock-in
- random vibrations

Figure 1.2.3.1. Illustrates these three primary modes of ice-structure interaction in terms of ice force $F(t)$ and corresponding displacement $u(t)$, as measured in the full scale structures in Bohai Bay. (ISO 19906, 2010)

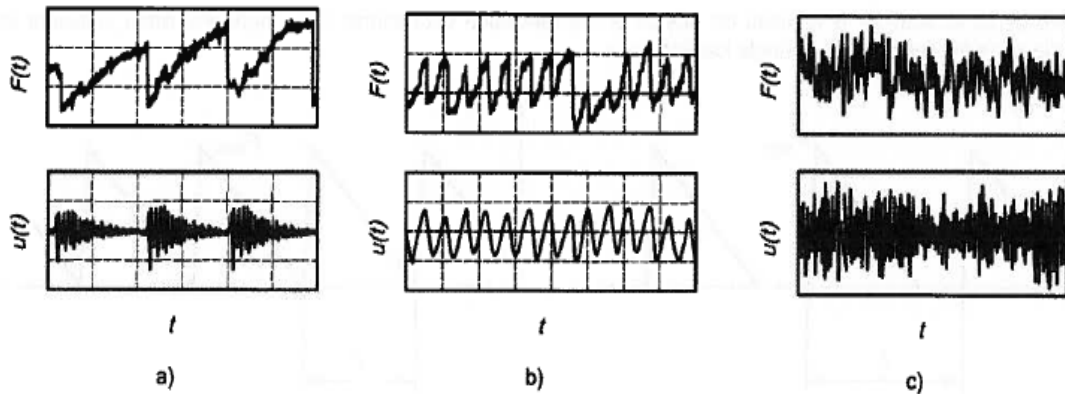


Figure 1.2.3.1. Modes of time-varying action due to ice crushing and the corresponding dynamic component of structure response. a) intermittent ice crushing b) frequency lock-in c) continuous brittle crushing. $F(t)$ is ice action, $u(t)$ is structure displacement, t is time. (ISO 19906, 2010)

Intermittent ice crushing mode, shown in Figure 1.2.3.1.a., occurs in a range of low ice velocity. Intermittent ductile-brittle crushing failure mode is responsible for this mode of ice-induced vibrations. Due to the fact that the ice velocity is low, ice edge starts to deform in a ductile manner. While ice force is gradually increasing, structure moves in the same direction as ice. When the ice action is reaching its maximal value, the brittle deformation starts to take place at the ice edge. Due to the brittle failure of ice the ice force decrease rapidly. In the intermittent crushing mode the structure exhibits relaxation vibrations, that decay due to the damping caused by the soil and the structure.

The ice action due to intermittent crushing can be simplified as shown in figure 1.2.3.2. In intermittent ice crushing mode the period T of the ice action is much longer than the longest natural period of the structure. The peak action F_{\max} can be determined by equation 1.

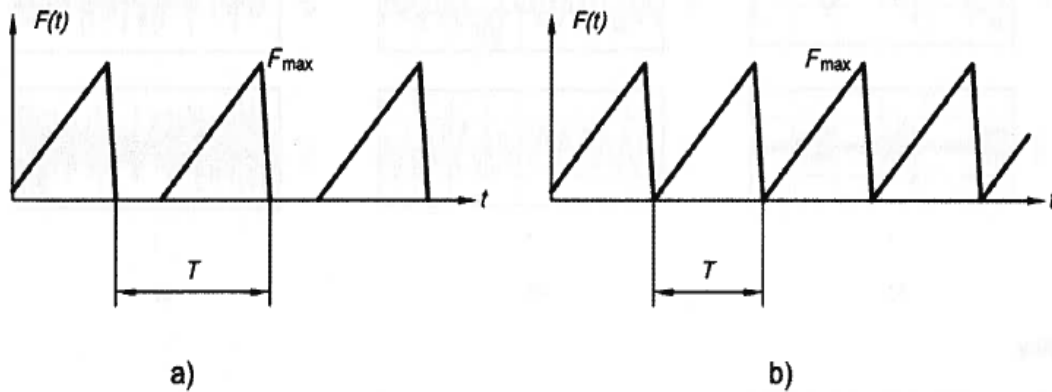


Figure 1.2.3.2. Idealized time histories of the ice action due to intermittent crushing. a) period of ice action greater than duration of loading/unloading cycle b) period of ice action equal to loading/unloading cycle. T is a period of ice action. t is time, $F(t)$ is ice action, F_{max} is a maximal value of ice action.(ISO 19906, 2010)

The frequency lock-in mode (Figure 1.2.3.1.b.), or self-excited vibrations, occurs when the ice is advancing against the structure with the range of intermediate ice speeds. In this mode vibrations are severe and therefore should be avoided. Typically, the ice speeds in the range from 0.04 m/s to 0.1 m/s can be considered as intermediate ice speeds. This vibration mode is associated with brittle crushing failure mode of ice. Similar to intermittent ice crushing mode, ice edge first exhibits ductile deformation that is replaced by brittle deformation once the ice force reaches the peak value. The problem arises when the time-varying ice action adapts to the frequency of the waterline displacements of the structure. Therefore, the time history of the ice action depends not only on the properties of ice but also on the characteristics of the structure. In the frequency lock-in mode the vibrations of the structure can be seen as sinusoidal. According to ISO structures with a fundamental frequency in the range of 0.4 to 10 Hz may experience self-excited vibrations.

In order to determine the structural response the time history of ice action due to frequency lock-in can be simplified as shown in Figure 1.2.3.3. ISO 19906 (2010) suggest to assume a constant peak value of ice action F_{max} and the difference ΔF between maximal F_{max} and minimal value of ice action F_{min} . The frequency $f=1/T$ of the forcing function is assumed to be equal to the frequency of one of the unstable natural modes that has a natural frequency below 10 Hz. The peak value F_{max} can be determined as a global ice action F_G , using equation 1, whereas the procedure of

finding ΔF is not so clear and controversial. ISO suggest to take the ΔF as the a fraction q of F_{\max} . Then the coefficient q should be scaled so that the velocity response at the waterline amount to value 1,4 times the highest ice velocity at which a lock-in conditions occur. The expression given in the ISO for estimation of this ice velocity is not correct, because according to that expression different types of structures will exhibit same vibrations what is not the case in reality.

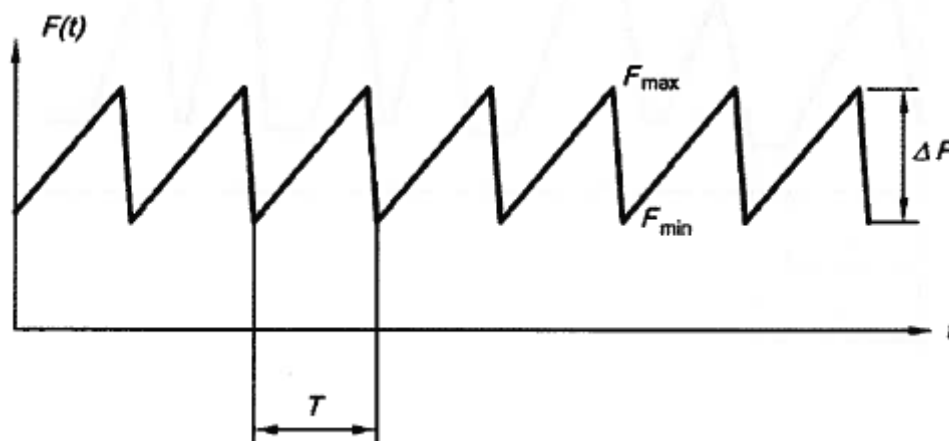


Figure.1.2.3.3. Assumed ice load history for frequency lock-in conditions. t is time, $F(t)$ is ice action, F_{\max} is a maximal value of ice action, F_{\min} is a minimal value of ice action, ΔF is a difference between maximal and minimal values of ice action, T is a period of ice action.(ISO 19906, 2010)

This vibration mode is associated with brittle crushing failure mode of ice. **Continuous brittle crushing** (Figure 1.2.3.1.c.) occurs at higher ice speeds. The ice speeds are typically higher than 100mm/s (ISO 19906, 2010). This vibration mode is characterized by random response of the structure and random ice action.

1.3. Ice properties and dynamic ice action

Although present ISO defines the conditions for frequency lock-in, they are still not so clear. Nevertheless, it is obvious that ice drift velocity has a significant influence on the process. However, it was observed that the lighthouse Nordstromgrund experienced more events of frequency lock-in in March, than in February, and this was not due to changes in the ice drift velocities.(personal communications) The reason for that might be the difference in the properties of ice. For instance due to the fact due to the warmer ice in March. However, it is not straight forward how the ice

properties may affect the process of ice-induced vibrations. None of the present dynamic ice-structure interaction models include the effect of changing ice properties.

Ice exhibits maximal stress near the structure. The stress gradually non-linearly decreases with increase of the distance to the structure. At a distance equal to several diameters of the structure ice still exhibits stresses. In the time domain the stress distribution is different. In the beginning of the process of ice-structure interaction the structure moves in the same direction as the ice. Then the ice starts to break in crushing within the narrow area around the structure and the structure displaces towards the ice. Then this process repeats. This means that when ice is approaching the structure it experiences cyclic loading with increasing amplitude.

Uniaxial cyclic compression tests of sea ice samples were performed at University Centre on Svalbard in 2007 (Sæbø, 2007). This experiment indicated that sample stiffness firstly increases and then decreases before the sample fails. This change in ice stiffness might have an influence on dynamic ice-structure interaction. Decrease of the sample can be explained by the development of damage in the sample. Increase in the sample stiffness is more difficult to explain within an elastic-plastic-damage framework. It can be explained by surface fluttering and/or by a visco-elastic ice material behavior.

In principle the behavior of ice is similar to behavior of metals due to the fact that ice is a polycrystalline material (Løset et al, 2006). However, the ordinary engineering approach to metals is not applicable to ice due to the fact that ice grains are relatively large and ice exists close to its freezing point in nature. The fact that sea ice consists of pure ice, brine, air and sometimes solid salts makes its behavior even more complicated. Therefore a material model of ice should include linear and non-linear aspects of elasticity, visco-elasticity, visco-plasticity. Numerous papers by Sihna (1978, 1982, 1984, 1989) and other researches explains this aspects of ice behavior. For example, the ice behavior can be described by well-known Burgers model (Løset et al, 2006).

1.4. Objective of the thesis

The goal of this work is to find out whether the increase of the stiffness of ice under cyclic loading can be explained by viscoelastic behavior of ice. In order to do that

numerical simulations of linear viscoelastic model of ice under the cyclic loading is performed.

Even though the linear viscoelastic model of ice does not capture all the aspects of the ice behavior, for instance it does not include fracture. It can be a good starting approximation of the ice response is such a complicated not fully understood process. This numerical model is simple and does not require a lot of computational power making it easy to perform and analyze many numerical experiments.

First, the concept of general viscoelasticity and linear viscoelasticity is discussed in this thesis, followed by the implementation of the model into the Matlab , validation of the model, sensitivity analysis, procedure of selecting the input parameter and results and discussion.

2. THEORY AND METHODS

Sections "viscoelasticity" and " The Boltzmann superposition principle " are based on "Continuum Mechanics" by Fridjov Irgens published in 2008.

2.1. Viscoelasticity

2.1.1. General Viscoelasticity

Viscoelasticity is a property of materials. Viscoelastic materials can exhibit both elastic and viscous behavior when undergoing deformation. Elastic materials return to their original shape once stress that deformed them is removed. Originally viscosity was introduced as a measure of resistance of a fluid which is being deformed by either shear or tensile stress. Later it was concluded that solids may be considered to have viscosity as well. The viscosity of solids is simply considered to be several orders higher than one of fluids.

Two different tests are often used to examine viscoelastic response of materials. One is the creep test and the other is relaxation test.

In creep test the specimen is subjected to a step constant stress during the time interval $[0, t_1]$. During the test viscoelastic materials exhibit a time-dependent deformation. This phenomena is known as viscoelastic creep. Time dependent strain response is a combination of elastic, delayed elastic and viscous strain responses. Each of these types of strain responses are explained further in this chapter. An example of a creep test is shown in figure 2.1.1.1.

The axial stress in the test specimen may be described by the following function:

$$\sigma(t) = \sigma_0[H(t) - H(t - t_1)] \quad (2.1.1.1)$$

where $H(t)$ is the Heaviside function.

The axial strain then is described as follows:

$$\varepsilon(\sigma_0, t) = \alpha(\sigma_0, t)\sigma_0 H(t) \quad (2.1.1.2)$$

where $\alpha(\sigma_0, t)$ is a creep function.

In relaxation test the specimen is subjected to a constant strain equal to ε_0 and the stress history is recorded. During the test the viscoelastic materials exhibit a time-dependent decrease in stress. An example of a relaxation test is shown in figure 2.1.1.2.

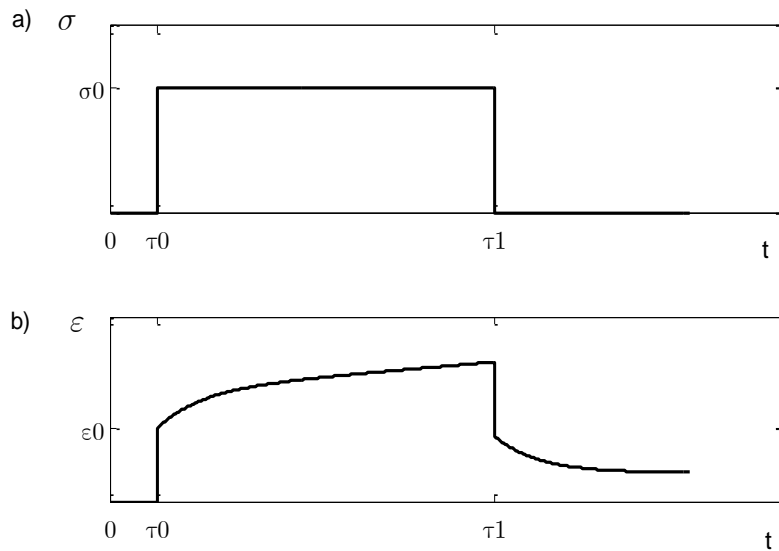


Figure 2.1.1.1. Creep test of a viscoelastic material. a) Applied stress b) Strain response.

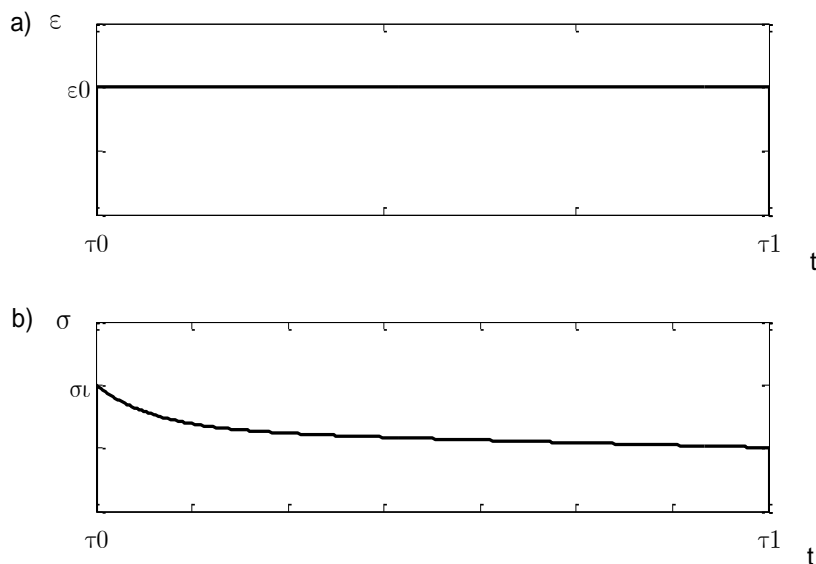


Figure 2.1.2. Relaxation test of a viscoelastic material. a) Applied strain b) Stress response.

The axial strain in the test specimen may be described by the following function:

$$\varepsilon(t) = \varepsilon_0 H(t) \quad (2.1.1.3)$$

The test result may be described by a relaxation function $\beta(\varepsilon_0, t)$ such that:

$$\sigma(\varepsilon_0, t) = \beta(\varepsilon_0, t) \varepsilon_0 H(t) \quad (2.1.1.4)$$

A viscoelastic material may be classified as a solid or a fluid. Figure 2.1.1.3. shows response of viscoelastic solid, viscoelastic fluid, elastic solid and viscous fluid from the creep and relaxation tests.

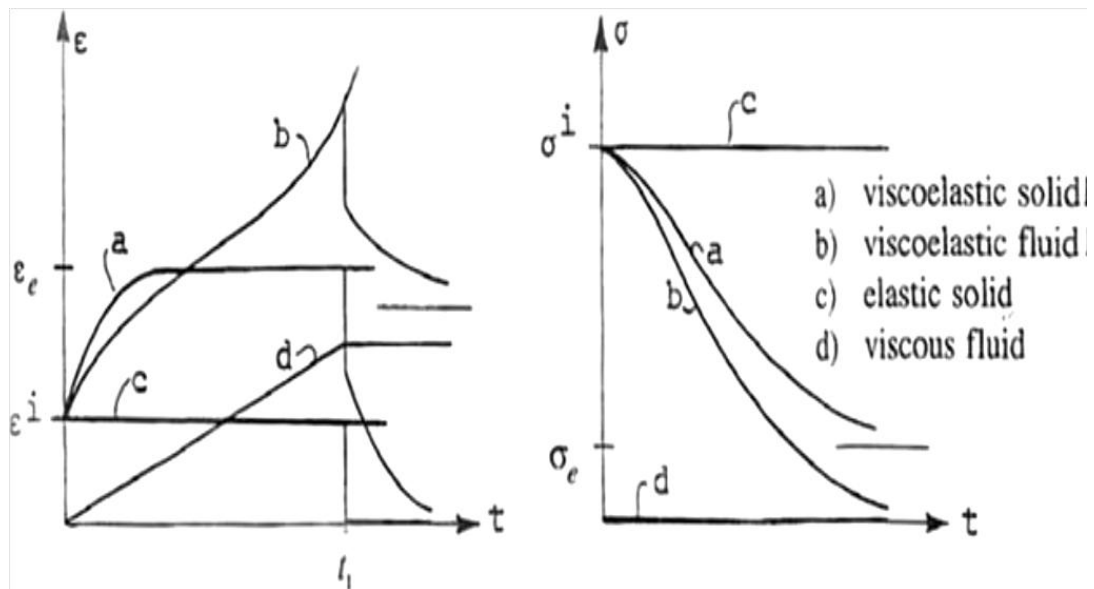


Figure 2.1.1.3. Fluid and solid response in creep(left) and relaxation(right) test.

(Irgens,2008)

During a creep test a viscoelastic solid will first exhibit initial elastic strain, primary creep (the stage with decreasing strain-rate), that can be described by delayed elastic strain in this case, and complete restitution without viscous strain. In a relaxation test of a viscoelastic solid the stress decreases towards an equilibrium stress $\sigma_e = \sigma_e(\varepsilon_0)$.

In creep test of viscoelastic fluid the test specimen can exhibit initial elastic strain, primary creep, secondary creep. During the secondary creep strain rate is constant.

During tertiary creep the rate of strain starts to increase until fracture occurs. After unloading the specimen exhibit elastic restitution (initial elastic strain disappears momentarily after the stress is removed) and then time dependent restitution. Viscous strain does not disappear. In relaxation test of viscoelastic fluid stress approaches zero asymptotically.

During creep test of elastic solid, strain is constant and equal to initial elastic strain. In relaxation test of an elastic solid the stress is constant and equal to initial stress σ_i that was applied to produce the constant strain ϵ_0 .

In creep test of viscous fluid, the strain rate is constant and after the stress is removed no restitution to initial shape occur. The specimen will get an irreversible viscous deformation. During relaxation test of viscous fluid the stress is equal to zero.

2.1.2. Linearly viscoelastic materials

The classical theory of viscoelasticity assumes small deformations(Irgens, 2008). The response of viscoelastic material can be represented by means of mechanical models. This models are the combination of spring and dashpots. Through this combination of the analogous responses of spring and dashpot the behavior of the material can be represented. The material shows linearly viscoelastic response when their creep and relaxation functions are functions only of time:

$$\alpha = \alpha(t), \beta = \beta(t). \quad (2.1.2.1)$$

Therefore plotting of this functions with respect to time can give a nice impression of how the corresponding graph of strain or stress should look like in case of creep or relaxation test respectively for a particular model considered. The instantaneous response is given by a glass compliance $\alpha_g = \alpha(0)$ and the glass modulus, also called the short time modulus, $\beta_g = \beta(0)$. $\alpha_e = \alpha(\infty)$ is equilibrium compliance and $\beta_e = \beta(\infty)$ is equilibrium modulus, or long time modulus.

2.1.2.1. Mechanical models

The response of linearly elastic material is the same as that of a linear spring.

The behavior of a linearly elastic material under uniaxial stress can be described by the response equation of the spring:

$$\sigma = E\varepsilon \quad (2.1.2.2)$$

where σ is stress, ε is strain, E is the modulus of elasticity. The linear spring shown in figure 2.1.2.1. is called **Hookean model**. This model have the following creep and relaxation functions respectively:

$$\alpha(t) = \frac{1}{E} = \alpha_g = \alpha_e, \quad \beta(t) = E = \beta_g = \beta_e \quad (2.1.2.3)$$

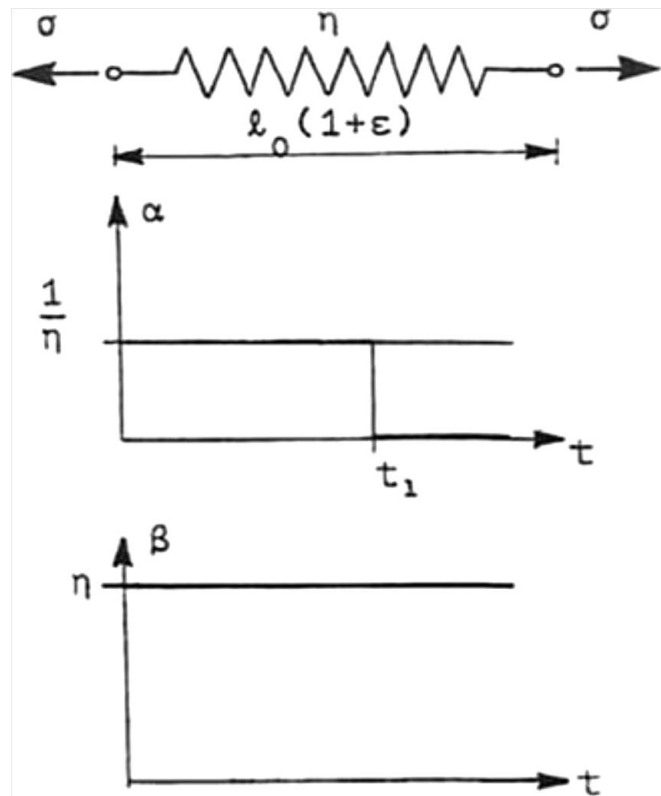


Figure 2.1.2.1. Hookean model. In this figure η is the modulus of elasticity.
(Irgens,2008)

Hookean model illustrates the concept of elastic response. When undergoing a creep test the specimen exhibits a elastic strain response.

The response of linearly viscous material is the same as that of linear dashpot. The behavior of a linearly viscous material under uniaxial stress can be described by the following response equation of the dashpot:

$$\sigma = \eta \dot{\varepsilon} \quad (2.1.2.4)$$

where η is viscosity of the material and $\dot{\varepsilon}$ is the time rate of strain, or strain rate. The linear dashpot shown in figure 2.1.2.2. is called **Newtonian model**.

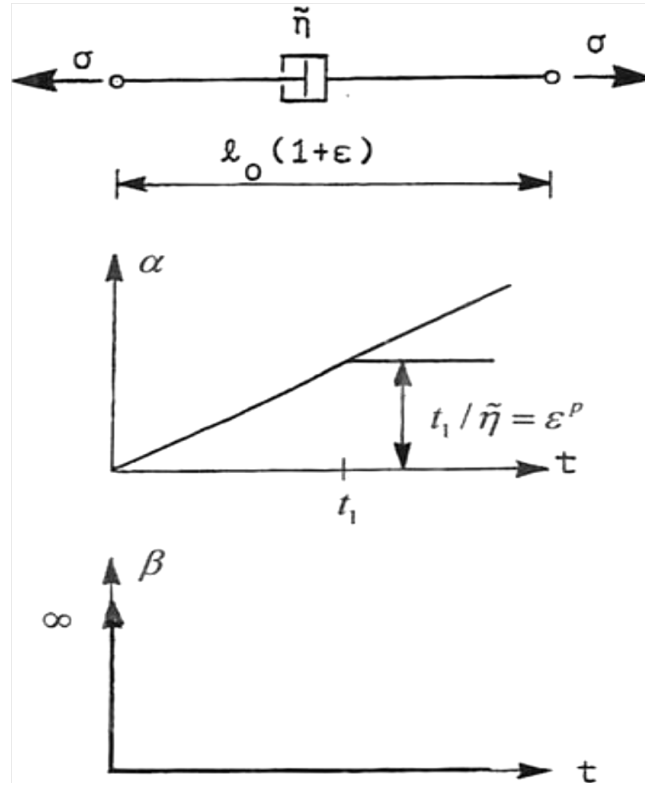


Figure 2.1.2.2. Newtonian model. In this figure $\tilde{\eta}$ represents viscosity. [Irgens,2008]

This model have the following creep function, glass compliance, equilibrium compliance, relaxation function, glass modulus, equilibrium modulus respectively:

$$\alpha(t) = \frac{t}{\eta}, \quad \alpha_g = 0, \quad \alpha_e = \infty, \quad \beta(t) = \eta \delta(t), \quad \beta_g = \infty, \quad \beta_e = 0 \quad (2.1.2.5)$$

where $\delta(t)$ is a Dirac delta function.

Newtonian model illustrates the concept of viscous response. When undergoing a creep test the specimen exhibits a viscous strain response.

The Maxwell model is a series of linear spring and linear dashpot. The response equation of the model is the following:

$$\dot{\varepsilon} = \frac{\dot{\sigma}}{E} + \frac{\sigma}{\eta} \quad (2.1.2.6)$$

The strain rate of the model is equal to the sum of strain rates of spring and of damper. The creep function, glass compliance, equilibrium compliance of the model are the following:

$$\alpha(t) = \frac{1}{E} \left[1 + \frac{t}{\lambda} \right], \quad \alpha_g = \frac{1}{E}, \quad \alpha_e = \infty \quad (2.1.2.7)$$

where $\lambda = \frac{\eta}{E}$ is the relaxation time. The relaxation function, glass modulus, equilibrium modulus of the model are the following:

$$\beta(t) = E \exp\left(-\frac{t}{\lambda}\right), \quad \beta_g = E, \quad \beta_e = 0 \quad (2.1.2.8)$$

The response of Maxwell model is the same as of a viscoelastic fluid. (Irgens, 2008).

By analyzing the graph (figure 2.1.2.3) of creep function several conclusions can be drawn. For instance, in case of creep test the total deformation of the material is combination of elastic and viscous deformation.

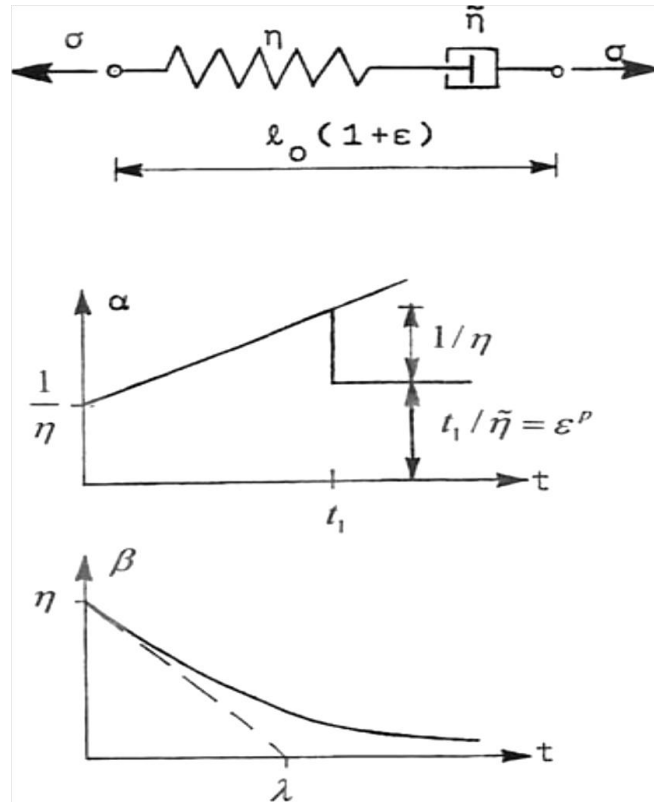


Figure 2.1.2.3. Maxwell model. In this figure $\tilde{\eta}$ represents viscosity and η is the modulus of elasticity. (Irgens, 2008)

The **Kelwin model** consists of a linear spring and a linear dashpot in parallel. This model is characterized by the following response equation:

$$\sigma = E\varepsilon + \eta\dot{\varepsilon} \quad (2.1.2.9)$$

The stress in the model is equal to the sum of the stress in the spring and stress in the dashpot. The creep function, glass compliance, equilibrium compliance of the model are the following:

$$\alpha(t) = \frac{1}{E} \left[1 - \exp\left(-\frac{t}{\lambda}\right) \right], \quad \alpha_g = 0, \quad \alpha_e = \frac{1}{E} \quad (2.1.2.10)$$

Here λ is retardation time and $\lambda = \eta/E$. The relaxation function, glass modulus, equilibrium modulus of the model are the following:

$$\beta(t) = E[1 + \lambda\delta(t)], \quad \beta_g = \infty, \quad \beta_e = E \quad (2.1.2.11)$$

The response of Kelvin model is the same as of a viscoelastic solid (Irgens, 2008).

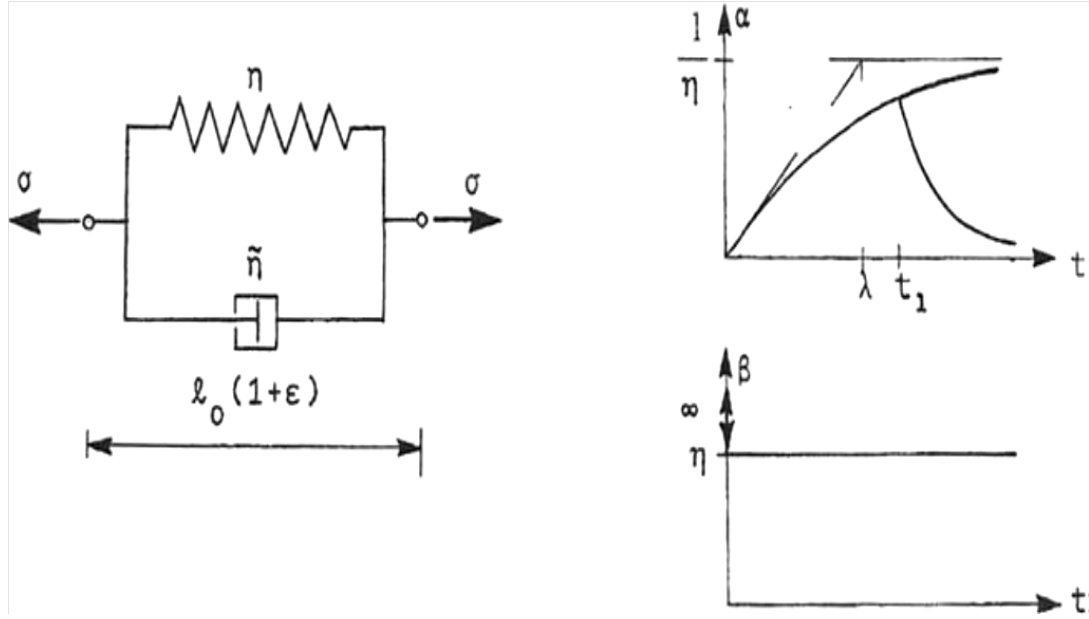


Figure 2.1.2.4 Kelvin model. In this figure $\tilde{\eta}$ represents viscosity and η is the modulus of elasticity. (Irgens, 2008)

Kelvin model illustrates the concept of delayed elastic response. When undergoing a creep test the specimen exhibits a delayed elastic strain response.

The **Burgers model** consists of a series of Maxwell elements and Kelvin element. This model has the following response equation:

$$\sigma + p_1 \dot{\sigma} + p_2 \ddot{\sigma} = q_1 \dot{\epsilon} + q_2 \ddot{\epsilon} \quad (2.1.2.12)$$

where:

$$p_1 = \lambda_1 \left[1 + \frac{E_1}{E_2} \right] + \lambda_2, \quad p_2 = \lambda_1 \lambda_2 \quad (2.1.2.13)$$

$$q_1 = \lambda_1 E_1, \quad q_2 = \lambda_2 \eta_1, \quad \lambda_1 = \frac{\eta_1}{E_1}, \quad \lambda_2 = \frac{\eta_2}{E_2}$$

The creep function, glass compliance, equilibrium compliance of the model are expressed as follows:

$$\alpha(t) = \frac{1}{E_1} \left[1 + \frac{t}{\lambda_1} \right] + \frac{1}{E_2} \left[1 - \exp\left(-\frac{t}{\lambda_2}\right) \right], \quad \alpha_g = \frac{1}{E_1}, \quad \alpha_e = \infty \quad (2.1.2.14)$$

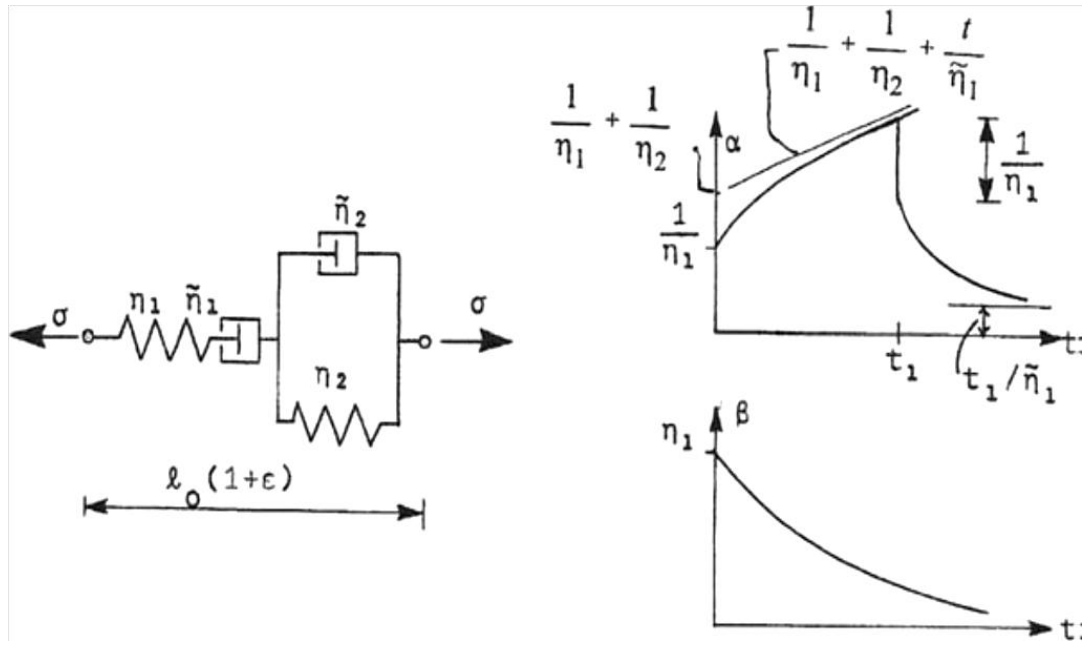


Figure 2.1.2.5. Burgers model. In this figure $\tilde{\eta}$ represents viscosity and η is the modulus of elasticity. (Irgens,2008)

The creep function of the Burgers model is equal to sum of the creep functions of Maxwell element and Kelvin element. The relaxation function, glass modulus, equilibrium modulus of the model are the following:

$$\beta(t) = \frac{1}{\sqrt{p_1^2 - 4p_2}} [(q_1 - \rho_2 q_2) \exp(-\rho_2 t) - (q_1 - \rho_1 q_2) \exp(-\rho_1 t)], \quad (2.1.2.15)$$

$$\beta_g = E_1, \quad \beta_e = 0$$

where:

$$\rho_{1,2} = \frac{1}{2p_2} [p_1 \pm \sqrt{p_1^2 - 4p_2}] \quad (2.1.2.16)$$

When undergoing a creep test, the strain response of a material, described by Burgers model, is a combination of elastic, delayed elastic and viscous strain responses.

It should be noted that by varying of viscosity η and the modulus of elasticity E it is possible to change the behavior of the model. For instance, let us consider the Kelvin model. Now if we increase value of η compare to E , basically this mean increasing of λ , the model will tend to behave like a Newtonian model. And conversely with decrease of λ the model will tend to behave like a Hookean model.

The Burgers model is a more sophisticated, model therefore by varying the material parameters it possible to get any model-like behavior, described in this chapter.

2.2. The Boltzmann superposition principle

It is of our interest to be able to predict a strain/stress history for a material in a state of uniaxial stress. For instant if the strain/stress history for a material is given it is interesting to compute the resulting stress or strain history. In order to do that the general response equation should be solved. The general response equation describes all different mechanical models that is constructed by adding together linear spring and linear dashpot in different combinations and is of the following form:

$$\sum_{n=0}^m p_n \frac{d^n \sigma}{dt^n} = \sum_{n=0}^{m+1} q_n \frac{d^n \varepsilon}{dt^n} \quad (2.2.1)$$

p_n and q_n are model parameters. The equation is developed from the basic response equations for the Hookean element and the Newtonian element.

The method of solving the response equation is based on the principle of superposition, introduced by Ludwig Boltzmann.

Let the strain history be given. Then the given strain history $\varepsilon(\bar{t})$ can be replaced by a step function $\tilde{\varepsilon}(\bar{t})$ (figure). The step function is constructed in the following way. Let t be the present time and \bar{t} be a "moving" time and $\bar{t} \leq t$. Let time interval $[t_0, t]$ be divided in m equal subintervals. And within each time subinterval $[t_n, t_{n-1}]$ \bar{t}_n is such that: $t_{n-1} \leq \bar{t}_n \leq t_n$. The condition $\varepsilon(\bar{t}) = 0$ for $\bar{t} < t_0$ should be satisfied. Then the step function $\tilde{\varepsilon}(\bar{t})$ is defined as follows:

$$\tilde{\varepsilon}(\bar{t}) = \sum_{n=1}^m \Delta \varepsilon_n H(\bar{t} - \bar{t}_n) \quad (2.2.2)$$

where:

$$\Delta \varepsilon_n \equiv \varepsilon(t_n) - \varepsilon(t_n - 1) = \dot{\varepsilon}(\bar{t}_n) \Delta t \quad (2.2.3)$$

The stress at the "moving" time \bar{t} due to the strain increment $\Delta \varepsilon_n$ is:

$$\Delta\sigma_n(\bar{t}) = \beta(\bar{t} - \bar{t}_n)\Delta\varepsilon_n H(\bar{t} - \bar{t}_n) = \beta(\bar{t} - \bar{t}_n)\dot{\varepsilon}(\bar{t})\Delta t H(\bar{t} - \bar{t}_n) \quad (2.2.4)$$

In order to get the stress at the present time t we may superimpose the stress contributions $\Delta\sigma_n(\bar{t})$. This is possible since the response equation (1) is linear. Hence the strain history $\tilde{\varepsilon}(\bar{t})$ results in the following stress at the present time t :

$$\tilde{\sigma}(t) = \sum_{n=1}^m \Delta\sigma_n(t) = \sum_{n=1}^m \beta(t - \bar{t}_n)\varepsilon(\bar{t}_n)\Delta\bar{t} \quad (2.2.5)$$

If $m \rightarrow \infty$ then approximated strain history $\tilde{\varepsilon}(\bar{t})$ approaches the actual strain history $\varepsilon(t)$ and the approximated stress history $\tilde{\sigma}(t)$ converges towards the actual stress history $\sigma(t)$. Therefore:

$$\sigma(t) = \int_{-\infty}^t \beta(t - \bar{t})\dot{\varepsilon}(\bar{t})d\bar{t} \quad (2.2.6)$$

Any response of a linearly viscoelastic material under uniaxial stress can be described by equation 2.2.6. The relaxation function $\beta(t)$ should be known beforehand (Irgens, 2008). For instance, it can be determined by performing relaxation tests of a material.

For a given stress history the solution can be obtained in the similar manner and the strain becomes:

$$\varepsilon(t) = \int_{-\infty}^t \alpha(t - \bar{t})\dot{\sigma}(\bar{t})d\bar{t} \quad (2.2.7)$$

The Boltzmann superposition principle illustrates how the response of any mechanical model in a uniaxial creep or relaxation test can be numerically solved. In this principle the assumption of small deformations is automatically fulfilled when the time step is small. In this method the creep function or relaxation function, depending on the test of interest, should be known beforehand. These functions represent the material response. Using the Boltzmann superposition principle the linear viscoelastic mechanical models were implemented into Matlab. The Matlab code is shown in appendix A.

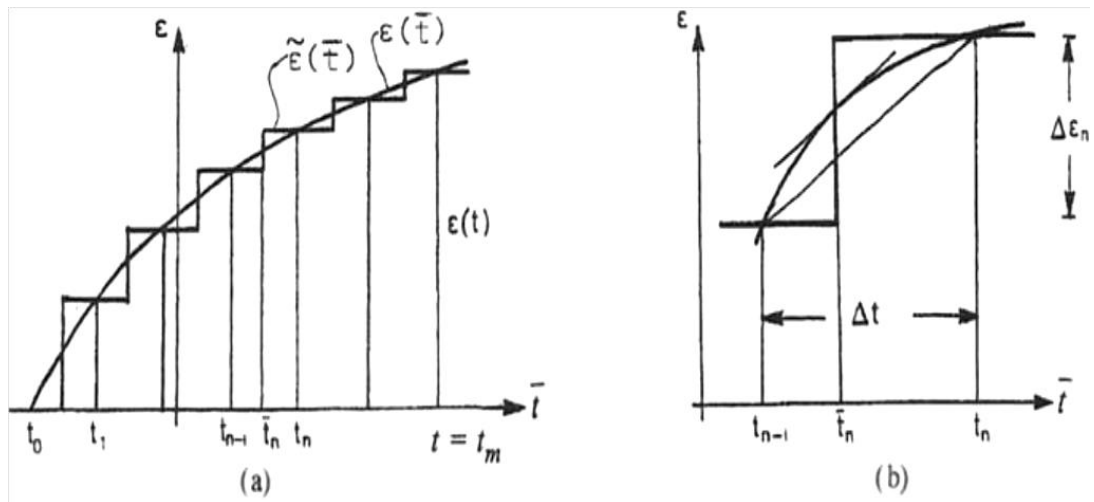


Figure.2.2.1. Superposition of strain increments.(Irgens,2008)

2.3.Validation of the Matlab code.

In order to verify that Matlab code were executed correctly, the numerical solutions for the response of Maxwell model obtained for two different creep tests were compared with its well-known analytical solutions. Two different types of loading were considered. For the first test the input was a stepwise constant stress and for the second one the input was a harmonic stress.

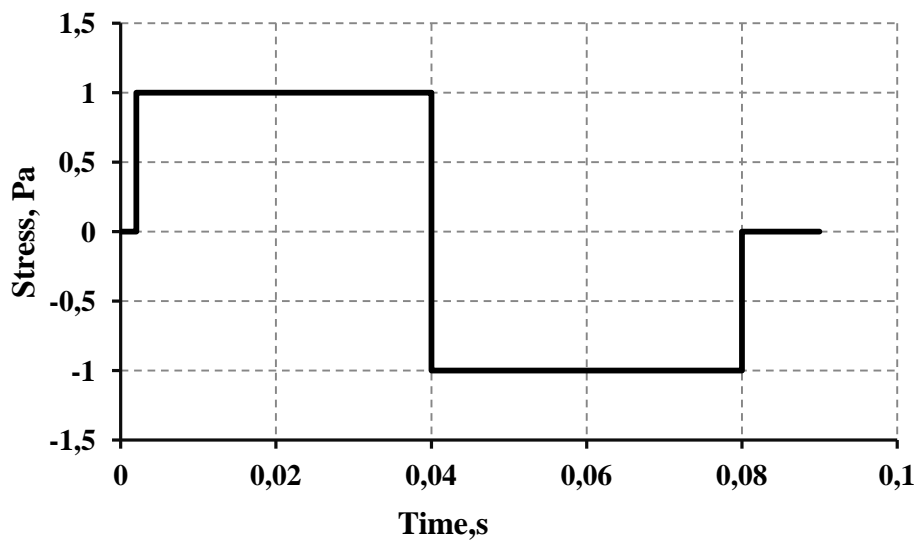


Figure 2.3.1. Stress history.

Assume that Maxwell model is exposed to stepwise axial stress, as shown in figure 2.3.1. The goal is to find the strain response $\varepsilon(t)$. The creep function for the Maxwell model can be written as follows:

$$\alpha(t) = \frac{1}{E} \left(1 + \frac{t}{\lambda} \right) \quad (2.3.1)$$

where E is a Young's Modulus, $\lambda = \eta / E$, where η is viscosity. For simplicity let us assume that $E = 1 \text{ Pa}$ and $\eta = 1 \text{ Pa} \cdot \text{s}$

The analytical solution of the strain response for the given stress history will be the following:

$$\varepsilon(t) = \frac{\sigma_0}{E} \left[\left(1 + \frac{t}{\lambda} \right) H(t) - 2 \left(1 + \frac{t-T}{\lambda} \right) H(t-T) + \left(1 + \frac{t-2T}{\lambda} \right) H(t-2T) \right] \quad (2.3.2)$$

where $H(t)$ is a Heaviside step function and $\sigma_0 = 1 \text{ Pa}$, $T = 0,04 \text{ s}$, $2T = 0,08 \text{ s}$, for a given stress history, shown in figure 1. It possible to calculate the strain response in Excel or any other software using equation 2.3.2. In order to do that the Heaviside step function can be approximated by the following equation:

$$H(x) = \frac{1}{1 + e^{-2kx}} \quad (2.3.3)$$

where the larger k corresponds to a sharper transaction at $x = 0$. $k = 1000$ was used in order to perform the calculations in Excel.

Now we are going to compare the results obtained by running the Matlab code based on Boltzmann principle of superposition and results obtained using equation 2. (figure 2.3.2.)

It follows from the figure that analytical and numerical solution give the same result. They differ a little bit in the transition regions when $t=0;0,04$ and $0,08\text{s}$. With increase of the value of k in equation 2.3.3 the analytical and numerical results will tend to be equal in the transition regions.

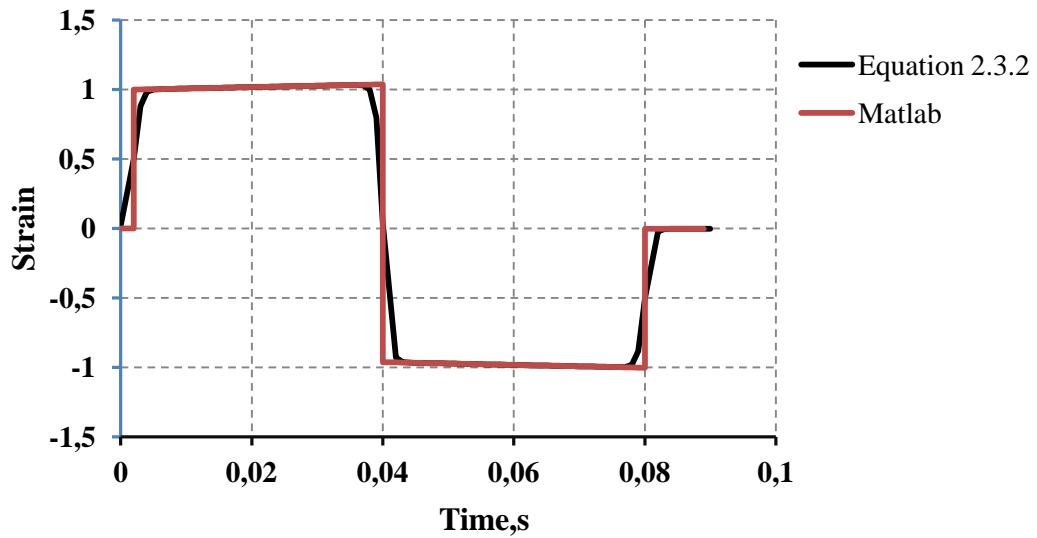


Figure 2.3.2. Comparison of numerical and analytical strain response.

Assume that Maxwell model is subjected to a harmonic uniaxial stress:

$$\sigma(t) = \sigma_0 \sin \omega t \quad (2.3.4)$$

The analytical solution for the strain response is as following:

$$\varepsilon(t) = [\alpha_1 \sin \omega t - \alpha_2 \cos \omega t] \sigma_0 H(t) + \alpha_2 \sigma_0 H(t) \quad (2.3.5)$$

where $H(t)$ is a Heaviside step function, α_1 and α_2 are the storage compliance and loss compliance respectively. For Maxwell model parameters α_1 and α_2 could be calculated using the following equations:

$$\alpha_1 = \frac{1}{\eta}, \quad \alpha_2 = \frac{1}{\lambda \omega \eta} \quad (2.3.6)$$

The strain response obtained by running the Matlab program based on Boltzmann principle of superposition and strain response obtained using equation 2.3.5 are shown in figure 2.3.3. The following values for the input parameters were used:

$$\eta = 1 \text{ Pa} \cdot \text{s}; \quad E = 1 \text{ Pa}; \quad \sigma_0 = 1 \text{ Pa}; \quad \omega = 1,26 \text{ rad} \cdot \text{s}^{-1}$$

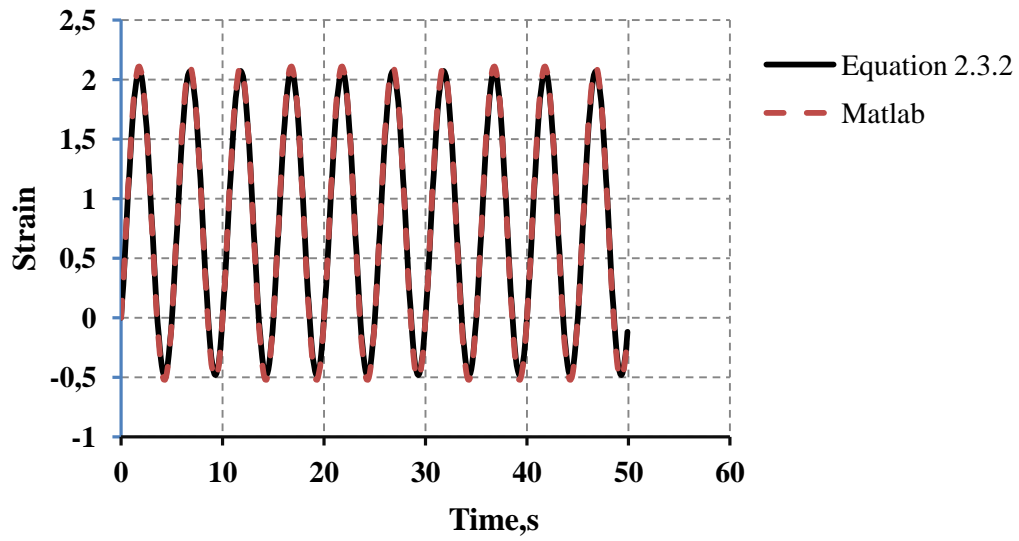


Figure 2.3.3. Comparison of strain response calculated using 2 different methods.

It follows from figure 2.3.3 that the Matlab program gives reasonable results.

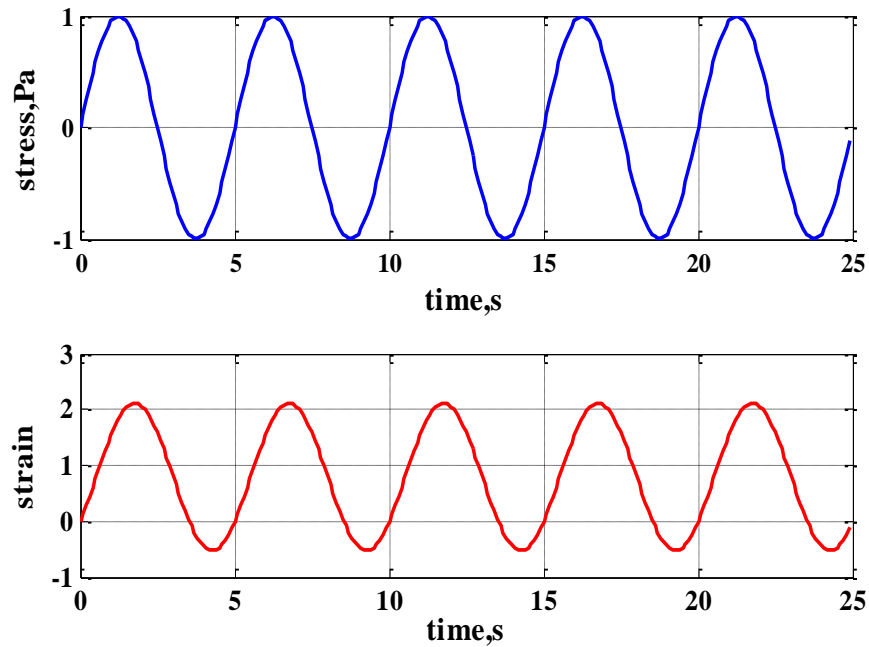


Figure 2.3.4. Stress history and corresponding numerically calculated strain response for 25s.

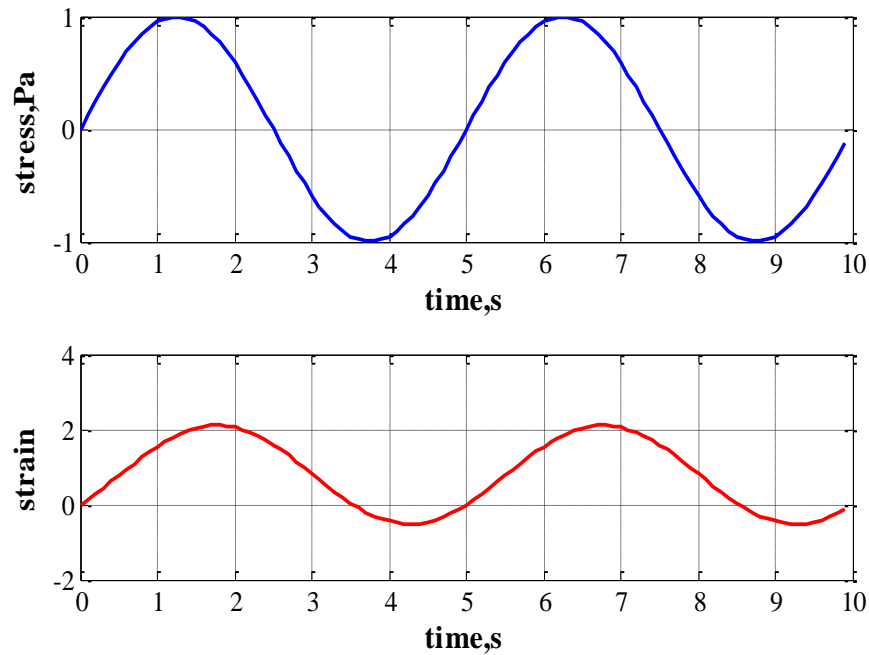


Figure 2.3.5. Stress history and corresponding numerically calculated strain response for 10s

From figure 2.3.4 and figure 2.3.5 it is clear that there is a phase lag between stress and corresponding strain. The phase lag is equal to δ/ω , where δ is a loss angle. For Maxwell model it can be calculated using the following equation:

$$\tan \delta = \frac{1}{\omega\lambda} \quad (7)$$

For the input values considered $\delta/\omega = 1\text{s}$. This does not contradict with the numerical result obtained.

2.4. Cyclic uniaxial compression test.

The test was conducted in the cold laboratory at University Centre on Svalbard in 2007. The aim of the experiment was to see the evolution of the stress-strain diagram in case where the specimen is subjected to a cyclic loading. In order to perform the test the "Kompis" machine was used (Figure 2.4.1.). The machine was set to have a constant nominal strain of 10^{-3} s^{-1} . The vertical test specimen, taken from Svea Bay, was used in the test. The ice sample had a diameter of 70 mm and the length of 175

mm. The test was conducted at the temperature about -10°C . After the sample was melted and its salinity was measured. During the test the ice sample was loaded and unloaded many time in order to reproduce cyclic loading.

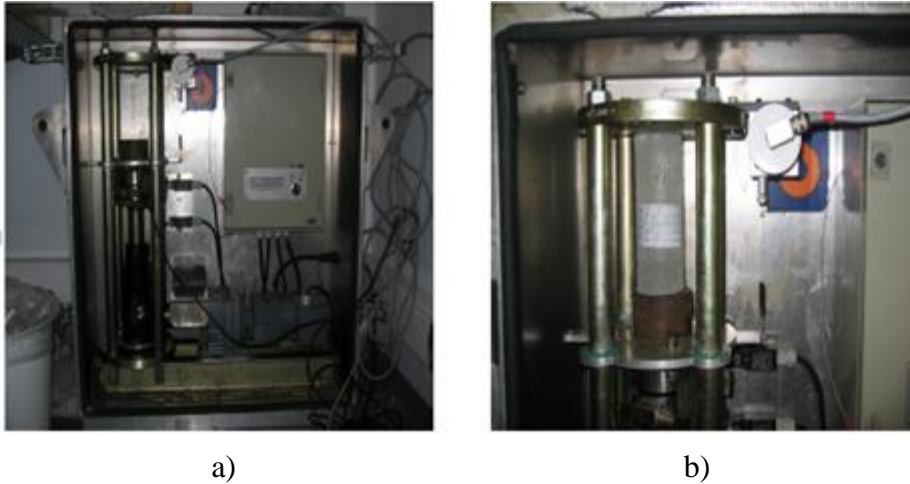


Figure 2.4.1. a) Kompis. b) Closer picture of a compressive unit. (Sæbø, 2007)

The stress history is shown in figure 2.5.2. The stress slowly increased in each cycle, starting with the load equal to 0,5-1,0 MPa.

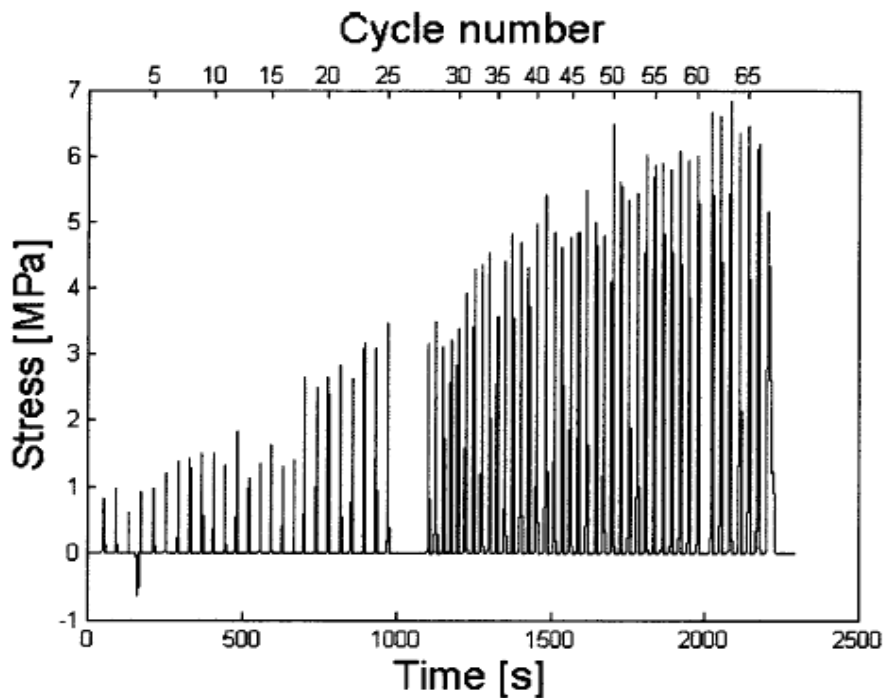


Figure 2.4.2. Stress plotted against time. 67 cycles are shown and numbered on the upper x-axis. (Sæbø, 2007)

During the test it was observed that the Young's modulus of ice sample first increases and then decreases when it subjected to cyclic loading with increasing amplitude (Figure 2.4.3.). The Young's Modulus was estimated every second cycle by linear least square regression (Figure 2.4.4.)

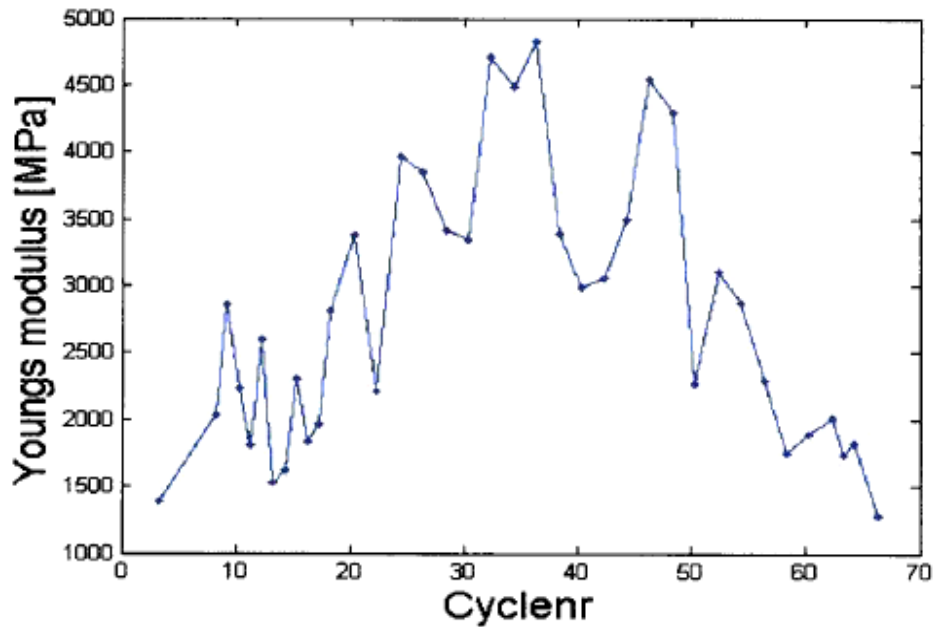


Figure 2.4.3. Young's modulus found by the linear regression for the different cycle numbers.(Sæbø, 2007)

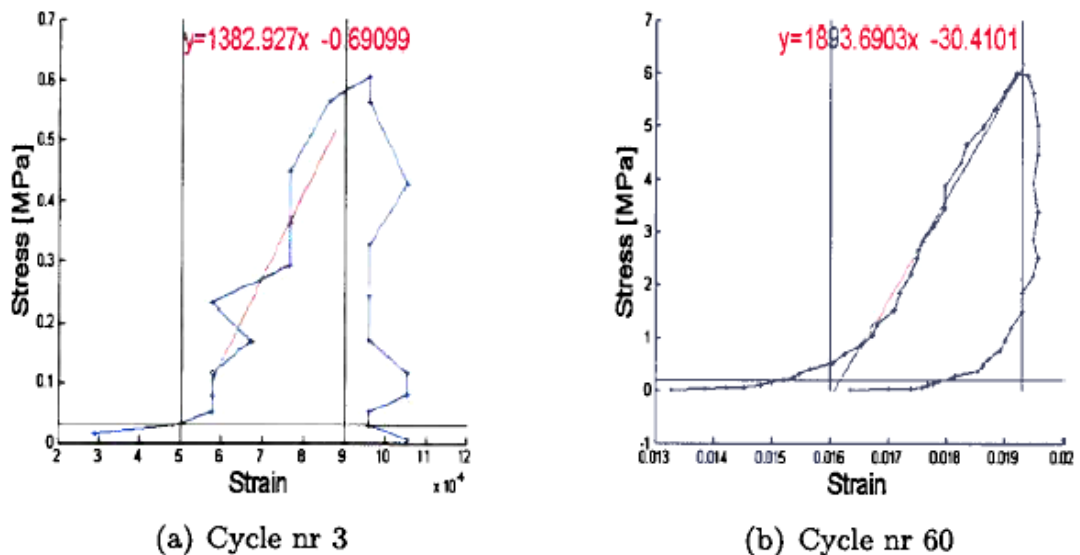


Figure 2.4.4. A stress-strain plot for cycle nr 3 and cycle nr 60. The horizontal and vertical lines limits the region where the best fit curves were calculated. The derivative of the equation on the top of the figures gives Young's Modulus. (Sæbø, 2007)

2.5. System's modulus of elasticity.

The goal of this work is to find out if the change of elastic modulus of ice under cyclic loading can be explained by viscoelastic properties of ice. In this work the behavior of ice is simulated by means of linearly viscoelastic mechanical models. These mechanical models are linear combinations of spring and dashpots. The input parameters for the creep functions of the model are not the same as properties of ice. For instance, the Young's modulus of spring element in mechanical model is not necessarily equal to modulus of elasticity of the simulated ice. From now on, the term system's modulus will be used when it comes to the modulus of elasticity of ice.

In order to say something about system's modulus the strain-stress curves should be analyzed. There is no one strict technique for definition of the modulus of elasticity from the stress-strain curve. In this thesis two definitions are used, shown in the figure 2.5.1. One is tangent system's modulus of elasticity E_t and the other one is secant system's modulus of elasticity E_s .

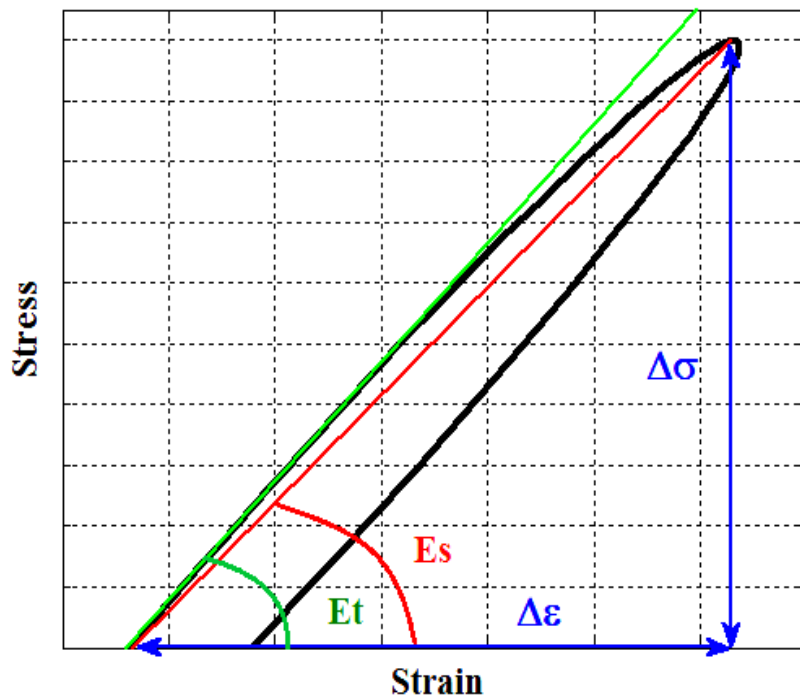


Figure 2.5.1. Tangent and secant system's modulus. Stress-strain curve in one cycle for Burgers model under cyclic loading is used in this figure.

The tangent system's modulus of elasticity E_t can be defined as slope of the tangent drawn from the initial point on the stress-strain curve. In this paper the secant system's modulus of elasticity E_s is defined as the slope of the line drawn from origin to the point, corresponding to the maximal stress in a stress-strain curve. Therefore E_s can be calculated as follows:

$$E_s = \frac{\Delta\sigma}{\Delta\varepsilon} \quad (2.5.1)$$

where E_s is a secant system's Young modulus [Pa], $\Delta\sigma$ is a difference between maximal and initial stress in a stress-strain diagram [Pa], $\Delta\varepsilon$ is corresponding to stress strain difference. Secant system's model capture the effects of non-elastic deformations.

2.6. Non-linear viscoelastic model for polycrystalline ice.

The model was proposed by N.K. Sinha and presented in several of his papers . In this thesis the paper "Rheology of columnar-grained ice", published in 1978 was used. The strain response of columnar-grained S-2 ice in a creep test can be expressed as follows:

$$\varepsilon_t(\sigma, T, t) = \varepsilon_e(\sigma) + \varepsilon_d(\sigma, T, t) + \varepsilon_v(\sigma, T, t) \quad (2.6.1)$$

where ε_t is total strain , ε_e is pure elastic strain, ε_d is recoverable, delayed elastic strain, ε_v is viscous permanent deformation. Explicit form of equation 2.5. is the following:

$$\varepsilon_t = \frac{\sigma}{E} + c \left(\frac{\sigma}{E} \right)^s \left[1 - \exp\left(- (a_T \cdot t)^b\right) \right] + \dot{\varepsilon}_v t |\sigma|^n \quad (2.6.2)$$

where $\dot{\varepsilon}_v = A \exp(-Q/RT)$, A is a constant for a given stress, R is a gas constant [J/mol/K], Q is the activation energy [KJ/mol], T is temperature [K], σ is stress [Pa], E is Young's modulus [Pa], t is time [s], a_T is inverse relaxation time [1/s], n is stress exponent, b, c, s are constants.

3.RESULTS

3.1. Sensitivity Analysis

Before starting the numerical experiments it is important to perform a sensitivity analysis in order to have a better understanding of how the input parameters are affecting the output of the model and which input parameters have a significant influence on the behavior of the model.

It is in our interest to analyze the behavior of the Burgers model in a creep test. As it was mentioned before Burgers model consists of Maxwell and Kelvin unit combined in series. The creep function of the model is a sum of creep functions of Maxwell and Kelvin unit. Therefore, it makes sense to perform the sensitivity analysis of these two units first. Thereby the sensitivity analysis of Kelvin, Maxwell and Burgers model is presented in this chapter.

At this stage of research using physically reasonable parameters is not so important. What is important is to try to combine the input parameters into dimensionless coefficients and see their influence on the behavior and output of the models. Therefore the input parameters used in this analysis are not suitable for simulating the ice behavior.

For each of the models two types of loading were considered: constant loading and cyclic loading. It is important to analyze the behavior of the models under constant loading first before looking into details into more complicated cyclic loading tests.

It was decided not to use dimensionless graphs in this section to be able to see clearly the influence of each input parameter.

3.1.1. Kelvin model

The model was subjected to a step constant stress σ_0 during the time interval $[t_0, t_1]$. The creep function of the model is described by equation 2.1.2.10.. The input parameters for Kelvin model are viscosity η , modulus of elasticity E , applied stress σ_0 and time $\Delta t = t_1 - t_0$, where t_0 is time when constant stress is applied and t_1 is time when stress is removed. The output is strain ε .

The parameter that has a significant influence on the strain response of the model is $\Delta t / \lambda$, where $\lambda = \eta / E$. For instance, it was concluded that if $\Delta t / \lambda = 5$ the strain reaches its maximal value equal to σ_0 / E at time t_1 . This phenomenon can be explained by the nature of the integral 2.2.7 and creep function 2.1.2.10. It is clear that with increase of the value of t / λ in equation 2.1.2.10 $\alpha(t)$ approaches the value of $1/E$ (Table 3.1.1.1). When calculating the strain response of the model using the Boltzmann principle of superposition we discretize the given stress history in order to solve the convolution integral 2.2.7. numerically. Therefore we are dealing with summation of the strain response obtained for values of moving time. So when $\Delta t / \lambda = 5$ the strain reaches its maximal value equal to σ_0 / E at time t_1 due to the behavior of $(1 - \exp(-t / \lambda))$ and summation. In order to validate this property of Kelvin model several tests were conducted numerically. The extensive results can be seen in appendix B. In figure 3.1.1. two selected cases are presented.

The ratio σ_0 / E has an influence on the values of strain response but not on the shape of the strain response curve.

Table 3.1.1.1. Values of creep function multiplied with modulus of elasticity for certain values of t/λ ratio.

t / λ	$\alpha(t) \cdot E = (1 - \exp(-t / \lambda))$
1	0.63212
2	0.86466
3	0.95021
4	0.98168
5	0.99326
6	0.99752
10	0.99995
100	1.00000

As it was already mentioned before it is possible to change the response of this viscoelastic model to either predominant elastic or viscous response just by varying the input parameters. It is of interest to check for the values of input parameters for which the Kelvin model will have a completely elastic behavior or viscous behavior. It is clear that for Kelvin model this strongly depends on the value of λ . Using the expression $\Delta t / \lambda = 5$ it is possible to set the condition for an elastic behavior.

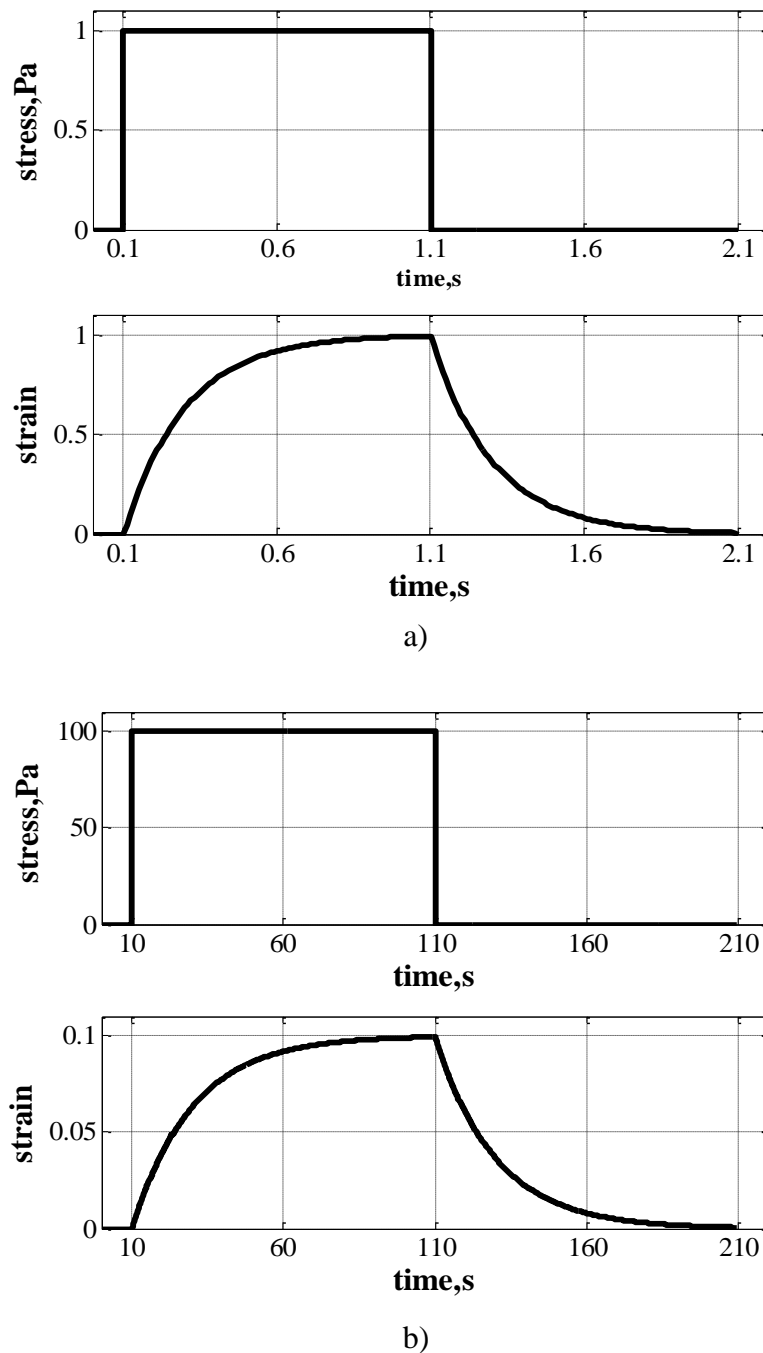


Figure 3.1.1.1. Stress history and strain response of Kelvin model in a creep tests. The value $\Delta t / \lambda$ were kept equal to 5. The following input parameters were selected for the tests:

- a) $\Delta t = 1s$; $\sigma_0 = 1 Pa$; $E = 1Pa$; $\eta = 0.2 Pa \cdot s$
b) $\Delta t = 100s$; $\sigma_0 = 100 Pa$; $E = 1000Pa$; $\eta = 20000 Pa \cdot s$

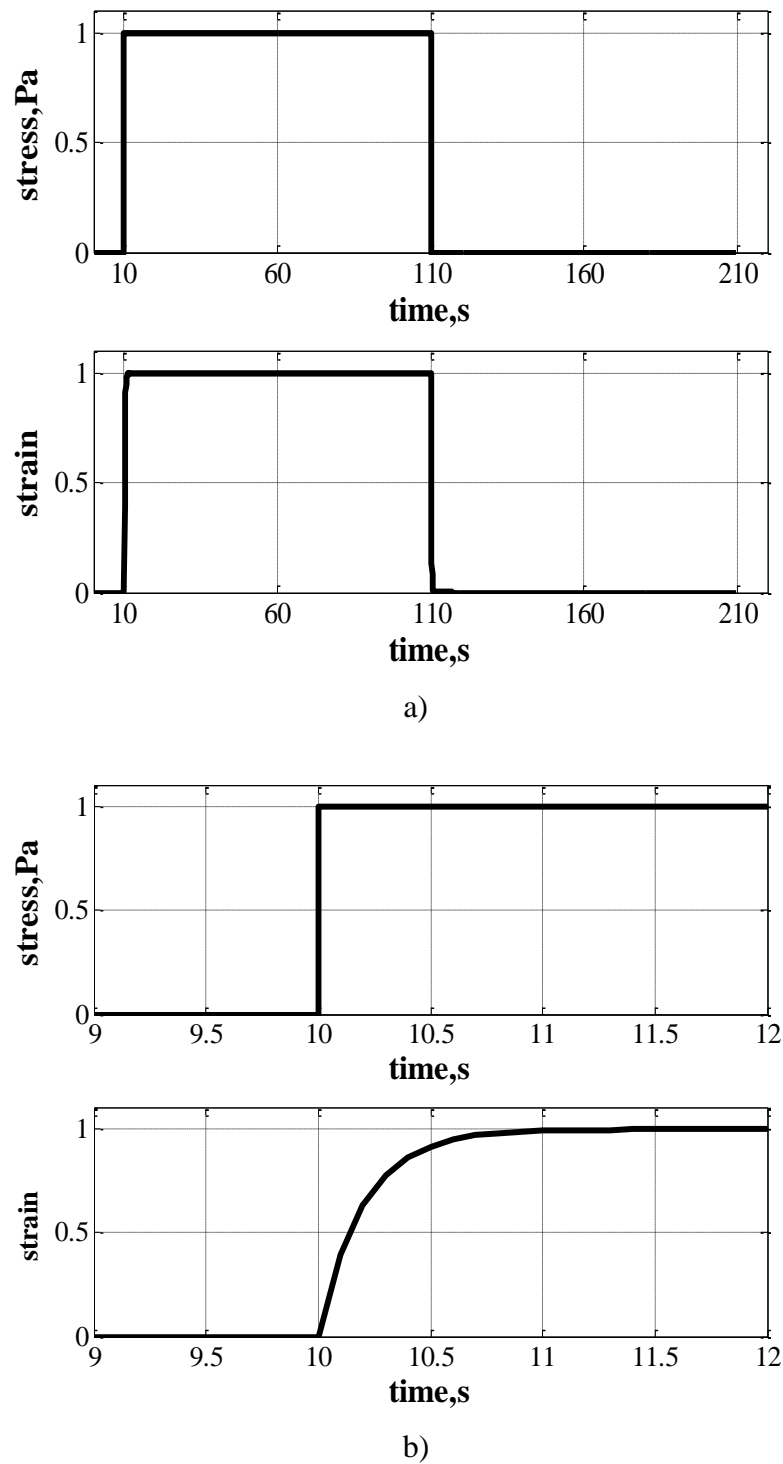


Figure 3.1.1.2. Selecting of a critical value of λ in order to obtain elastic behavior of the Kelvin model. The following values of the input parameters were assigned to the model: $\Delta t = 100$ s; $\sigma_0 = 1$ Pa; $E = 1$ Pa; $\eta = 0.2$ Pa·s. a) Strain response of the model for 210s. b) Strain response of the model for first 12s.

Instead of assigning the difference of t_1 and t_0 to Δt , we can give a relatively small time step compared to total loading time in which the strain response should reach it's maximal value equal to σ_0/E . For example if we have a 100s stress history we may assume that the model shows elastic behaviour if the strain reaches value of σ_0/E within first second after loading. Out of this condition we can derive the critical value for λ . And if $\lambda \leq \lambda_{critical}$ then we have elastic behavior of the model. The example is shown in Figure 3.1.1.2. For viscous behavior of Kelvin model viscosity should be much less than elasticity of the model. It is harder to give a clear criterion of initiation of predominantly viscous response of Kelvin model. Even though, the following condition may be used: $\Delta t / \lambda \geq 0.01$, where $\Delta t = t_1 - t_0$. An example of the viscous response of the model is shown in figure 3.1.1.3.

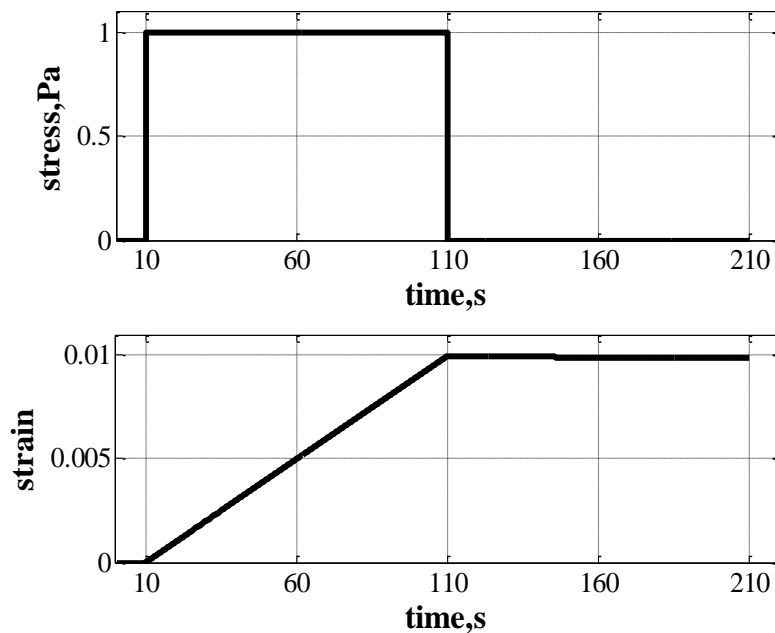


Figure 3.1.1.3. Viscous response of Kelvin model. The following values of the input parameters were used: $\Delta t = 1s$; $\sigma_0 = 100 Pa$; $E = 1Pa$; $\eta = 10000 Pa \cdot s$.

Using the condition $\Delta t / \lambda = 5$ we may also judge how the model will behave for a given stress history and value of λ .

Harmonic stress was described by the following equation:

$$\sigma = \sigma_0 \sin \omega t \quad (3.1.1.1.)$$

where σ_0 is an amplitude of the stress [Pa], ω is an angular frequency [rad/s], t is time [s]. It is also of our interest to analyze the response of the model to absolute value of harmonic stress described in equation 3.1.1.

$$\sigma = |\sigma_0 \sin \omega t| \quad (3.1.1.2.)$$

Once again it is useful to establish some kind of criterion that explains for which combination of the input parameters Kelvin model acts like a elastic or like a viscous model. The criterion can be derived from the following basis. When viscoelastic model is subjected to harmonic or cyclic stress there will be a phase lag between the stress and strain response (Figure 3.1.1.4.).

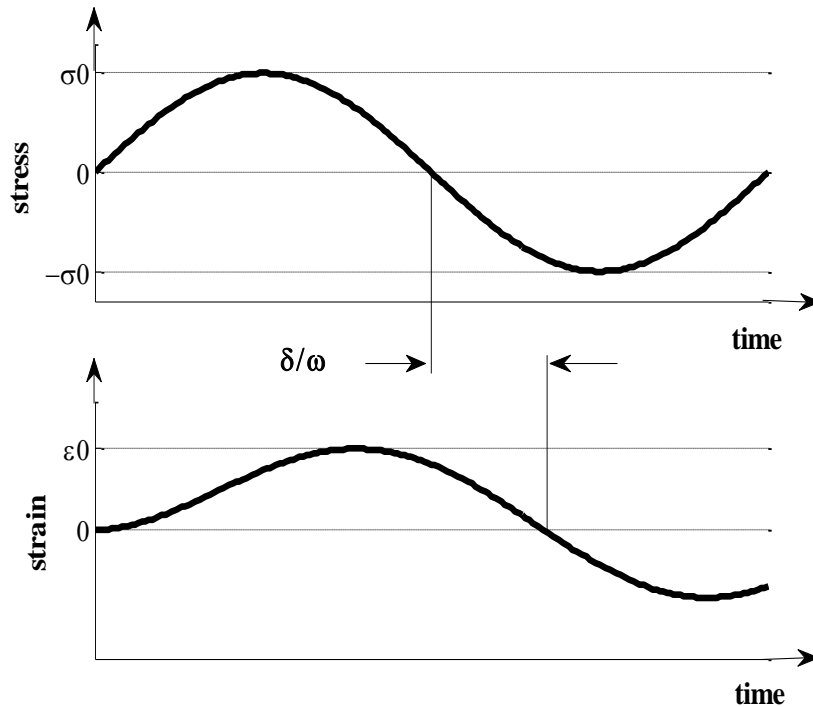


Figure 3.1.1.4. Phase lag between harmonic stress and corresponding strain response.

For Kelvin model tangent of the phase angle δ can be expressed by the following equation:

$$\tan \delta = \lambda \omega \quad (3.1.1.3.)$$

Elastic behavior of model is characterized by instantaneous strain response to applied stress. Therefore δ should be equal 0 and hence $\tan \delta$ should be 0. This means that $\lambda \omega \rightarrow 0$. In case of viscous response of the model we may say that δ should be

equal $\pi/2$. However $\tan(\pi/2)$ is undefined, but this condition will be fulfilled when $\lambda\omega \rightarrow \infty$. For engineering purposes it is useful to know what values of $\lambda\omega$ will correspond to either case when $\tan\delta$ equal 0 or $\pi/2$. Therefore the model was tested for different combination of the input parameters. When ratio T/λ is greater than or equal to 1000 Kelvin model acts like a Hookean model, whereas if T/λ is less than or equal to 0.001 Kelvin model acts like a Newtonian model. Here T is a period of harmonic loading or double time of one cycle in case of cyclic loading. Elastic behavior of Kelvin model is shown in figure 3.1.1.5. It is characterized by instantaneous strain response to applied stress. Strain is in phase with stress and reaches its maximal value equal to σ_0/E during each cycle. Viscous behavior of Kelvin model is shown in figure 3.1.1.6. Strain response is out of phase with applied stress. Phase angle is equal to $\pi/2$.

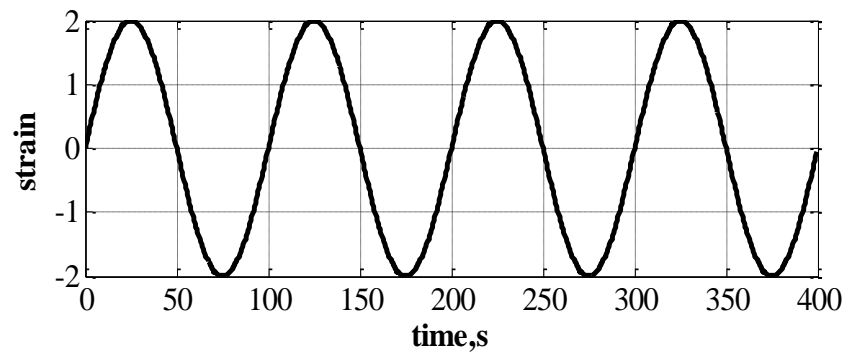
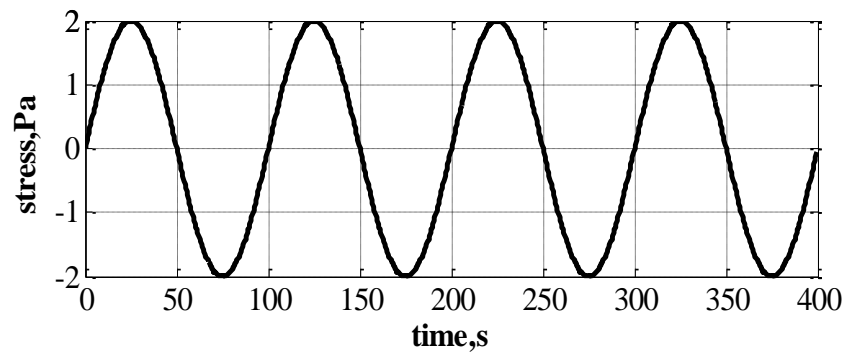
The input parameters were combined into the dimensionless coefficients described by equation 3.1.4. and the influence of these coefficients on the strain response of Kelvin model under cyclic loading, described by equation 3.1.1.2 was analyzed.

$$K = \frac{f\eta}{E} = f\lambda; \quad M = \frac{\sigma_0}{E} \quad (3.1.1.4)$$

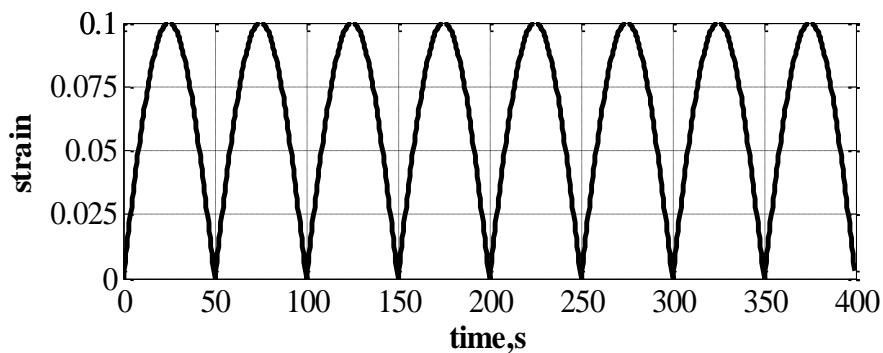
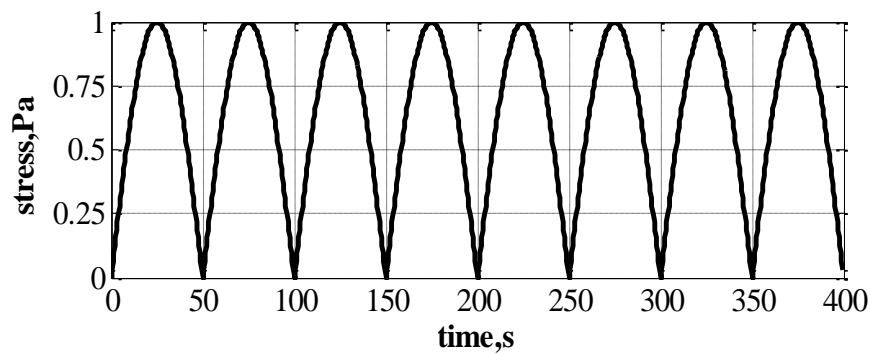
where $f = \omega/2\pi$ is frequency [Hz].

The following cases were considered:

1. The coefficients K and M were kept constant and equal to 1. The modulus of elasticity and the stress amplitude were fixed and equal to 1 Pa. Frequency, number of cycles and viscosity were being changed during the tests.
2. The coefficients K and M were kept constant and equal to 1. Frequency was kept equal to 0.0667 Hz. Viscosity, modulus of elasticity and stress amplitude were being changed during the tests.
3. The coefficient M was kept constant and equal to 1. Frequency was fixed and equal to 0.0667 Hz. Viscosity was being changed during the tests.
4. The coefficient K was kept constant and equal to 1. Frequency was fixed and equal to 0.0667 Hz. Amplitude of stress was fixed and equal to 1. Relation between viscosity and Young's modulus were kept constant and equal to 15. The values for coefficient M were being changed.

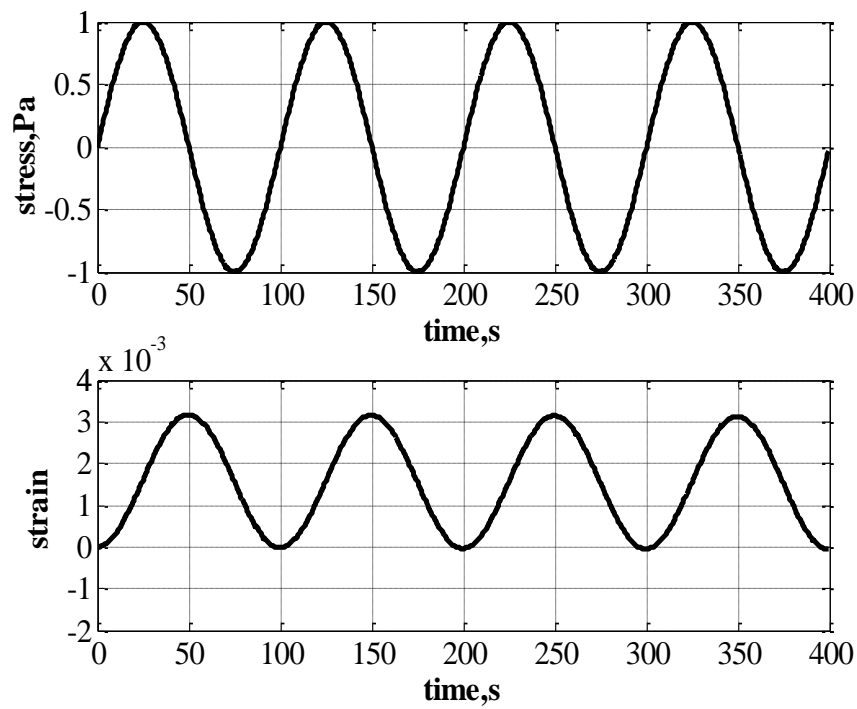


a) $\sigma_0 = 2 \text{ Pa}$; $T = 100 \text{ s}$; $E = 1 \text{ Pa}$; $\eta = 0.1 \text{ Pa} \cdot \text{s}$

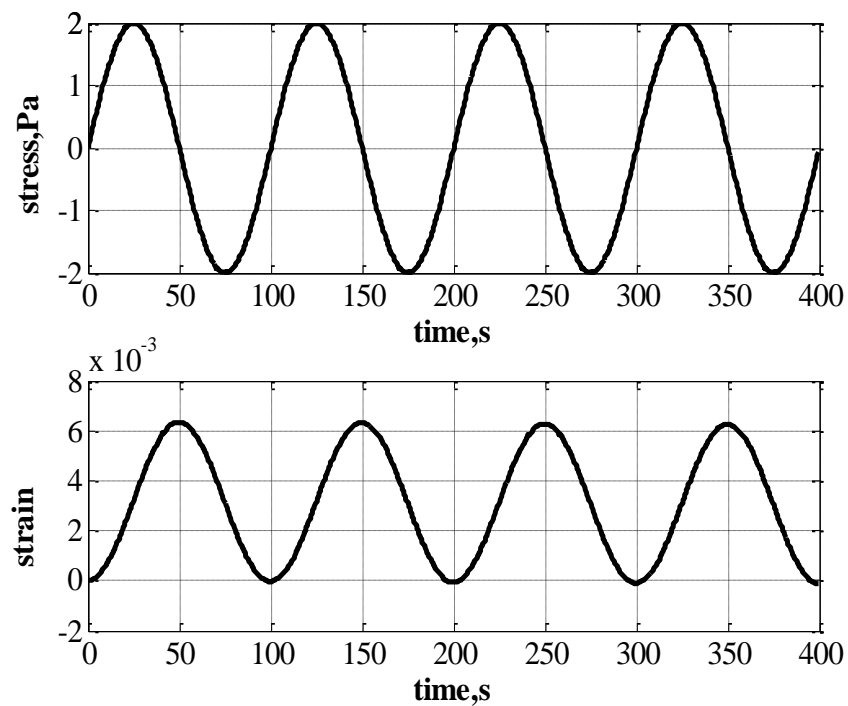


b) $\sigma_0 = 1 \text{ Pa}$; $T = 2 \cdot 50 \text{ s}$; $E = 10 \text{ Pa}$; $\eta = 0.01 \text{ Pa} \cdot \text{s}$

Figure 3.1.1.5. Elastic response of the Kelvin model under harmonic loading.



a) $\sigma_0 = 1 Pa$; $T = 100s$; $E = 1 Pa$; $\eta = 100000 Pa \cdot s$



b) $\sigma_0 = 2 Pa$; $T = 100s$; $E = 1 Pa$; $\eta = 100000 Pa \cdot s$

Figure 3.1.1.6. Viscous response of the Kelvin model under harmonic loading.

The results for each case are presented below. In case 2 there was no difference between the strain response curves, due to the fact that ratios T/λ and σ/E were kept constant. Therefore case 2 is not included below.

From figures 3.1.1.7.-3.1.1.9. it is clear that when the cyclic loading is applied to Kelvin model the strain starts to increase during a certain amount of time and then it reaches mean value and after that only oscillations around this mean value of the strain occur. This mean value of strain is the same for all tests conducted and equal to $2/\pi \cdot (\sigma_0/E)$, where $2/\pi$ is a mean value of $|\sin(\omega t)|$. The time, strain need to reach the phase ,where only oscillations around the mean value equal to $2/\pi \cdot (\sigma_0/E)$ occur ,can be obtained from the following expression: $\Delta t/\lambda = 5$, where Δt is time that is needed. The basis for using this expression has been discussed above in this section. For instance from figure 3.1.1.7. it is clear that higher the value for viscosity more time required for strain to reach the stationary oscillation around the mean value. The amplitude of this stationary oscillation is proportional to λ .(figure 3.1.1.8.) Higher the value of λ smaller the amplitude. From figure 3.1.1.9. it is clear that the ratio of the amplitude of stationary strain oscillations to mean strain value is constant for case 4.

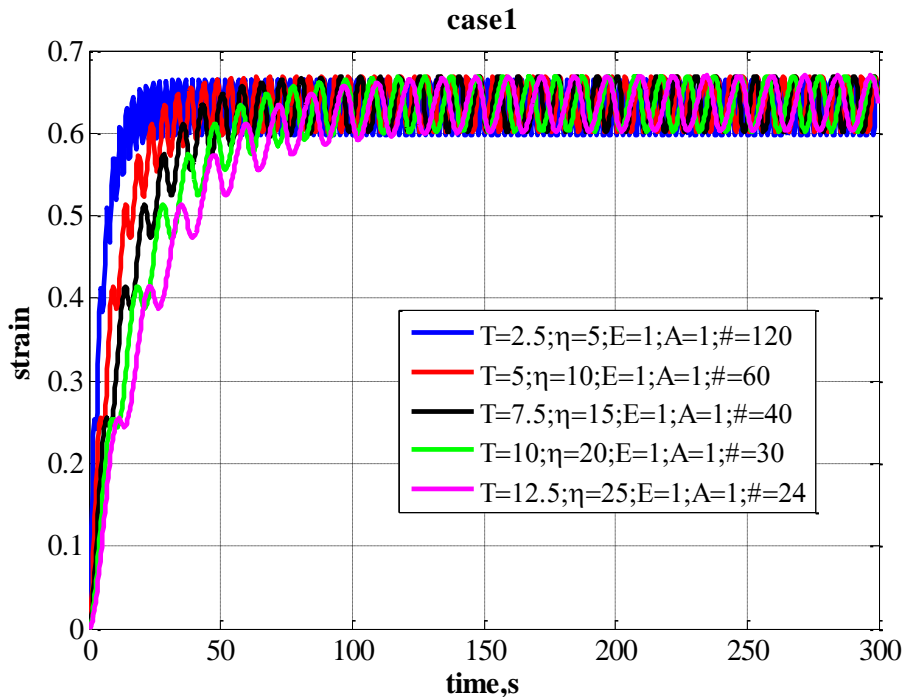


Figure 3.1.1.7. Strain responses of Kelvin model in case 1. In the legend: T is duration of one cycle [s], η is viscosity [Pa·s], E is modulus of elasticity, $A = \sigma_0$ is an amplitude of cyclic stress [Pa], $\#$ is number of cycles.

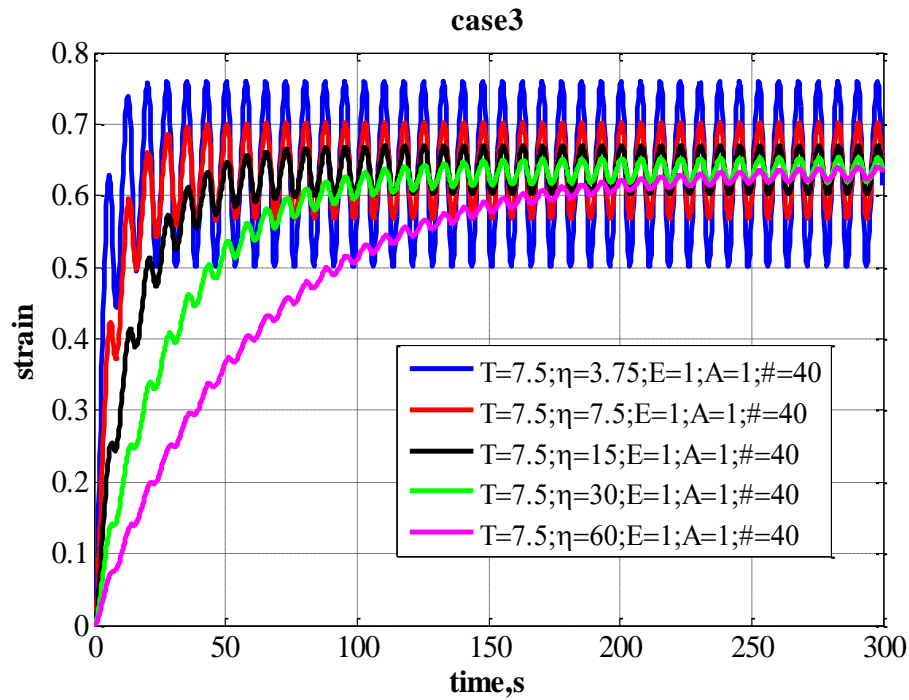


Figure 3.1.1.8. Strain responses of Kelvin model in case 3. In the legend: T is duration of one cycle [s], η is viscosity [Pa·s], E is modulus of elasticity, $A = \sigma_0$ is an amplitude of cyclic stress [Pa], $\#$ is number of cycles.

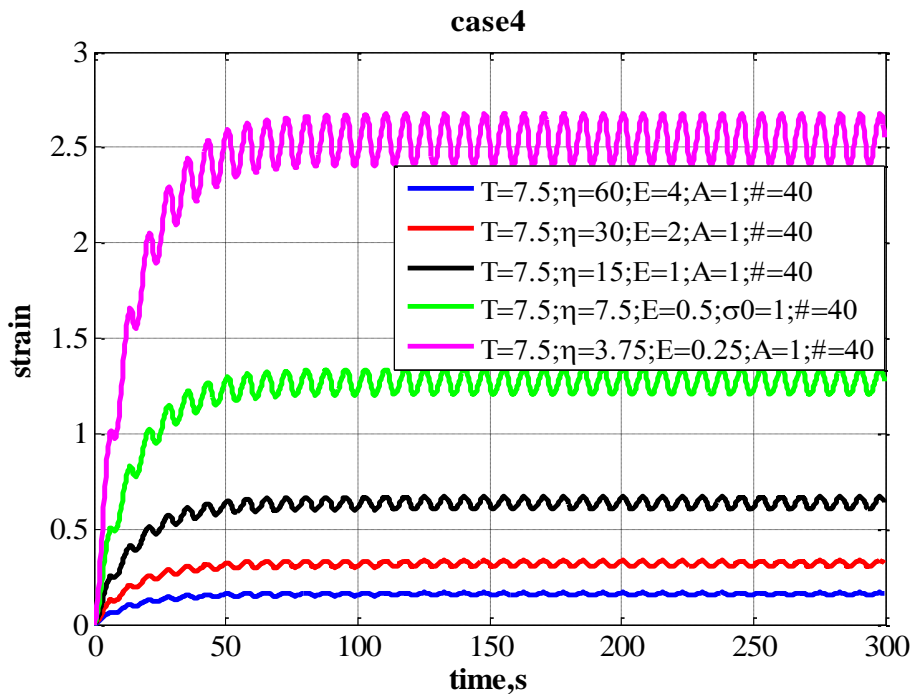


Figure 3.1.1.9. Strain responses of Kelvin model in case 4. In the legend: T is duration of one cycle [s], η is viscosity [Pa·s], E is modulus of elasticity, $A = \sigma_0$ is an amplitude of cyclic stress [Pa], $\#$ is number of cycles.

3.1.2. Maxwell model.

The Maxwell model and its creep and relaxation function are shown in Figure 2.1.2.3

The case when the model is subjected to a constant stress σ_0 during the time interval $[t_0, t_1]$. is considered in this part. The creep function of the model is described by equation 2.1.2.7. The input parameters that may influence the behavior of the model are viscosity η , modulus of elasticity E , applied stress σ_0 and time $\Delta t = t_1 - t_0$, where t_0 is time when constant stress is applied and t_1 is time when stress is removed. The output is strain ε . An example of creep test is shown in figure 3.1.2.1. By analyzing the strain response of Maxwell model in creep test the following conclusions can be drawn:

- At time t_0 model exhibits an instantaneous strain equal to σ_0 / E , which completely vanishes once the loading is removed.
- The ratio $(t_1 - t_0) / \lambda$ could be seen as a slope angle of the strain response curve during the time interval $[t_0, t_1]$. The value of this ratio multiplied on σ_0 / E determines to what level the strain will grow during the time $[t_0, t_1]$ in addition to instantaneous strain.
- The ratio of $(t_1 - t_0) / \eta$ determines the value of irreversible deformation.

In order to get elastic response of Maxwell model the ratio of $(t_1 - t_0) / \lambda$ should be relatively small. The assumption of $(t_1 - t_0) / \lambda \leq 0.01$ works quite well, since the ratio of σ_0 / E is less than 1 for ice. In order to get viscous response of Maxwell model the ratio of $(t_1 - t_0) / \lambda$ should be relatively big. The assumption of $(t_1 - t_0) / \lambda \geq 100$ works quite well in this case. It should be mentioned that the model will still exhibit instantaneous strain of value σ_0 / E so we just need to select the value of input parameters in such a way that this instantaneous strain can be

considered negligible. The elastic and viscous strain response of the Maxwell model are shown in figure 3.1.2.2. and 3.1.2.3. respectively.

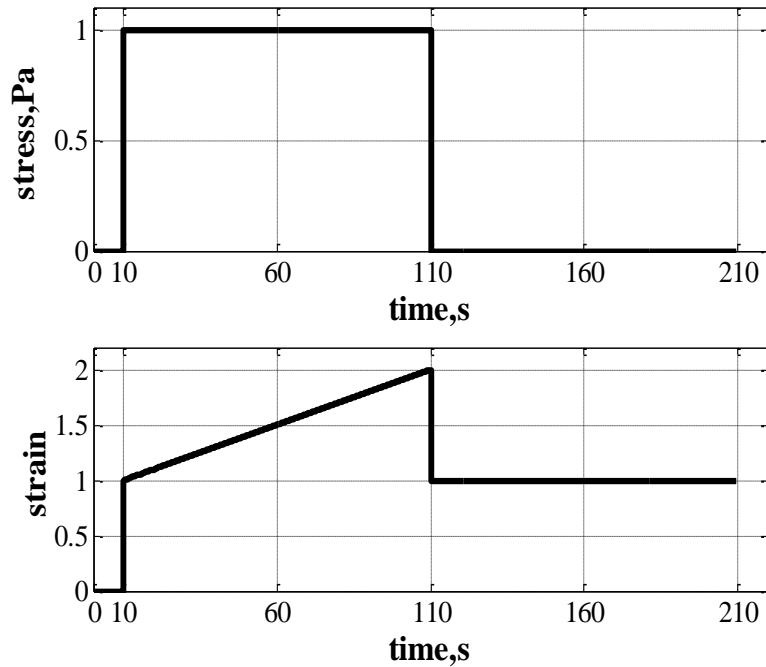


Figure 3.1.2.1. Maxwell model. Creep test. Input parameters:

$$\sigma_0 = 1 \text{ Pa}; \quad \Delta t = 100 \text{ s}; \quad E = 1 \text{ Pa}; \quad \eta = 100 \text{ Pa} \cdot \text{s}$$

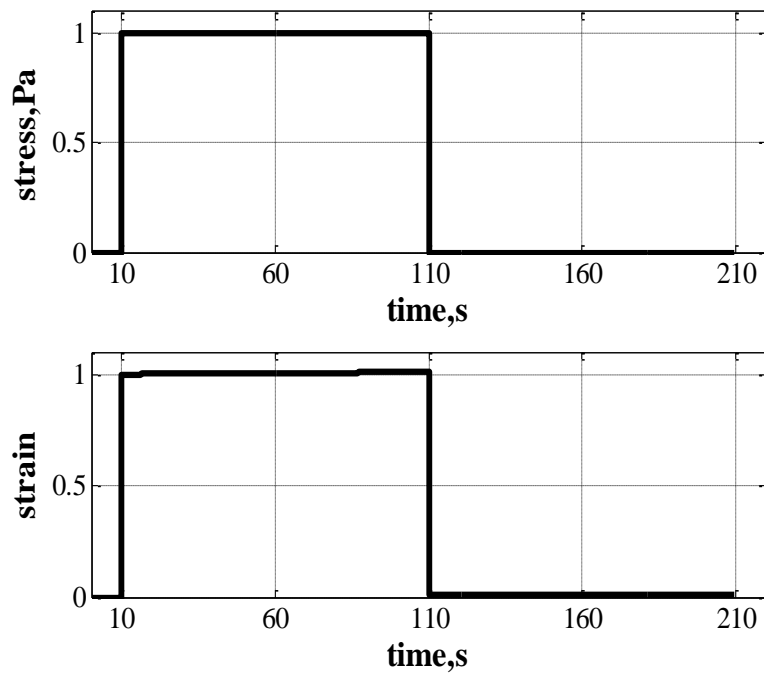


Figure 3.1.2.2. Elastic behavior of Maxwell model in creep test. Input parameters:

$$\sigma_0 = 1 \text{ Pa}; \quad \Delta t = 100 \text{ s}; \quad E = 1 \text{ Pa}; \quad \eta = 10000 \text{ Pa} \cdot \text{s}$$

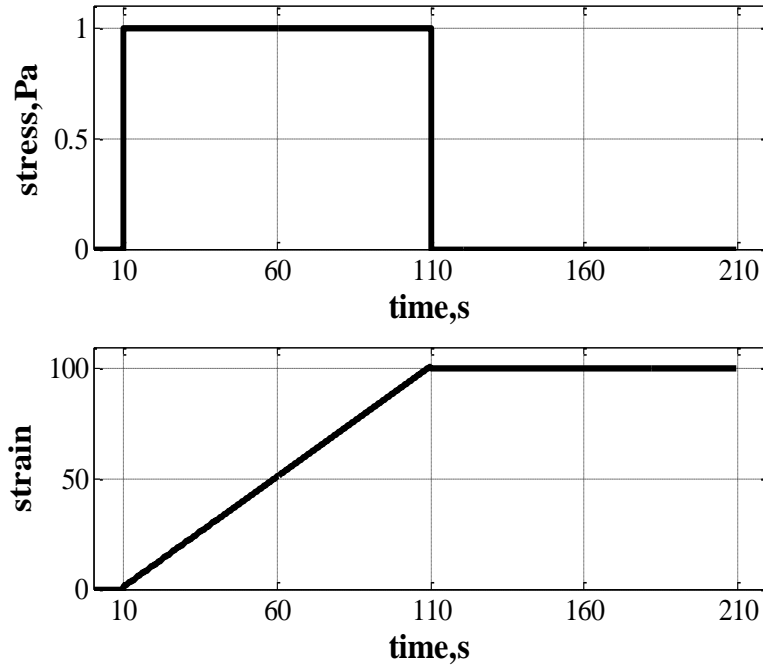


Figure 3.1.2.3. Viscous behavior of Maxwell model in creep test. Input parameters:

$$\sigma_0 = 1 \text{ Pa}; \quad \Delta t = 100 \text{ s}; \quad E = 1 \text{ Pa}; \quad \eta = 1 \text{ Pa} \cdot \text{s}$$

The case when the model is subjected to a cyclic stress is considered in this part. Applied harmonic stress is described by equation 3.1.1.1 and cyclic stress by equation 3.1.1.2. When Maxwell model is subjected to harmonic or cyclic stress there will be a phase lag between the stress and strain response. For Maxwell model the tangent of the phase angle δ can be expressed by the following equation :

$$\tan \delta = \frac{1}{\lambda \omega} \quad (3.1.2.1.)$$

For elastic behavior of the model δ should be equal 0 and hence $\tan \delta$ should be 0. This means that $\lambda \omega \rightarrow \infty$. For viscous response of the model δ should be equal $\pi/2$. Hence, $\lambda \omega \rightarrow 0$. When ratio T/λ greater or equal to 1000 Maxwell model acts like Newtonian model (figure 3.1.2.4.), whereas if T/λ less or equal to 0.001 Maxwell model acts like Hookean model (figure 3.1.2.5.). Here T is a period of harmonic loading or double time of one cycle in case of cyclic loading.

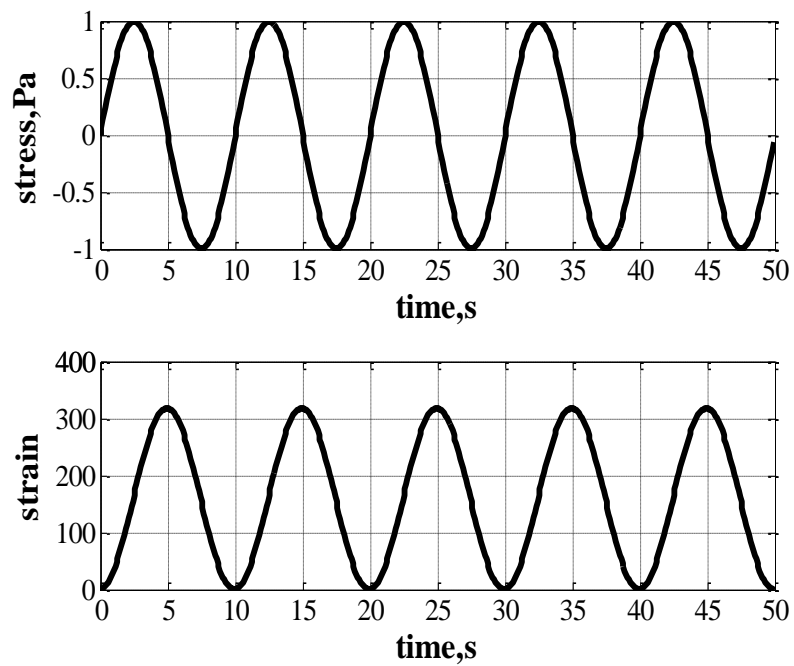


Figure.3.1.2.4. Viscous response of the Maxwell model under harmonic loading.

Input: $\sigma_0 = 1 Pa$; $\Delta t = 10s$; $E = 1Pa$; $\eta = 0.01 Pa \cdot s$

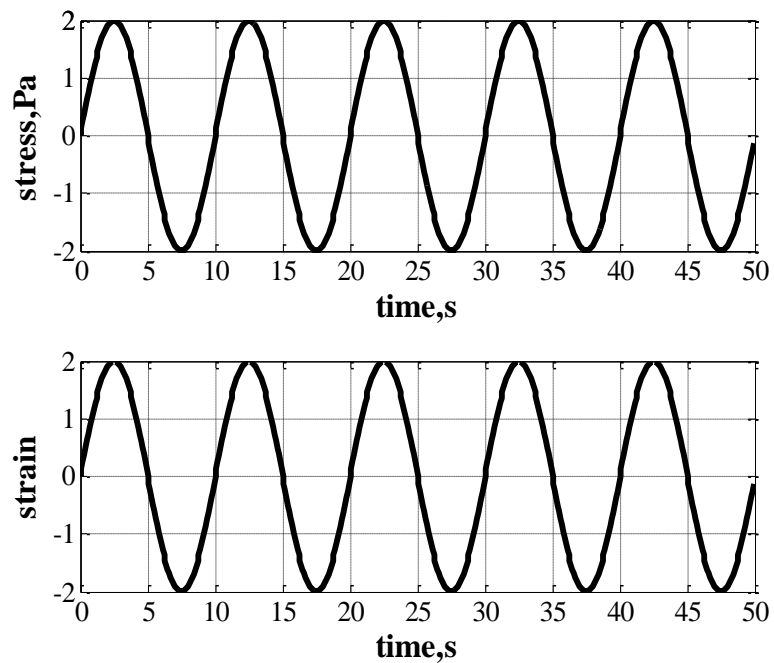


Figure.3.1.2.5. Elastic response of the Maxwell model under harmonic loading.

Input: $\sigma_0 = 2 Pa$; $T = 10s$; $E = 1Pa$; $\eta = 1000 Pa \cdot s$

The influence of the input parameters, combined into the dimensionless coefficients, described by equation 3.1.1.4, on the strain response curves under cyclic loading were analyzed. The similar combinations of the input parameters as for Kelvin model were used. This means the same cases 1-4 we considered. The results for each case are presented figures 3.1.2.6.-3.1.2.8. In case 2 there was no difference between the strain response curves, since ratios of T to λ and σ_0 to E were kept constant. Therefore case 2 is not presented.

From figures 3.1.2.6-3.1.2.8 the following conclusion can be drawn. The maximal value of the strain in the tests is equal to $(1/E + \Delta t/\lambda) \cdot \sigma_0 \cdot (2/\pi)$, where Δt is duration of the test and $2/\pi$ is a mean value of $|\sin(\omega t)|$. From case 3 it is clear that when ratio σ_0/E is constant the value of strain depends on λ . Greater the value of λ , less is strain ε . In case 4 the value strain depends on the ratio σ_0/E .

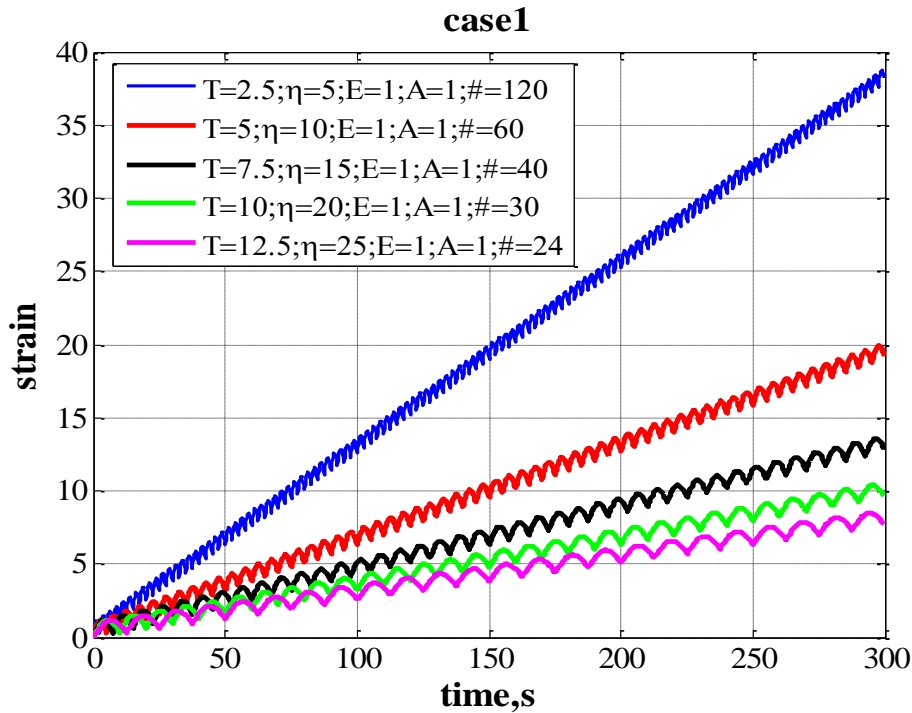


Figure 3.1.2.6. Strain responses of Maxwell model in case 1. In the legend: T is duration of one cycle [s], η is viscosity [Pa·s], E is modulus of elasticity, $A = \sigma_0$ is an amplitude of cyclic stress [Pa], $\#$ is number of cycles.

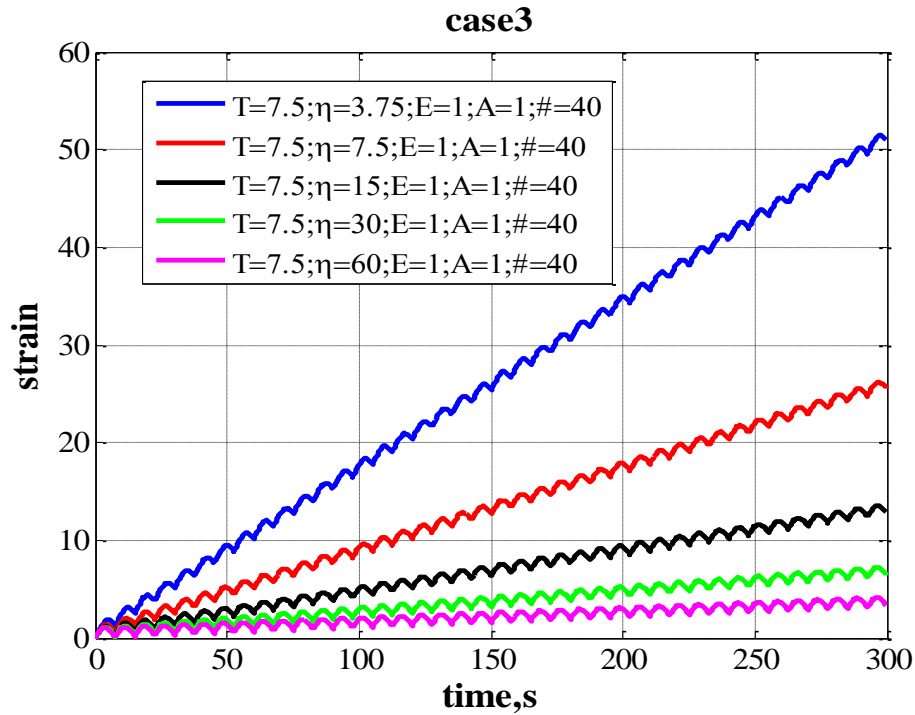


Figure 3.1.2.7. Strain responses of Maxwell model in case 3. In the legend: T is duration of one cycle [s], η is viscosity [Pa·s], E is modulus of elasticity, $A = \sigma_0$ is an amplitude of cyclic stress [Pa], $\#$ is number of cycles.

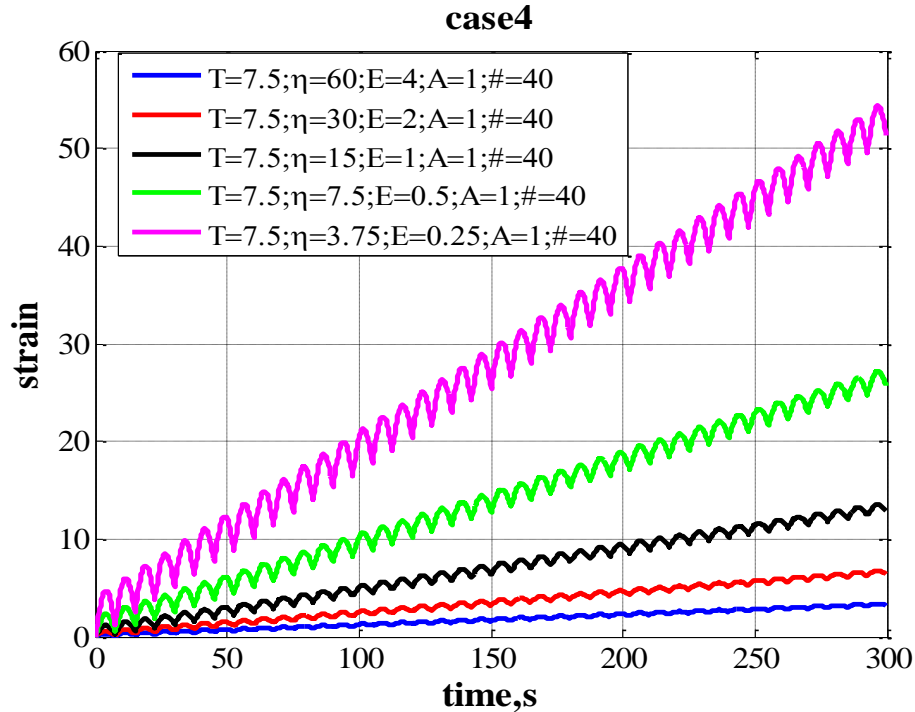


Figure 3.1.2.8. Strain responses of Maxwell model in case 4. In the legend: T is duration of one cycle [s], η is viscosity [Pa·s], E is modulus of elasticity, $A = \sigma_0$ is an amplitude of cyclic stress [Pa], $\#$ is number of cycles.

3.1.3. Analysis of Burgers model

Burgers model and its creep and relaxation function are shown in figure 2.1.2.5.

The case when the model is subjected to a constant stress is considered in this part. The model is supposed to be subjected to a step constant stress σ_0 during the time interval $[t_0, t_1]$. The creep function of the model is described by equation 2.1.2.14. The input parameters that may influence the behavior of the model are viscosity of Maxwell unit η_1 , modulus of elasticity of Maxwell unit E_1 , viscosity of Kelvin unit η_2 , modulus of elasticity of Kelvin unit E_2 , applied stress σ_0 and time $\Delta t = t_1 - t_0$, where t_0 is time when constant stress is applied and t_1 is time when stress is removed. The output is strain ε . An example of creep test is shown in figure 3.1.3.1.

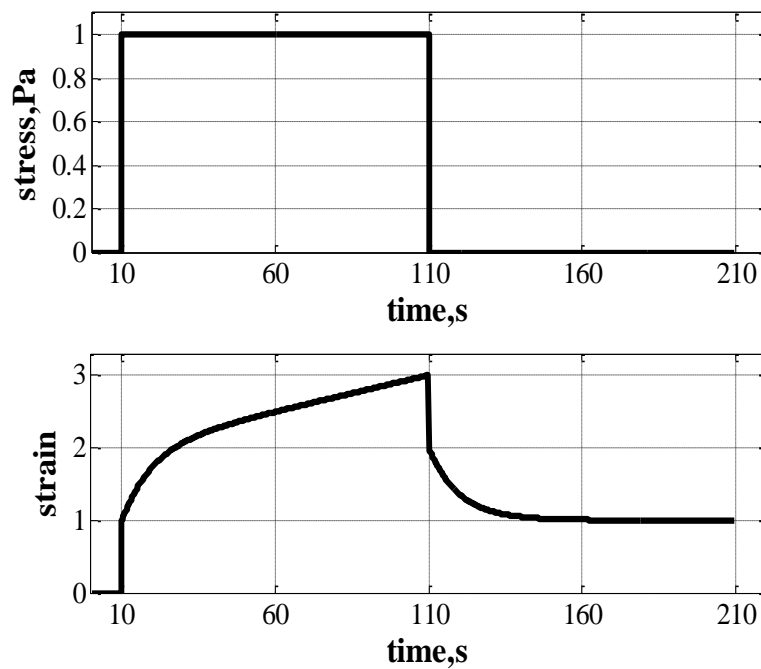


Figure 3.1.3.1. Burgers model. Creep test. Input parameters:

$$\sigma_0 = 1 \text{ Pa}; \quad \Delta t = 100 \text{ s}; \quad E_1 = 1 \text{ Pa}; \quad \eta_1 = 100 \text{ Pa} \cdot \text{s}; \quad E_2 = 1 \text{ Pa}; \quad \eta_2 = 10 \text{ Pa} \cdot \text{s}.$$

By analyzing the strain response of Burgers model in creep test the following conclusions can be drawn:

- At time t_0 model exhibits an instantaneous strain equal to σ_0 / E_1 , that vanishes once the loading is removed.

- The ratio of $(t_1 - t_0) / \eta_1$ determines the value of irreversible deformation.
- The value of $\left(\frac{1}{E_1} + \frac{1}{E_2} + \frac{t_1 - t_0}{\eta_1} \right)$ multiplied on σ_0 determines the limit that strain is trying to reach during the creep test.
- The curvature of the strain response is determined from the condition for Kelvin unit. Condition $(\Delta\tau / \lambda_2) = 5$ determines the time $\Delta\tau$ when strain contribution of Kelvin unit reaches it's maximal value equal to σ_0 / E_2 and stay constant until the load is removed. After the time $\Delta\tau$ the strain of the Burgers model is equal to $\left(\frac{1}{E_1} + \frac{1}{E_2} + \frac{t_1 - t_0}{\eta_1} \right) \cdot \sigma_0$
- In order to stay in the framework of Burgers model the contribution of both Kelvin and Maxwell unit should be significant. This gives the following limits for the input parameters:

$$\begin{aligned}
 0.01 < \frac{E_2}{E_1} < 100; \\
 0.01 < \frac{\Delta t \cdot E_2}{\eta_1} < 100.
 \end{aligned}
 \tag{3.1.3.1.}$$

The conditions for elastic response of Kelvin and Maxwell model were discussed before. Since the creep function of Burgers model is a sum of creep function of Maxwell and Kelvin model, both conditions one for Kelvin and one for Maxwell unit should be fulfilled in order to get an elastic response of Burgers model, unless one of the units is irrelevant. For Maxwell unit the condition is $(t_1 - t_0) / \lambda_1 \leq 0.01$. For Kelvin unit the condition is $\Delta\tau / \lambda_2 = 5$, where $\Delta\tau$ is selected relatively small time interval, after which the strain response of Kelvin unit does not change in time and can be seen as an elastic response. Elastic response of Burgers model in creep test is shown in figure 3.1.3.2. In creep test shown in the figure both Maxwell and Kelvin units are giving significant contributions, since $E_1 = E_2$. The input parameters were selected in such a way that both Maxwell and Kelvin unit act completely elastic and therefore Burgers model is transformed into two Hookeans elements combined in series. Hence the strain response is determined by $(1/E_1 + 1/E_2) \cdot \sigma_0$.

Now let us consider the case when condition for elastic behavior is fulfilled only for Maxwell unit and the contribution of the Kelvin unit is significant. In this case the model will respond as series of Hookean unit and Kelvin unit.(Figure 3.1.3.3.) And vice versa if condition for elastic behavior is fulfilled for Kelvin unit only and the contribution of Maxwell unit is significant the model will respond as series of Hookean unit and Maxwell unit.(Figure 3.1.3.4.)

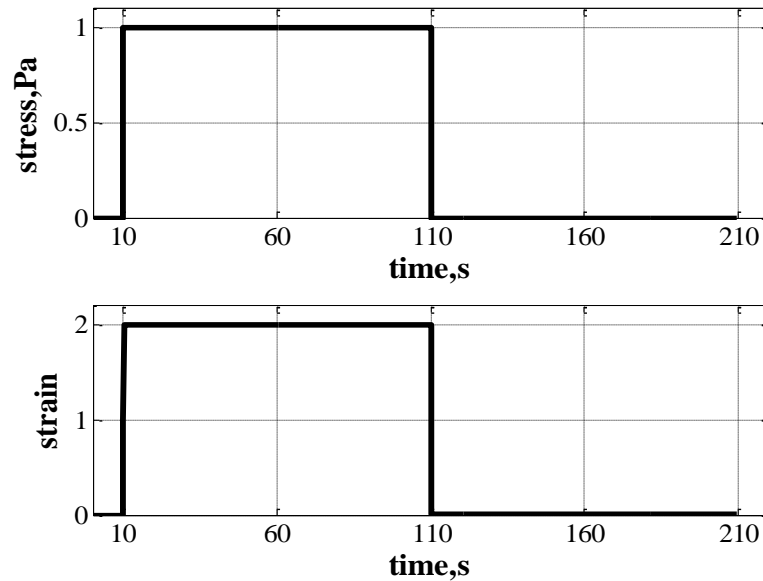


Figure 3.1.3.2. Elastic response of Burgers model. Input parameters:

$$\sigma_0 = 1 \text{ Pa}; \quad \Delta t = 100 \text{ s}; \quad E_1 = 1 \text{ Pa}; \quad \eta_1 = 10000 \text{ Pa} \cdot \text{s}; \quad E_2 = 1 \text{ Pa}; \quad \eta_2 = 0.002 \text{ Pa} \cdot \text{s}.$$

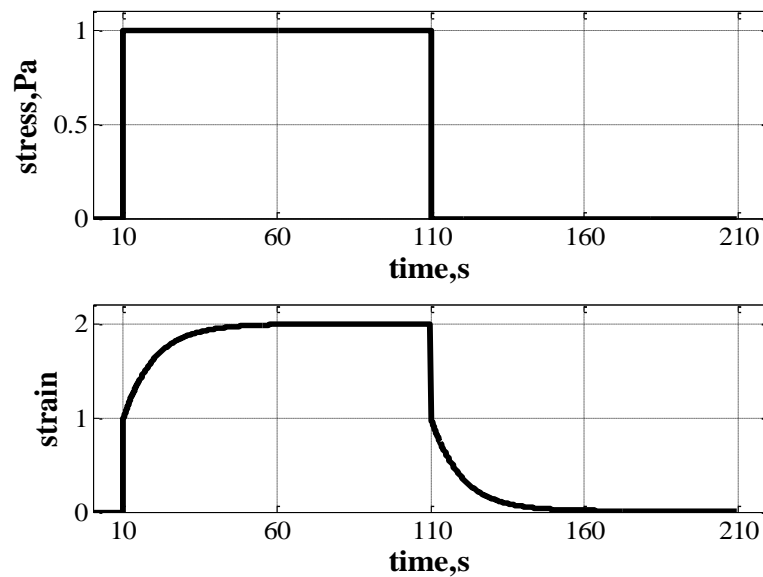


Figure 3.1.3.3. Burgers model. Creep test. Input parameters:

$$\sigma_0 = 1 \text{ Pa}; \quad \Delta t = 100 \text{ s}; \quad E_1 = 1 \text{ Pa}; \quad \eta_1 = 10000 \text{ Pa} \cdot \text{s}; \quad E_2 = 1 \text{ Pa}; \quad \eta_2 = 10 \text{ Pa} \cdot \text{s}.$$

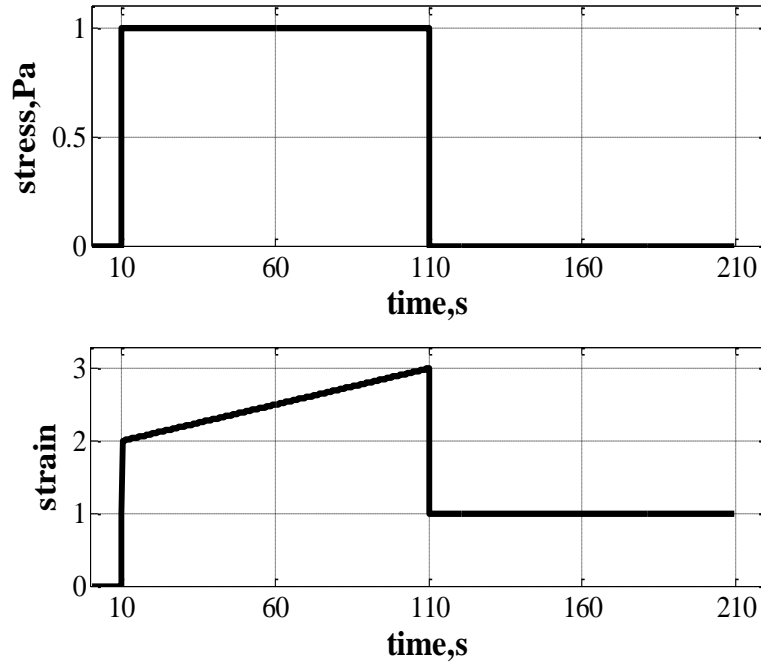


Figure 3.1.3.4. Burgers model. Creep test. Input parameters:

$$\sigma_0 = 1 \text{ Pa}; \quad \Delta t = 100 \text{ s}; \quad E_1 = 1 \text{ Pa}; \quad \eta_1 = 100 \text{ Pa} \cdot \text{s}; \quad E_2 = 1 \text{ Pa}; \quad \eta_2 = 0.002 \text{ Pa} \cdot \text{s}.$$

The conditions for viscous response of Kelvin and Maxwell model were discussed before. In order to get a viscous response of Burgers model conditions for Kelvin and Maxwell unit should be fulfilled. The condition for Kelvin model is $(t_1 - t_0) / \lambda_2 \geq 0.01$. The condition for Maxwell model is $(t_1 - t_0) / \lambda_1 \geq 100$. Viscous response of Burgers model is shown in figure 3.1.3.5.

Now let us consider the case when condition for viscous behavior is fulfilled only for Maxwell unit the model will respond as Newtonian model (Figure 3.1.3.6.) unless the contribution of Kelvin unit is extremely significant. (Figure 3.1.3.7.) This is reasonable since the strain response of Maxwell unit is not limited, whereas the strain response of Kelvin unit is limited by the value of σ_0 / E_2 . If condition for viscous behavior is fulfilled for Kelvin unit only the model will respond as Maxwell model. (Figure 3.1.3.8.).

The Behavior of Burgers model is more complicated than that of Kelvin or Maxwell. The relative contribution of Kelvin and Maxwell unit should be taken into account when

giving the conditions for elastic or viscous response of the Burgers model. Moreover, Maxwell unit has a bigger contribution to the model, since the strain response of this unit is not limited and constantly grow during the test depending with the rate dependent on the input parameters for the unit. However, it of course depend on the input parameters.

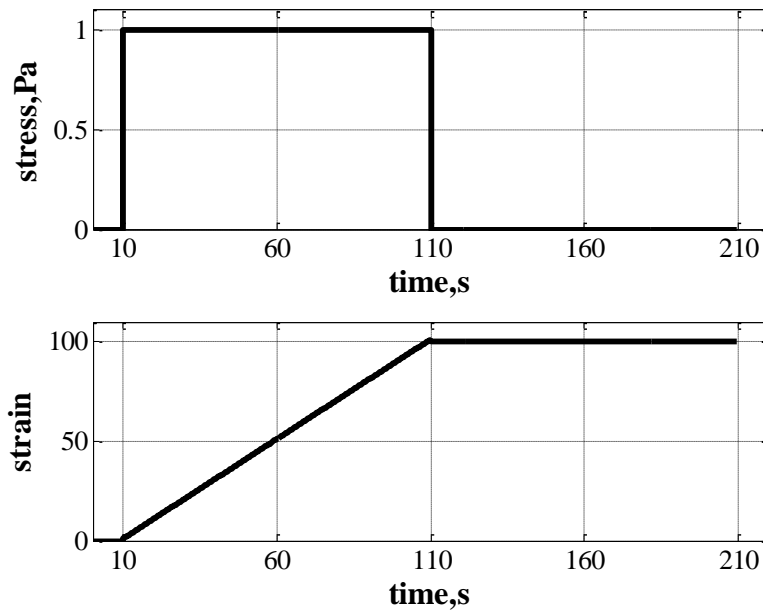


Figure 3.1.3.5. Viscous response of Burgers model. Input parameters:
 $\sigma_0 = 1 Pa$; $\Delta t = 100s$; $E_1 = 1 Pa$; $\eta_1 = 1 Pa \cdot s$; $E_2 = 1 Pa$; $\eta_2 = 10000 Pa \cdot s$.

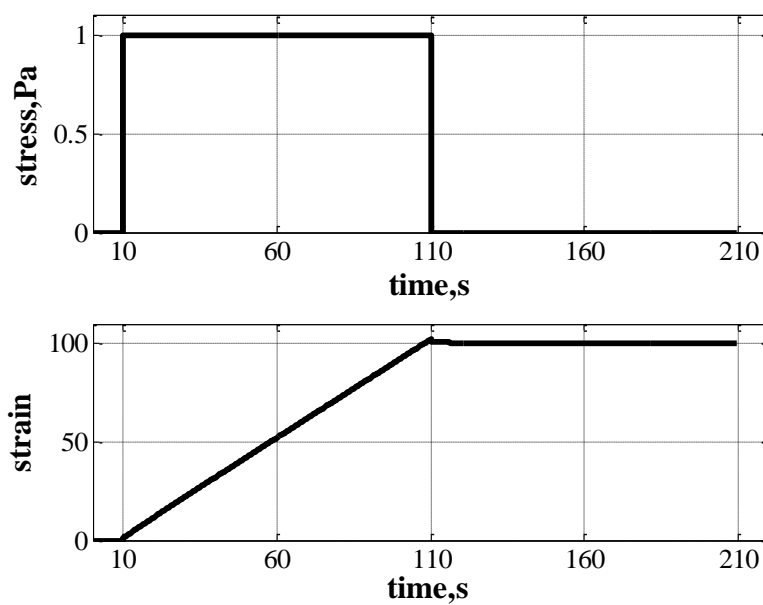


Figure 3.1.3.6. Burgers model. Creep test. Input parameters:

$$\sigma_0 = 1 \text{ Pa}; \quad \Delta t = 100 \text{ s}; \quad E_1 = 1 \text{ Pa}; \quad \eta_1 = 1 \text{ Pa} \cdot \text{s}; \quad E_2 = 1 \text{ Pa}; \quad \eta_2 = 10 \text{ Pa} \cdot \text{s}.$$

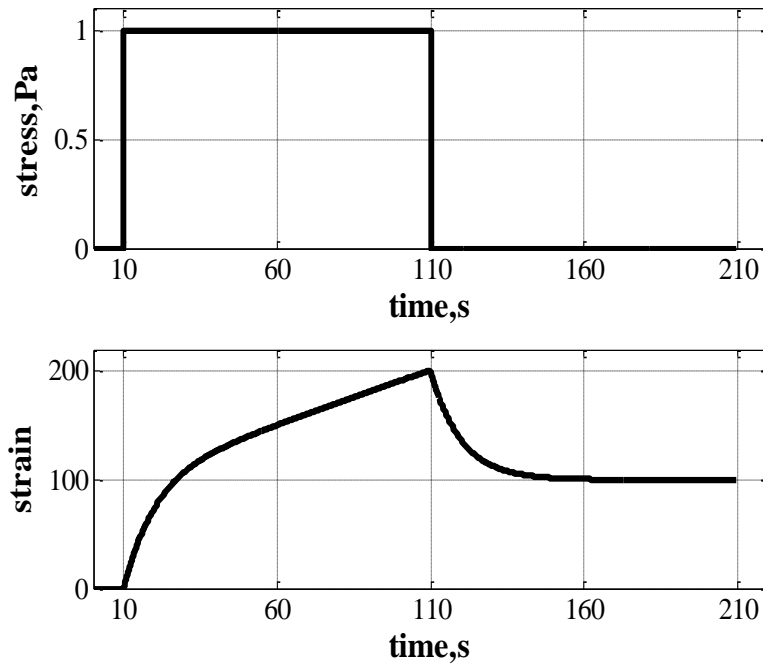


Figure 3.1.3.7. Burgers model. Creep test. Input parameters:

$$\sigma_0 = 1 \text{ Pa}; \quad \Delta t = 100 \text{ s}; \quad E_1 = 1 \text{ Pa}; \quad \eta_1 = 1 \text{ Pa} \cdot \text{s}; \quad E_2 = 0.01 \text{ Pa}; \quad \eta_2 = 0.1 \text{ Pa} \cdot \text{s}.$$

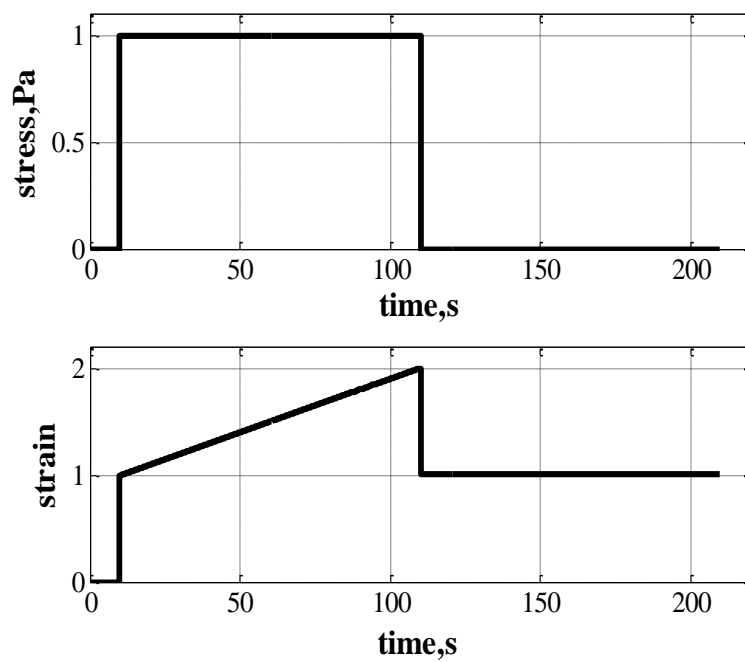


Figure 3.1.3.8. Burgers model. Creep test. Input parameters:

$$\sigma_0 = 1 \text{ Pa}; \quad \Delta t = 100 \text{ s}; \quad E_1 = 1 \text{ Pa}; \quad \eta_1 = 100 \text{ Pa} \cdot \text{s}; \quad E_2 = 1 \text{ Pa}; \quad \eta_2 = 10000 \text{ Pa} \cdot \text{s}.$$

Burgers model consists of the Kelvin and Maxwell unit combined in series. Therefore, in order to get predominantly viscous or elastic response of Burgers model under cyclic loading conditions for predominantly viscous or elastic response for Kelvin and Maxwell unit should be fulfilled. These conditions were discussed before. Also the contribution of one unit compare to another should be taken into account. In order to get a predominantly viscous response of Burgers model the input parameters should fulfill the following conditions: $T / \lambda_1 \geq 1000$ and $T / \lambda_2 \leq 0.001$, where T is a period of harmonic loading or double duration of one cycle in case of cyclic loading, $\lambda_1 = \eta_1 / E_1$ is the parameter of Maxwell unit and $\lambda_2 = \eta_2 / E_2$ is a parameter of Kelvin unit. If $T / \lambda_1 \leq 0.001$ and $T / \lambda_2 \geq 1000$, the response of Burgers model is predominantly elastic.

The influence of the input parameters, combined into the dimensionless coefficients, described by equation 3.1.1.4, on the strain response curves under cyclic loading were analyzed. The similar combinations of the input parameters as for Kelvin and Maxwell model were considered. The difference in the analysis of Burgers model is that there is two pairs of the dimensionless coefficients described by equation 3.1.1.4., one for Kelvin and one for Maxwell unit.

It was decided to change the input parameters for Kelvin unit first and kept the ratio λ_1 for Maxwell unit constant. Secondly, the input parameters for Maxwell unit were being changed while the ratio λ_2 for Kelvin unit was kept constant. The Young's modulus of Kelvin unit was equal to Young's modulus of Maxwell unit for all the cases examined. In total 8 cases were considered. Input parameter were changed 5 times within each case. It was decided to stick to the previous abbreviator. Therefore the cases corresponding to change of the input parameters in Maxwell unit carry index "a". The results are presented in figures 3.1.3.9. to 3.1.3.12. Case 1, case 1a, case 2 and case 2a are excluded. In case 2 and case 2a the strain response is equal for all five combinations of the input parameters considered. In the legend of figures 3.1.3.9. to 3.1.3.12. T is duration of one cycle [s], η_1 is viscosity of Maxwell unit [Pa·s], E_1 is modulus of elasticity of Maxwell unit, η_2 is viscosity of Kelvin unit

[Pa·s], E_2 is modulus of elasticity of Kelvin unit, $A = \sigma_0$ is an amplitude of cyclic stress [Pa], # is number of cycles.

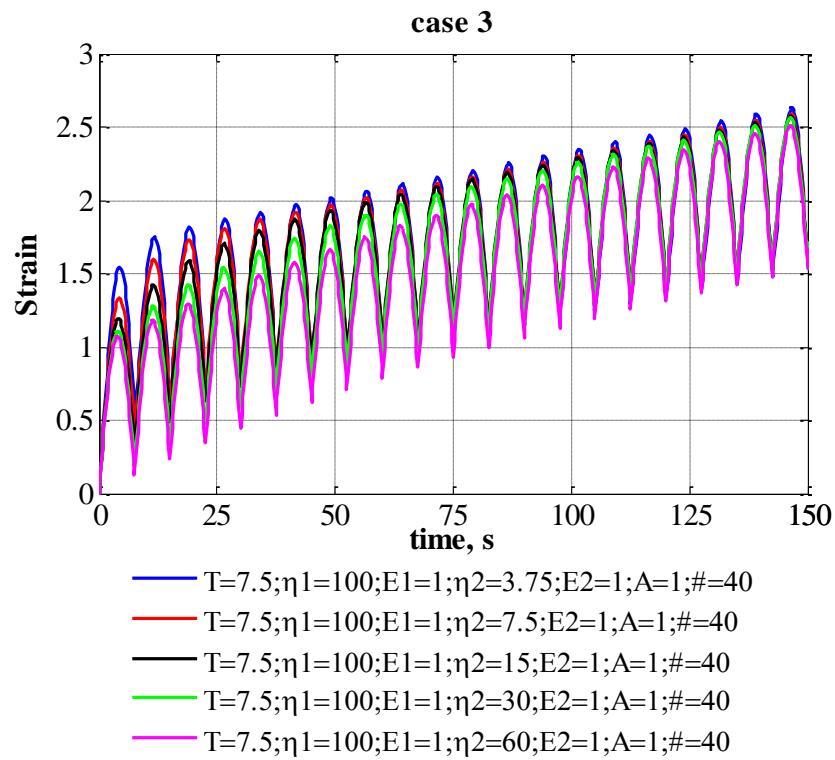


Figure 3.1.3.9. Strain responses of Burgers model in case 3 for first 20 cycles.

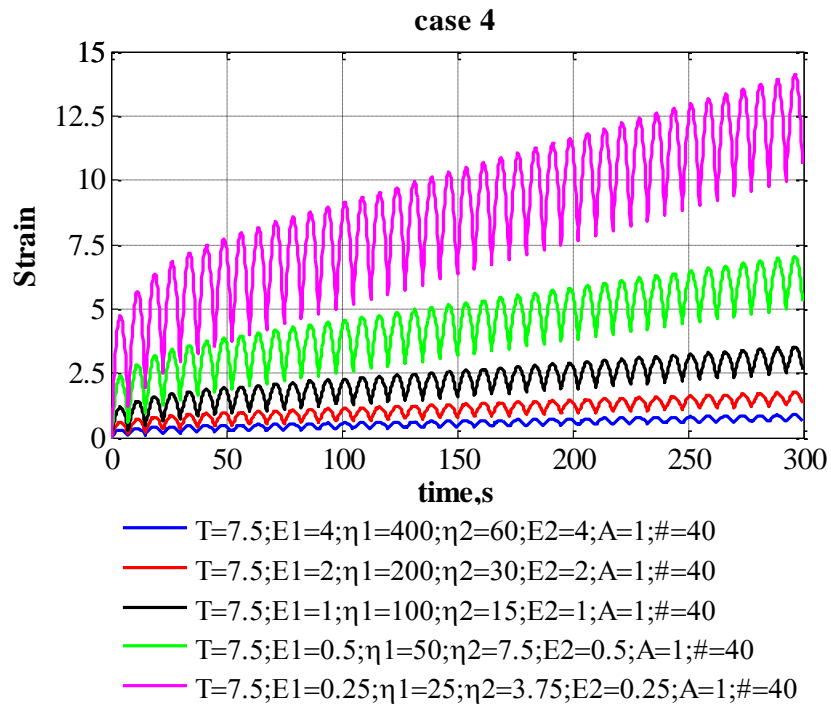


Figure 3.1.3.10. Strain responses of Burgers model in case 4.

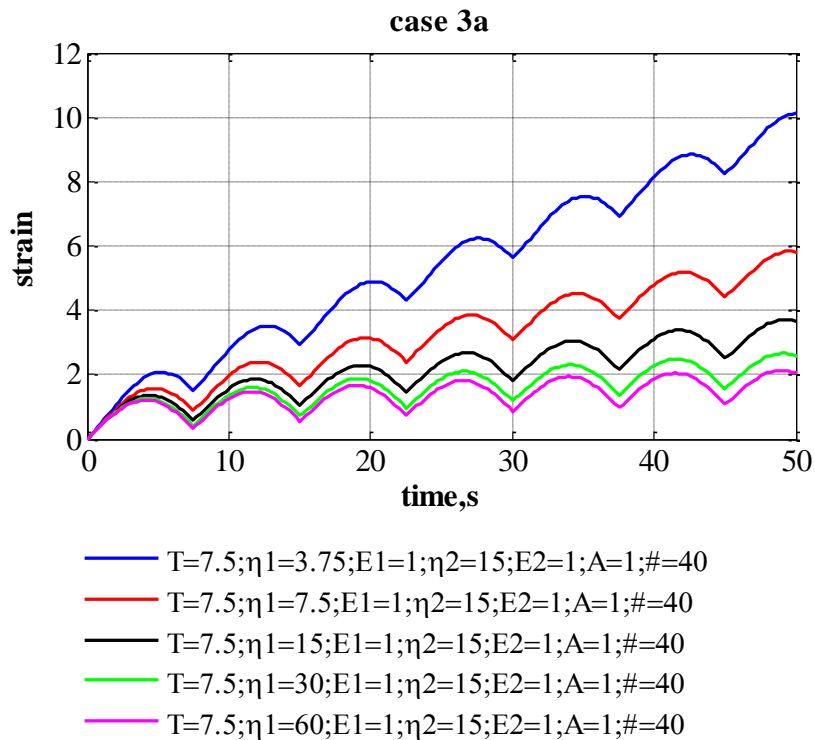


Figure 3.1.3.11. Strain responses of Burgers model in case 3a during first 50 seconds.

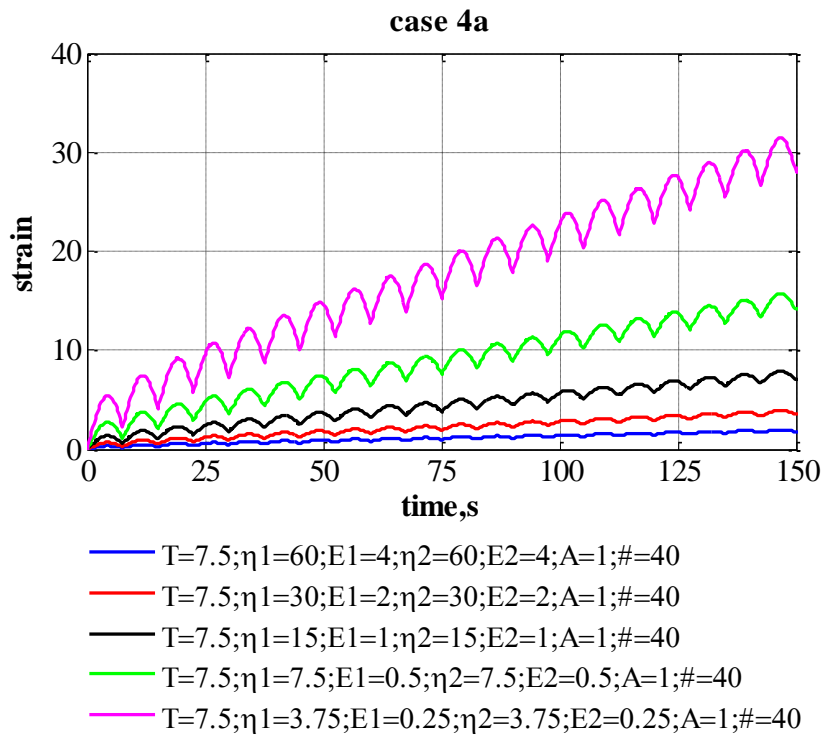


Figure 3.1.3.12. Strain responses of Burgers model in case 4a during first 20 cycles.

From figures 3.1.3.9.-3.1.3.12. it follows that Maxwell unit is strongly influence on the shape of the strain response curves of Burgers model. This is due to the fact that the damper in Maxwell unit can experience unlimited deformations and it's response is simply governed by ration T / λ_1 , where T is duration of a cycle [s]. With a decrease in ratio λ_2 / λ_1 the response of the Burgers model becomes more similar to the response of Kelvin unit and a spring combined in series (figure 3.1.3.10 and figure 3.1.3.11). The delayed-elastic deformations are fully-developed after the time equal to $5\lambda_2$. This is a property of Kelvin model, that was already explained earlier

3.2. Sensitivity analysis of the secant system's modulus.

Numerical results obtained during the sensitivity analysis are used in this part in order to analyze the change in secant system's modulus of elasticity during the cyclic loading creep tests.

3.2.1. Kelvin model

The stress-strain curves for case 2 to 4 are shown in the figures 3.2.1.1.a-3.2.1.3.a. The secant system's modulus of elasticity was estimated for each cycle for all of the

cases considered in the previous section. The method of estimation of this modulus is explained in section 2.5. The results are presented in figures 3.2.1.1.b-3.2.1.3.b.. In the legend of all figures below T is duration of one cycle [s], η is viscosity of a damper [Pa·s], E is modulus of elasticity of spring, $A = \sigma_0$ is an amplitude of cyclic stress [Pa], $\#$ is number of cycles.

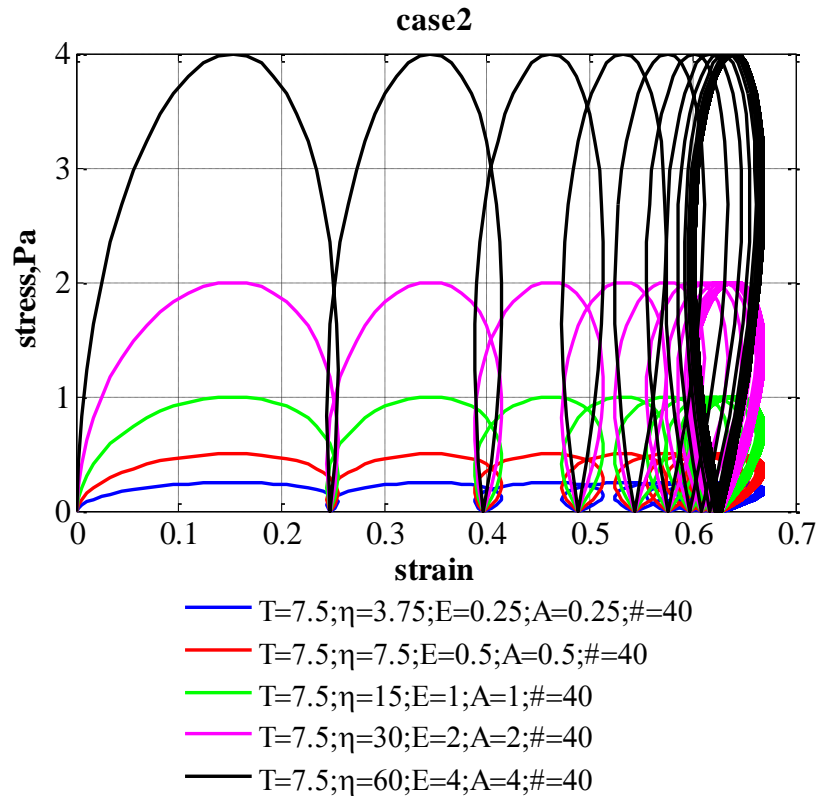


Figure 3.2.1.1.a. Kelvin model response under cyclic loading. Stress-strain curve in case 2.

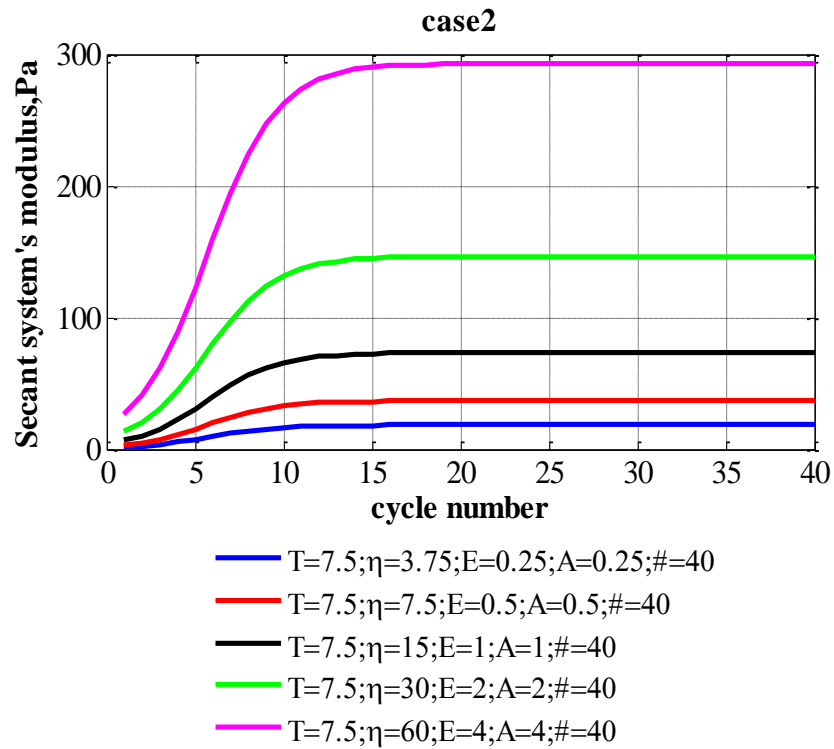


Figure 3.2.1.1.b. Secant system's modulus of elasticity estimated for each cycle in case 2 when material, represented by Kelvin model, exhibit cyclic loading.

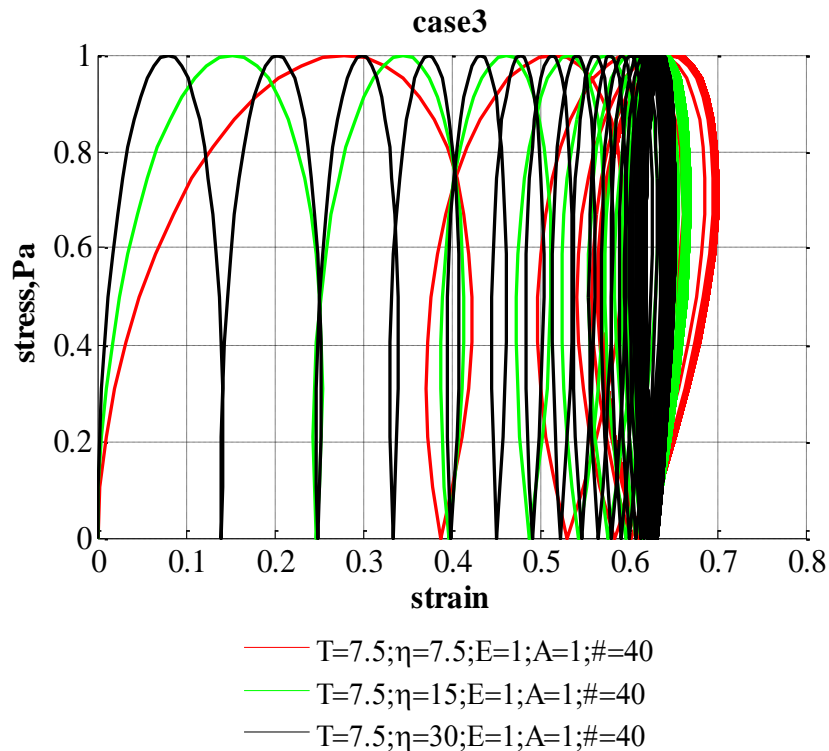


Figure 3.2.1.2.a. Kelvin model response under cyclic loading. Stress-strain curve in case 3.

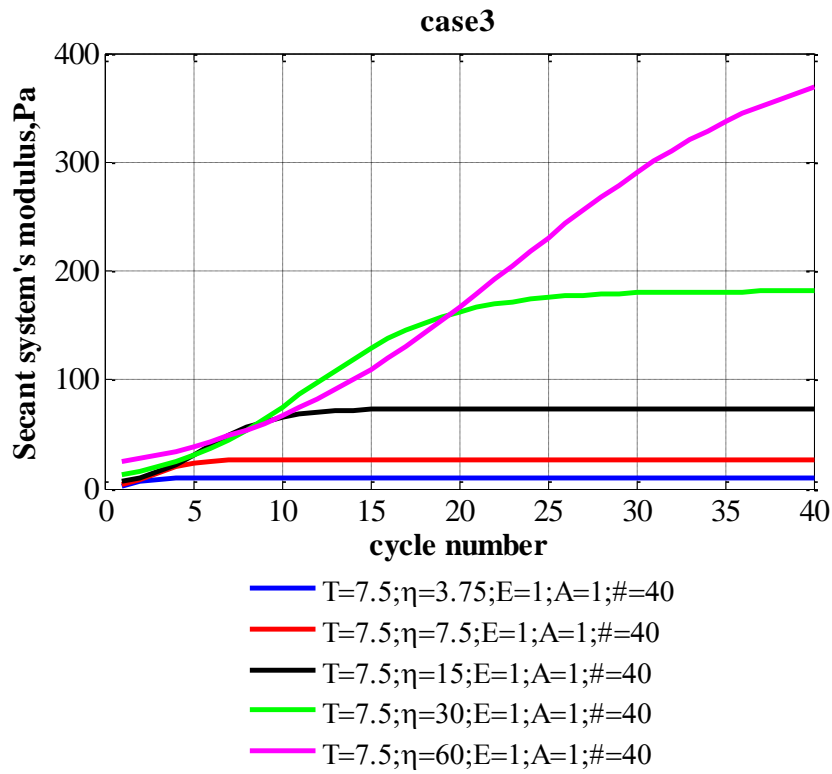


Figure 3.2.1.2.b. Secant system's modulus of elasticity estimated for each cycle in case 3 when material, represented by Kelvin model, exhibit cyclic loading.

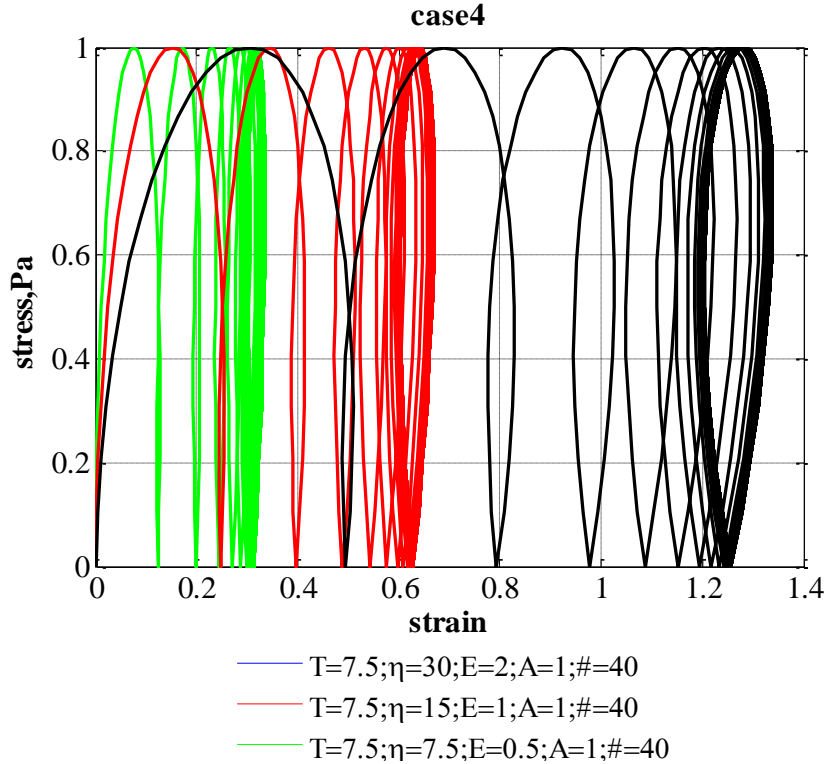


Figure 3.2.1.3.a. Kelvin model response under cyclic loading. Stress-strain curve in case 4.

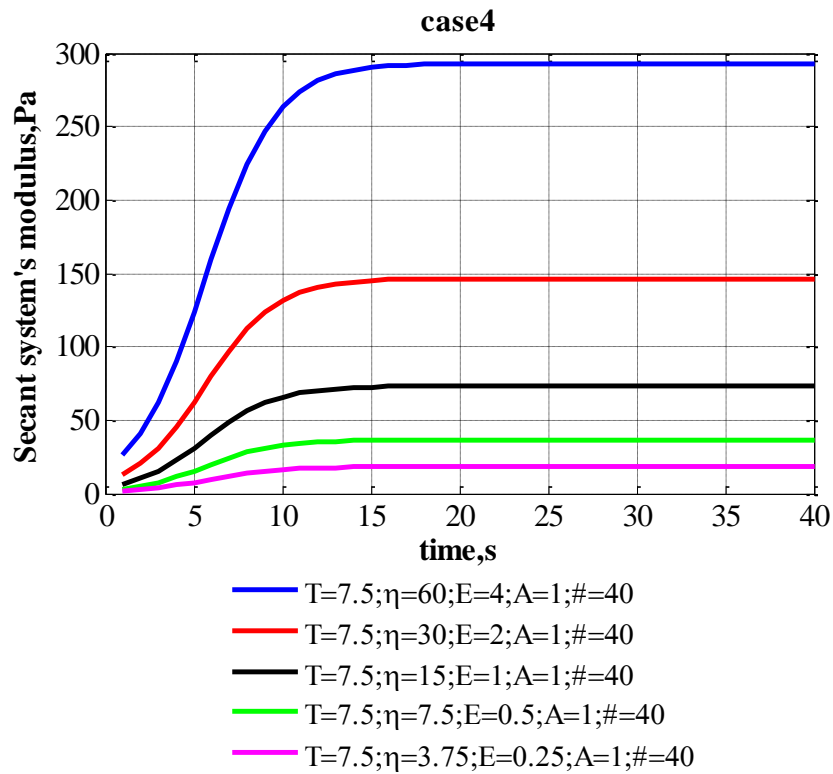


Figure 3.2.1.3.b. Secant system's modulus of elasticity estimated for each cycle in case 3 when material, represented by Kelvin model, exhibit cyclic loading.

3.2.2. Maxwell model

The stress-strain curves for cases 2 to 4 are shown in the figures 3.2.2.1.a-3.2.2.3.a. The secant system's modulus of elasticity was estimated for each cycle for all of the cases considered in the previous section. The method of estimation of this modulus is explained in section 2.5. The results are presented in figures 3.2.2.1.b-3.2.2.3.b.. In the legend of all figures below T is duration of one cycle [s], η is viscosity of a damper [Pa·s], E is modulus of elasticity of spring, $A = \sigma_0$ is an amplitude of cyclic stress [Pa], $\#$ is number of cycles.

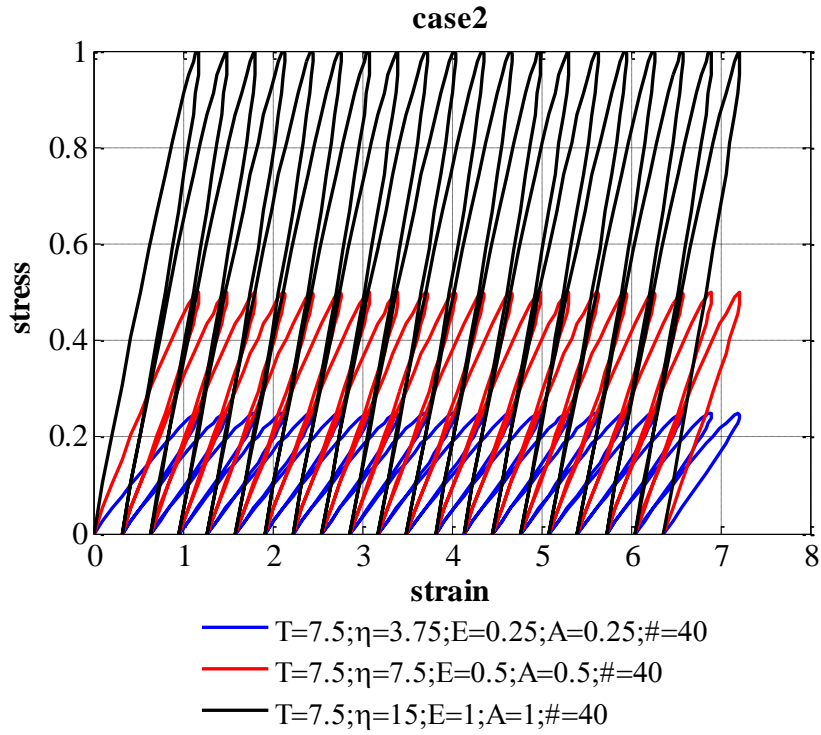


Figure 3.2.2.1.a. Maxwell model response under cyclic loading. Stress-strain curve in case 2 for first 20 cycles.

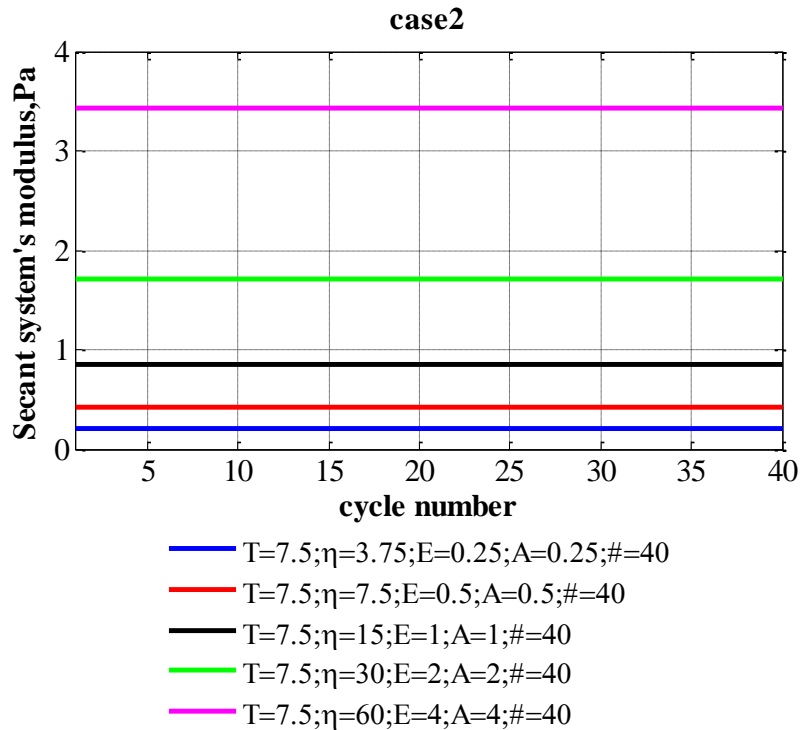


Figure 3.2.2.1.b. Secant system's modulus of elasticity estimated for each cycle in case 2 when material, represented by Maxwell model, exhibit cyclic loading.

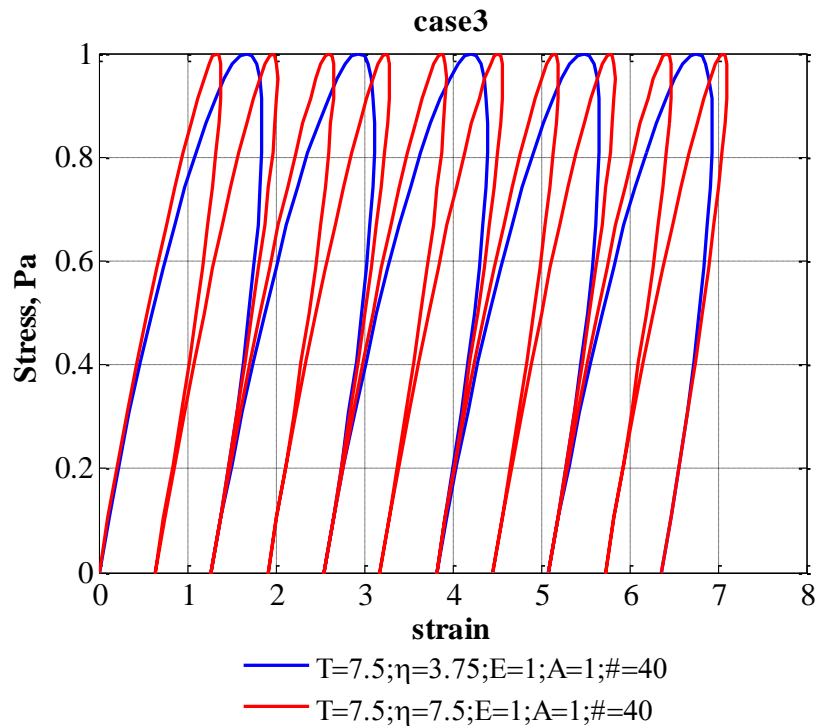


Figure 3.2.2.2.a. Maxwell model response under cyclic loading. Stress-strain curve in case 3 for first 5 cycles for navy line and first 10 cycles for red line.

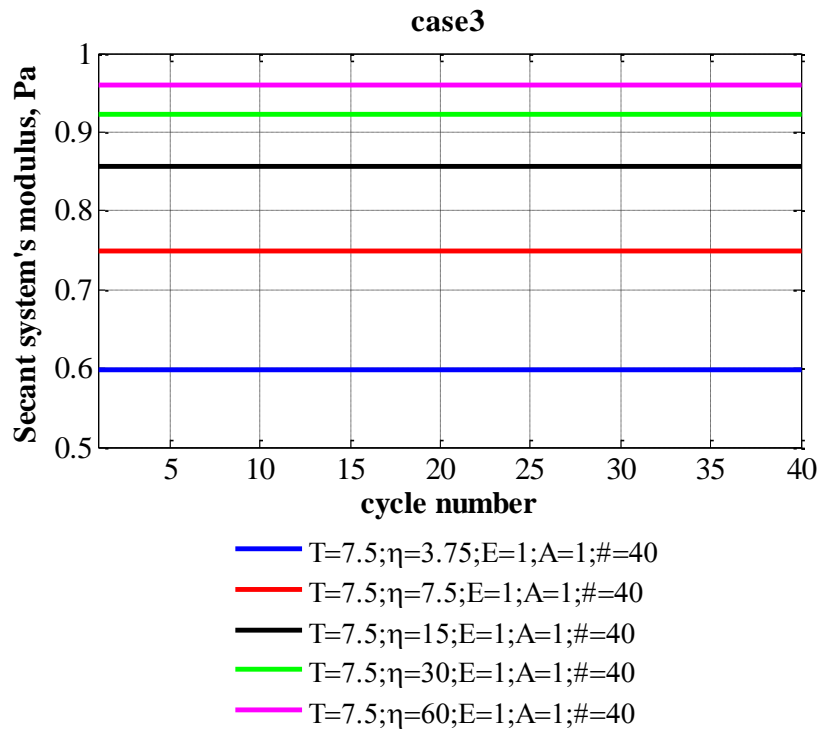


Figure 3.2.2.2.b. Secant system's modulus of elasticity estimated for each cycle in case 3 when material, represented by Maxwell model, exhibit cyclic loading.

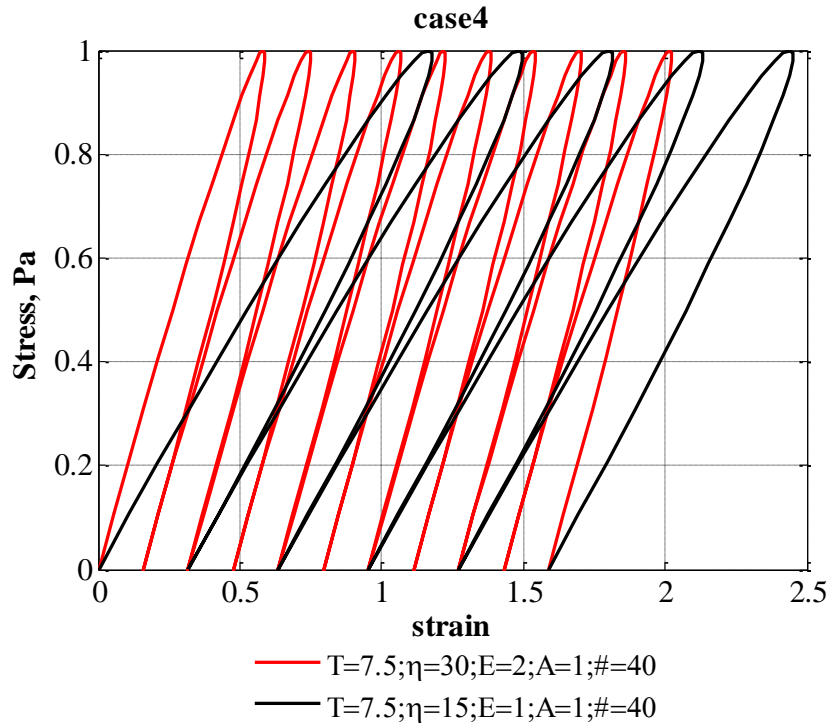


Figure 3.2.2.3.a. Maxwell model response under cyclic loading. Stress-strain curve in case 4 for first 5 cycles for black line and first 10 cycles for red line.

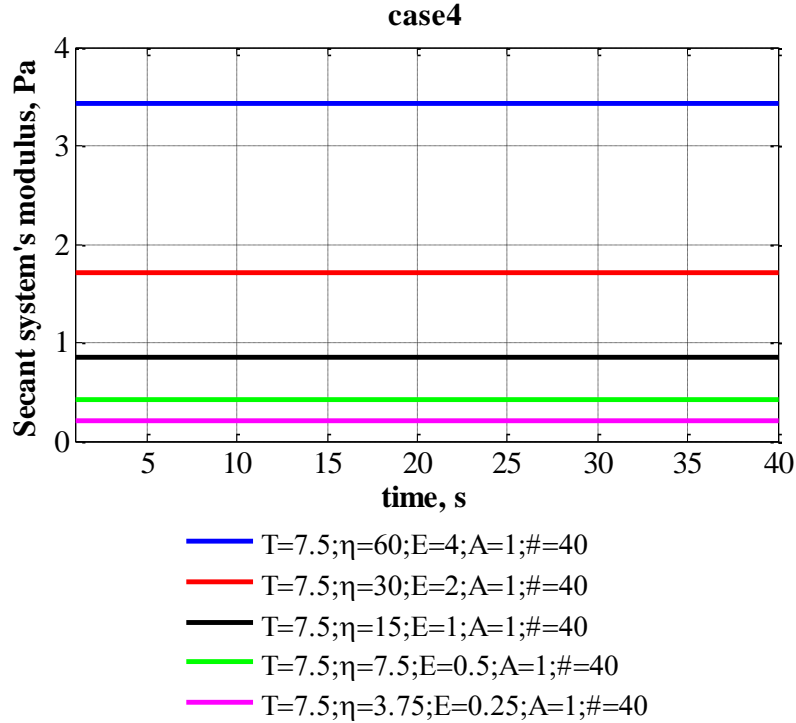


Figure 3.2.2.3.b. Secant system's modulus of elasticity estimated for each cycle in case 4 when material, represented by Maxwell model, exhibit cyclic loading.

3.2.3. Burgers model

The stress-strain curves for cases 2 to 4 are shown in figures 3.2.3.1.a-3.2.3.3.a and cases 3a and 4a are shown in the figures 3.2.3.4.a and 3.2.1.4.a. The secant system's modulus of elasticity was estimated for each cycle for all of the cases considered. The method of estimation of this modulus is explained in section 2.5. The results are presented in figures 3.2.3.1.b-3.2.3.5.b. In the legend of figures 3.1.3.9. to 3.1.3.12. T is duration of one cycle [s], η_1 is viscosity of Maxwell unit [Pa·s], E_1 is modulus of elasticity of Maxwell unit, η_2 is viscosity of Kelvin unit [Pa·s], E_2 is modulus of elasticity of Kelvin unit, $A = \sigma_0$ is an amplitude of cyclic stress [Pa], # is number of cycles.

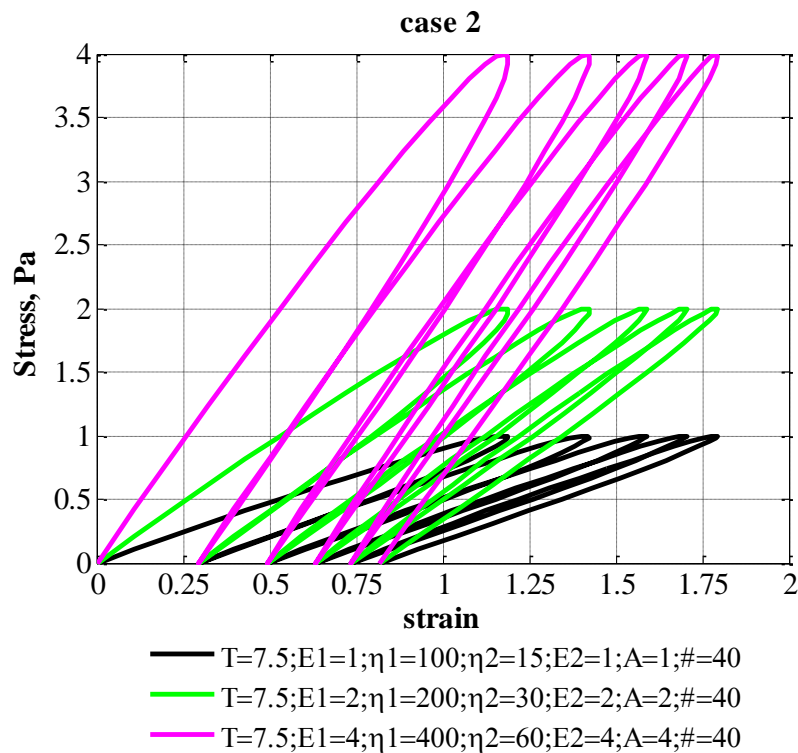


Figure 3.2.3.1.a. Burgers model response under cyclic loading. Stress-strain curve for first 5 cycles in case 2.

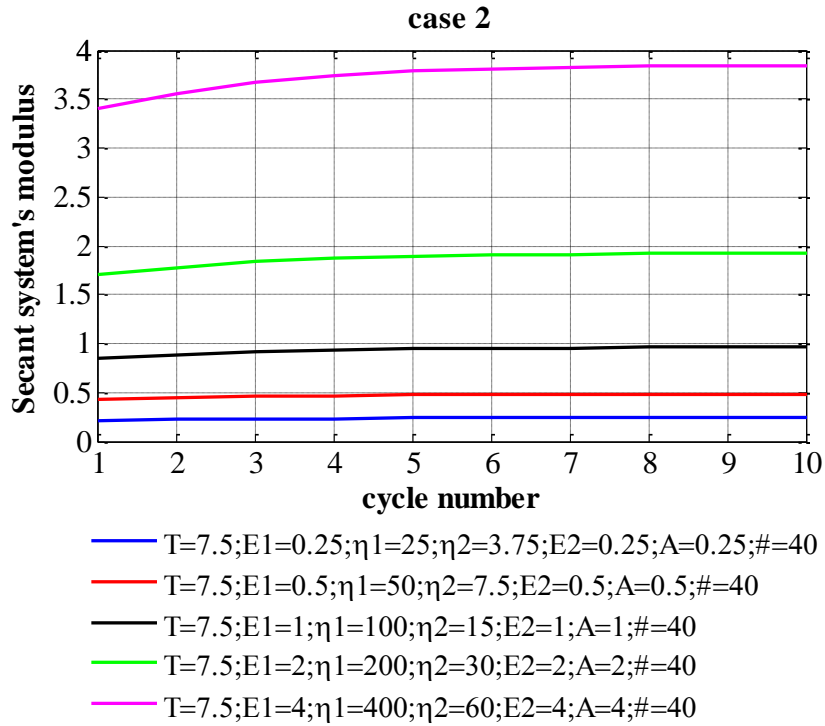


Figure 3.2.3.1.b. Secant system's modulus of elasticity estimated for each cycle in case 2 when material, represented by Burgers model, exhibit cyclic loading.

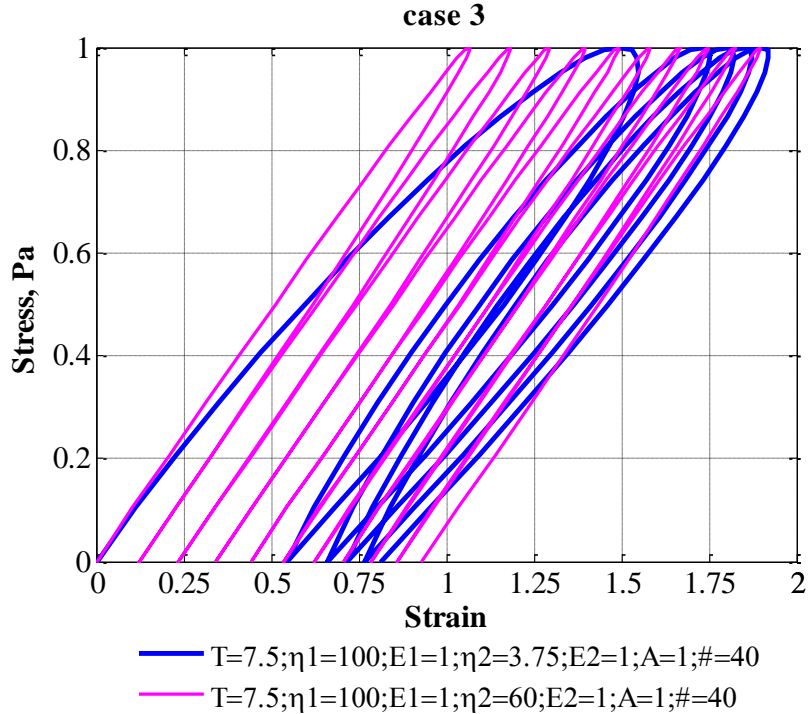


Figure 3.2.3.2.a. Burgers model response under cyclic loading. Stress-strain curve in case 3 for first 4 cycles for a navy line and first 10 cycles for a pink line.

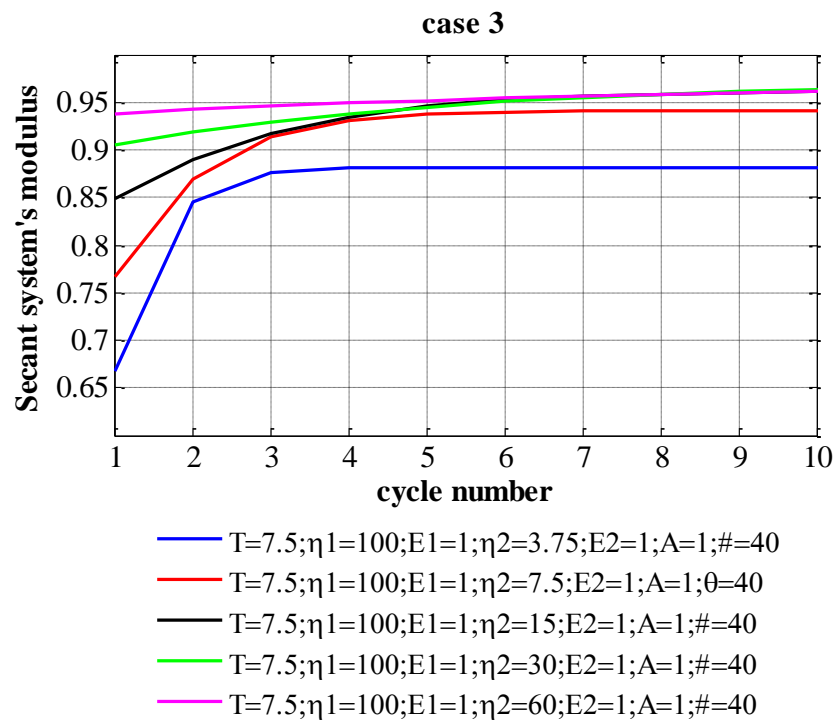


Figure 3.2.3.2.b. Secant system's modulus of elasticity estimated for each cycle in case 3 when material, represented by Burgers model, exhibit cyclic loading.

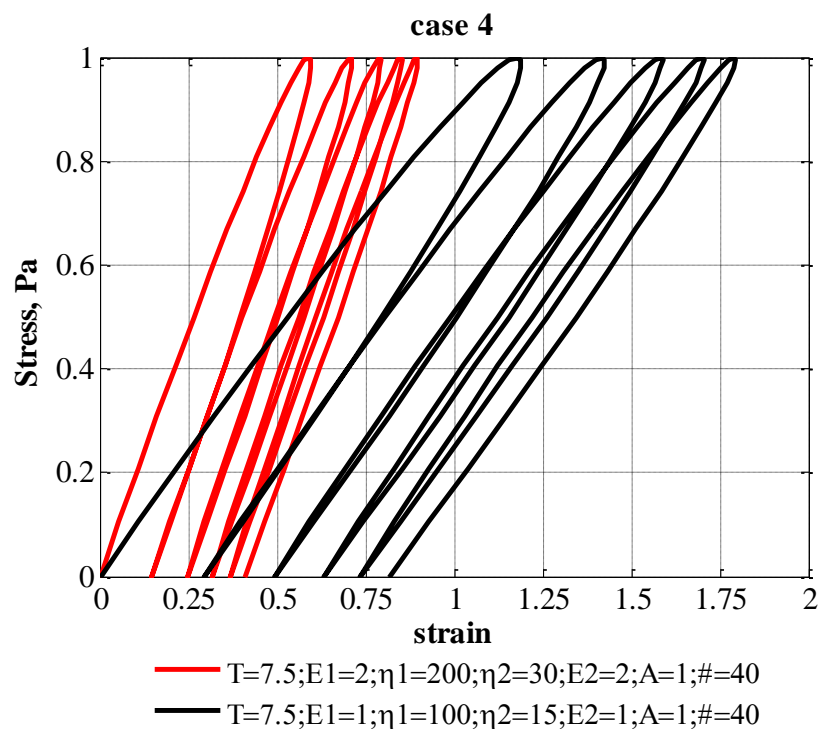


Figure 3.2.3.3.a. Burgers model response under cyclic loading. Stress-strain curve for first 4 cycles in case 4.

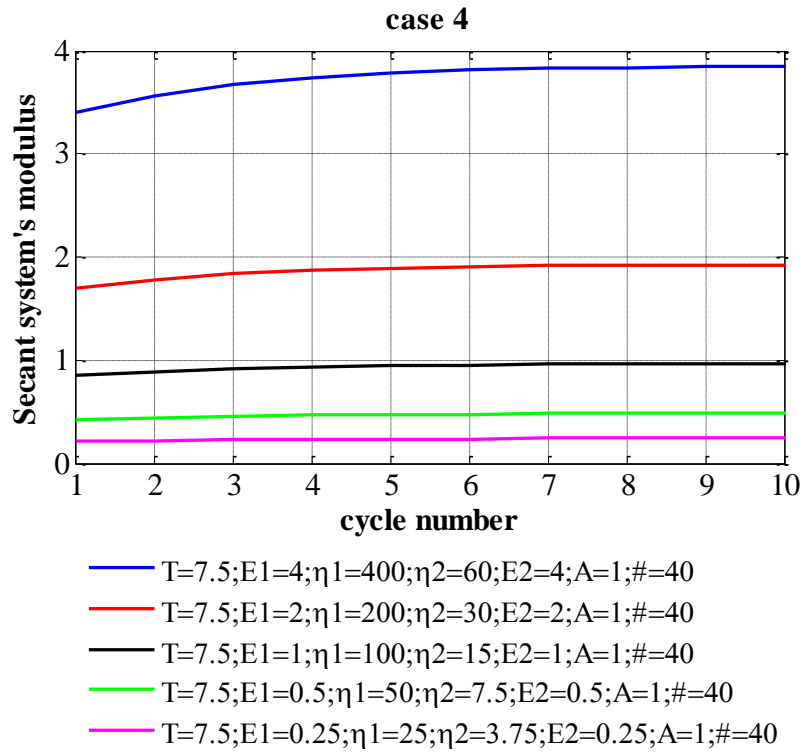


Figure 3.2.3.3.b. Secant system's modulus of elasticity estimated for each cycle in case 4 when material, represented by Burgers model, exhibit cyclic loading.

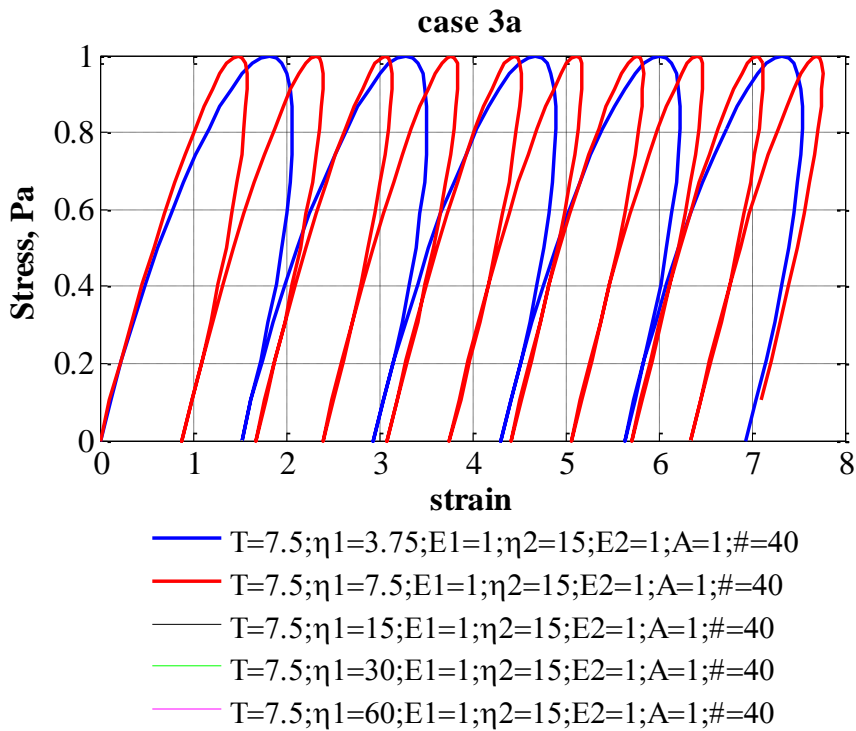


Figure 3.2.3.4.a. Burgers model response under cyclic loading. Stress-strain curve in case 3a for first 5 cycles for navy line and first 10 cycles for red line.

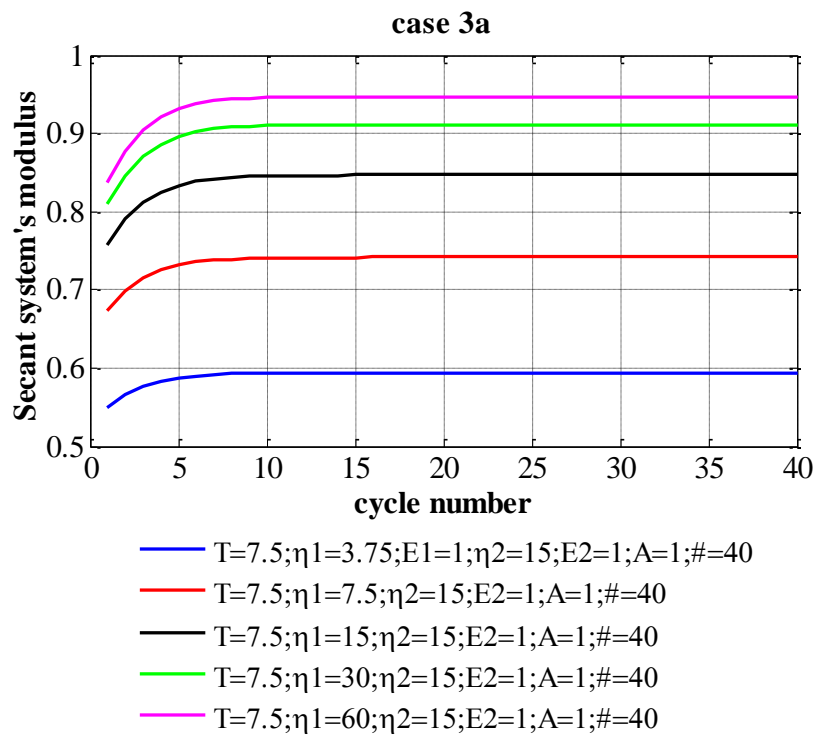


Figure 3.2.3.4.b. Secant system's modulus of elasticity estimated for each cycle in case 3a when material, represented by Burgers model, exhibit cyclic loading.

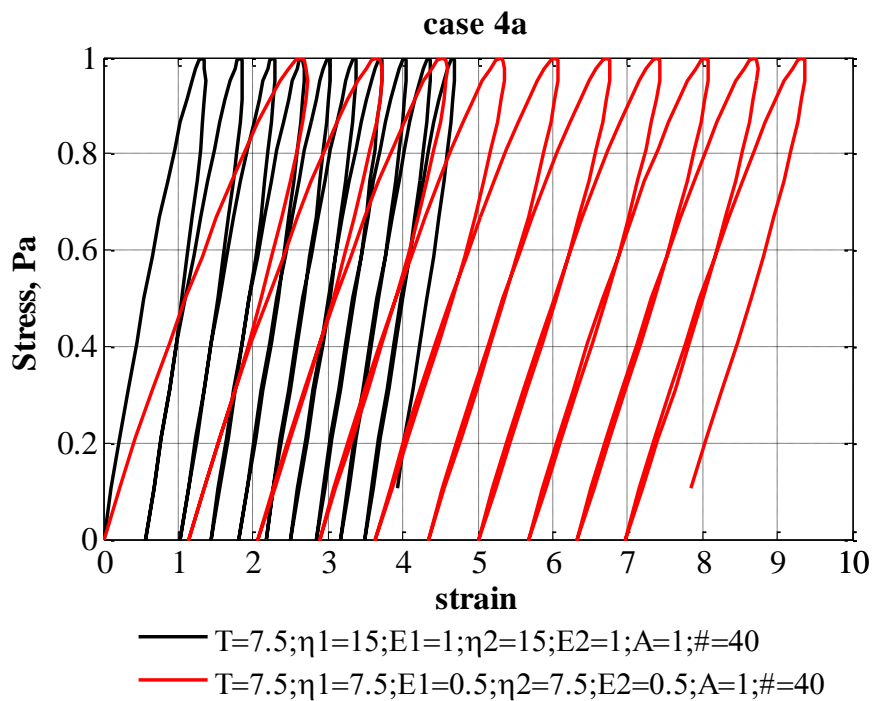


Figure 3.2.3.5.a. Burgers model response under cyclic loading. Stress-strain curve in for first 10 cycles in case 4a.

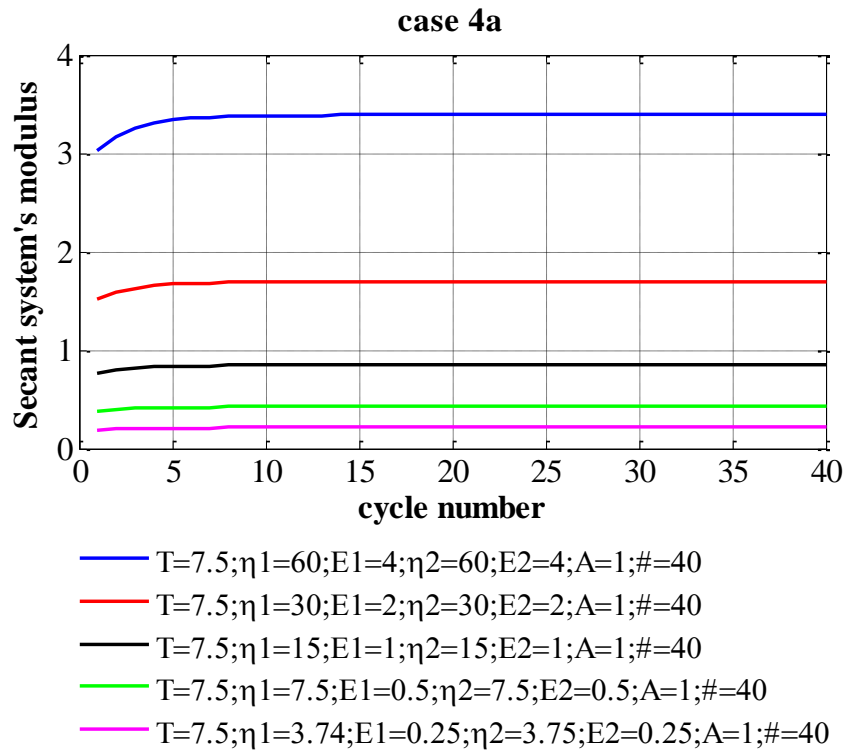


Figure 3.2.3.5.b. Secant system's modulus of elasticity estimated for each cycle in case 4a when material, represented by Burgers model, exhibit cyclic loading.

3.3. Calibration of the model.

Sinha (1978) performed uniaxial compressive creep test of ice made in a cold room at -10°C from deaerated water. The specimens had a rectangular form with the following dimensions: $5 \times 10 \times 25 \text{ cm}^3$. The long direction of the grains was perpendicular to the $10 \times 25 \text{ cm}^2$ face. In this paper he also presented a non-linear viscoelastic model to describe the strain response observed during the experiment

The Sinha's non-linear model was implemented into Matlab using The Boltzman principle of superposition and equation (2.5.2.) in order to get the creep curves instead of picking the values manually from the graphs presented in his paper. The Matlab code can be seen in the appendix C. Two creep tests were selected when ice temperature was -19.8°C and -10°C . The strain response curve of linear viscoelastic model was fitted onto Sinha's strain response curves from creep tests by varying the input parameters for creep function of the Burgers model (figure 3.3.1 and figure 3.3.2.). By this, input parameters for linear viscoelastic model were obtained. This process also served to compare linear viscoelastic model with a non-linear one. The following input parameters for linear viscoelastic model were obtained.

For ice at -10°C : $E_1 = E_2 = 9.3 \text{ GPa}$; $\eta_1 = 4570 \text{ GPa}\cdot\text{s}$; $\eta_2 = 1116 \text{ GPa}\cdot\text{s}$

For ice at -19.8°C : $E_1 = E_2 = 9.3 \text{ GPa}$; $\eta_1 = 100000 \text{ GPa}\cdot\text{s}$; $\eta_2 = 2325 \text{ GPa}\cdot\text{s}$

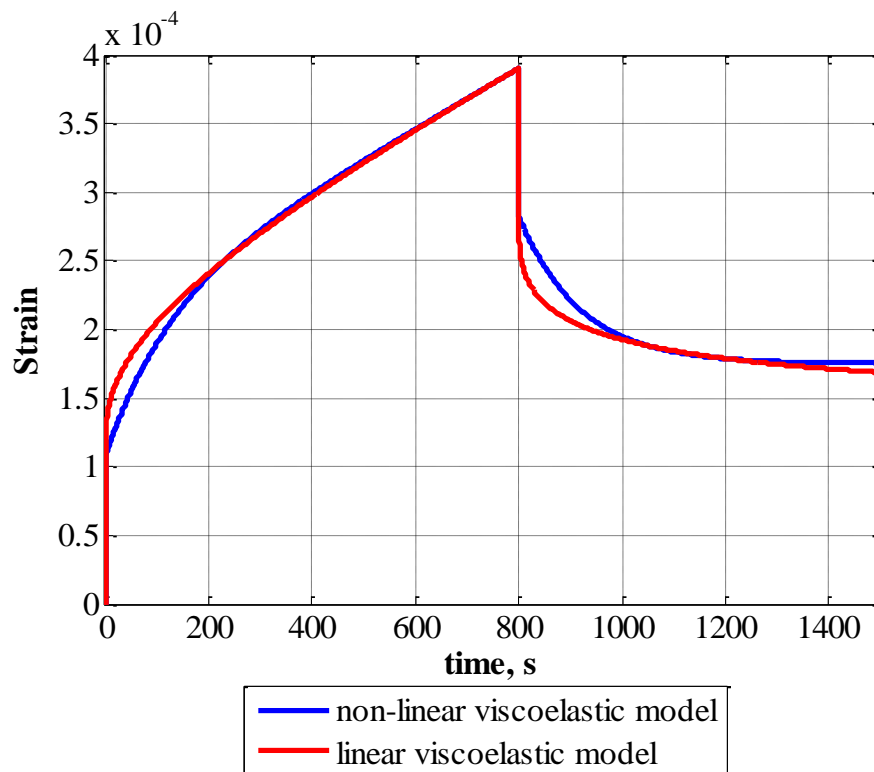


Figure 3.3.1. Creep and recovery of ice at -10°C . Constant stress of 1 MPa was applied during first 800 seconds.

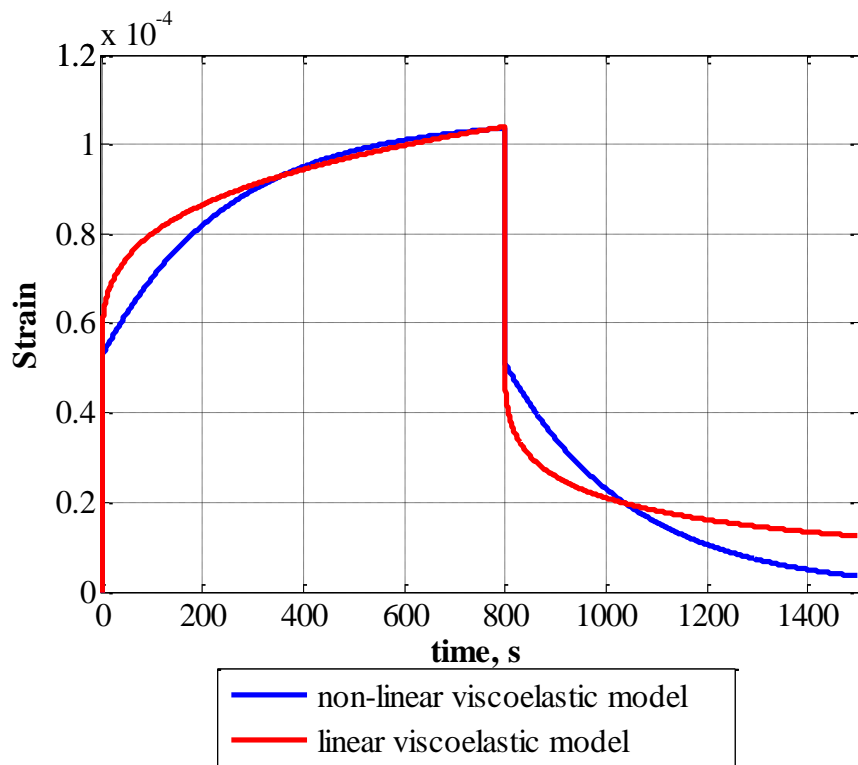


Figure 3.3.2. Creep and recovery of ice at -19.8°C . Constant stress of 0.49 MPa was applied during first 800 seconds.

3.4. Numerical simulation of cyclic uniaxial compression test.

In order to get similar strain response of ice as in the uniaxial compression cyclic test performed at UNIS different variation of the input parameters for linear viscoelastic Burgers model were considered. The best fitted curve were obtained when the input parameters were 15 times smaller than the ones got during the calibration of linear viscoelastic model by means of Sinha's creep test with -10°C fresh ice. The reduction in the values of the input parameters can be explained by the fact that sea ice is weaker than the fresh ice. It should be noted that the ratios λ_1 and λ_2 were kept the same to the ones obtained for fresh ice. Strictly speaking this ratios might not be the same for sea ice. However, no information regarding this topic was found or available. The real stress history of the cyclic uniaxial compression test were used as the input for the model (Figure 3.4.1).

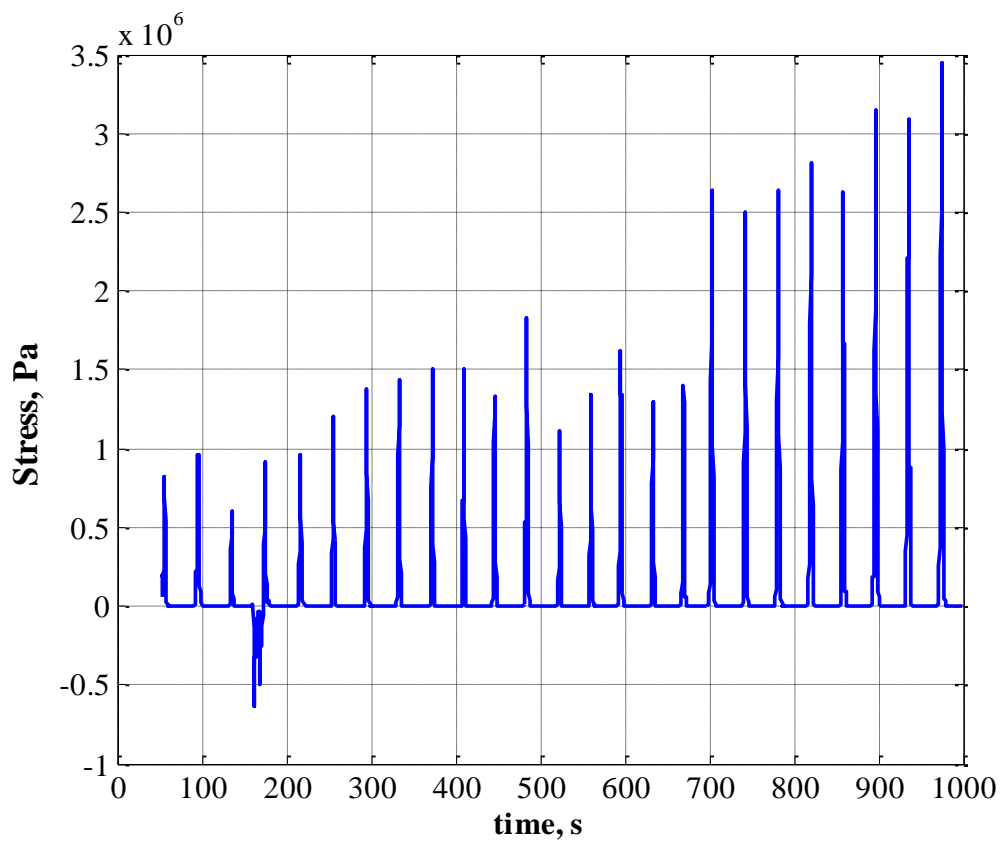


Figure 3.4.1. Stress-history of uniaxial cyclic compression test performed at UNIS.

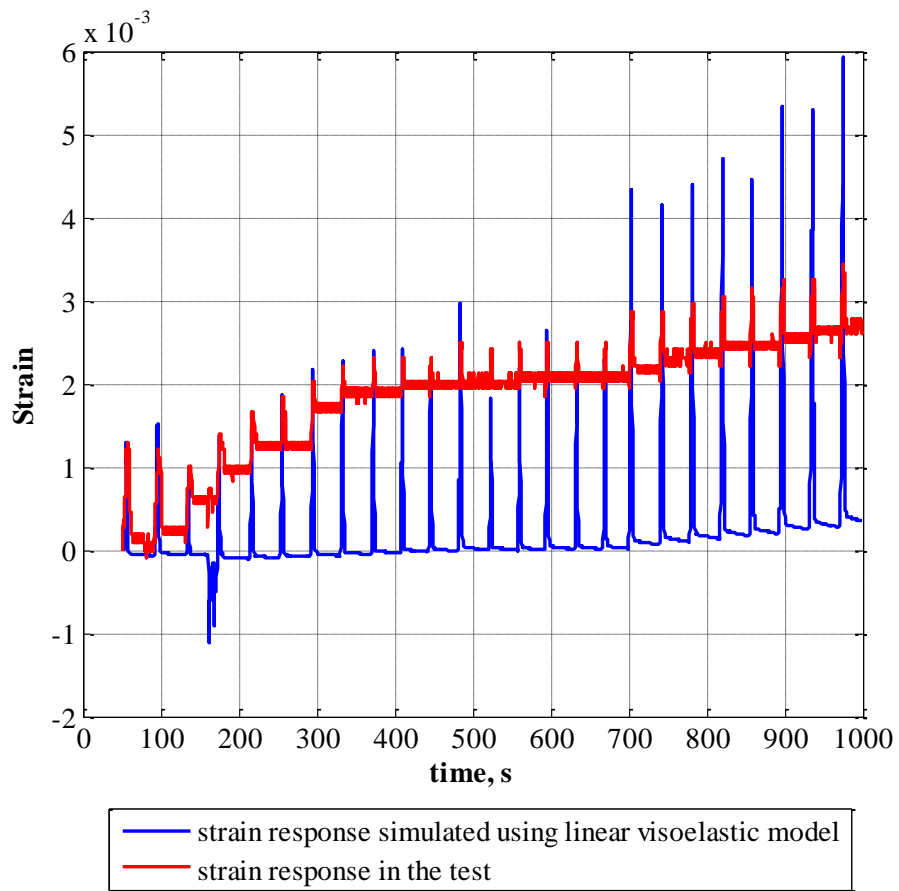


Figure 3.4.2. Comparison of strain response in uniaxial cyclic test with strain response simulated by linear viscoelastic model.

4. ANALYSIS AND DISCUSSION.

4.1. Sensitivity analysis.

The sensitivity analysis showed that the case when mechanical model is subjected to a cyclic stress can be considered as a creep test, in which the stress is oscillating around its constant mean value. This explains that the final stress of mechanical model can be estimated as the value of creep function of the model for time equal the duration of test multiplied on average value of applied cyclic stress.

The ratio $\Delta t / \lambda$, where Δt is duration of the application of the stress and $\lambda = \eta / E$ is a parameter of the model, determines the shape of, so to speak, the "viscous" part of the creep function and therefore the shape of the "viscous" strain response curve for all the mechanical models considered. Here by term "viscous" I meant both viscous and delayed-elastic deformations, or in other words all deformations except elastic ones. Strictly speaking, one may predict the behavior of a material in the framework of selected mechanical model just by knowing the value of $\Delta t / \lambda$, duration of the application of the stress, Δt , can be seen as $n \cdot T$, where T is duration of one cycle and n is a number of cycles. In case of constant loading the number of cycles is equal 1 and duration of the cycle is just equal to duration of the application of the stress. In case of Burgers model there will be two different λ , one for Maxwell unit and one for Kelvin unit, since the Burgers model is a combination of two of those.

More extensive information on the input parameters affecting the strain response of mechanical models in a creep test is presented in the corresponding part in Results section. This was done in order to make it easier for a reader to follow the conclusions drawn from the sensitivity analysis. One of the important observations during sensitivity analysis was that for Kelvin when if $\Delta t / \lambda = 5$ the strain reaches its maximal value equal to $\bar{\sigma} / E$ at time t_1 . Variable t_1 is time when stress is removed, $\bar{\sigma}$ is mean stress, E is Young's modulus of a spring element in Kelvin model. This feature of Kelvin model will be frequently used in the following discussions.

To compare different creep tests results under same loading conditions the same number of points should be used in approximation of the input stress curve. This is especially important when the model is subjected to time-varying stress. For

example, mechanical model is subjected to a cyclic stress $\sigma = \sigma_0 |\sin(\omega t)|$ and several tests should be performed. There can be two different cases. The first one, when the number of cycles is the same for the tests and the second one, when the duration of the test is the same. In order to get the accurate and comparable results in the first case the number of points approximating the sinus simply should be kept constant. Whereas in the second case the ratio of $T / \Delta t_i$ should be kept constant and equal to number of points approximating the cycle. In this ratio T is duration of the cycle and Δt_i is time step. In order to get the accurate numerical creep tests results the input stress curve should be approximated with sufficient number of points. For both cases the number of points approximating the sinus should be selected beforehand and greater or equal 10.

4.2. Sensitivity analysis of the secant system's modulus.

4.2.1. Kelvin model

When Kelvin model under cyclic loading is considered, the secant system's modulus of elasticity E_s is increasing during the test until a certain value after which it is a constant. The time Δt required for E_s to reach this constant value could be derived from relationship $\Delta t / \lambda = 5$. The time Δt could be seen as n / f , where n is the number of cycles and f is frequency of a cyclic loading [Hz]. $f = 1 / T$, where T is time of one cycle [s].

$$\frac{n}{f\lambda} = 5 \quad (4.2.1.1.)$$

Using expression 4.2.1.1. it is possible to say after which number of cycles n the system modulus E_s can be considered as constant.

In case 2 (Figure 3.2.1.1.a and Figure 3.2.1.1.b) the ratio $n / (f\lambda)$ and ratio σ_0 / E were kept constant. If both of this ratios are keeping constant the corresponding strain responses of Kelvin model are equal. However, the system modulus will change with change of σ_0 , since the value of secant system's modulus of elasticity E_s is proportional to amplitude of the cyclic loading. With increase of σ_0 the

modulus E_s increases (Figure 3.2.1.1.b.). From expression 4.2.1.1. for case 2, it follows that after cycle number 10 the secant system's modulus of elasticity can be considered to be constant. The values for system modulus E_s in case 2 are shown in the table 4.2.1.1. From the table it follows that the ratio $(E_{s,40} - E_{s,11}) / (E_{s,40} - E_{s,1})$ is less than 0.1, where $E_{s,40}$ is the value of system modulus at cycle 40, $E_{s,11}$ is the value of system modulus at cycle 11 and $E_{s,1}$ is the value of system modulus at cycle 1. This means that after cycle 10 the value of system modulus increases less than in 10%. Therefore equation 4.2.1.1. can be used for prediction the number of cycles n , after which the system modulus E_s can be considered as constant.

Table 4.2.1.1. The values for secant system's modulus of elasticity E_s for case 2.

n	Input parameters				
	$\eta = 3.75Pa \cdot s,$ $T = 7.5s,$ $E = 0.25Pa,$ $\sigma_0 = 0.25Pa.$	$\eta = 7.5Pa \cdot s,$ $T = 7.5s,$ $E = 0.5Pa,$ $\sigma_0 = 0.5Pa.$	$\eta = 15Pa \cdot s,$ $T = 7.5s,$ $E = 1Pa,$ $\sigma_0 = 1Pa.$	$\eta = 30Pa \cdot s,$ $T = 7.5s,$ $E = 2Pa,$ $\sigma_0 = 2Pa.$	$\eta = 60Pa \cdot s,$ $T = 7.5s,$ $E = 4Pa,$ $\sigma_0 = 4Pa.$
	E_s				
1	1.638692	3.277384	6.554767	13.10953	26.21907
11	17.1252	34.25041	68.50081	137.0016	274.0032
40	18.29829	36.59658	73.19316	146.3863	292.7726

In case 4 (Figure 3.2.1.3.a and Figure 3.2.1.3.b) the ratio $n / (f\lambda)$ and was kept constant, while the ratio σ_0 / E were being changed. The ratio of σ_0 / E affects on the value of the strain response and therefore has an influence on the value of E_s . With increase of E secant system's modulus of elasticity E_s increases (Figure 3.2.1.3.b.).

In case 3 (figure 3.2.1.2.a and figure 3.2.1.2.b) viscosity η was not kept constant and therefore the ratio $n / (f\lambda)$ was not constant as well. From expression 6.1. it follows that different number of cycles in each test were required for system modulus E_s to reach the constant value. Moreover the constant value of system modulus E_s

was different in each test, due to the fact that viscosity was different for each test. From figure 3.2.1.2.b it follows that the value of system modulus E_s increase with an increase of viscosity. The value of λ changes the shape of the hysteresis loops (Figure 4.2.1.4.). With an increase of viscosity hysteresis loops becomes narrower and less tilted. This results in an increase of the system modulus.

From figures 3.2.1.1b-3.2.1.3.b it follows that the final values of secant system's modulus are several orders higher that the Young's modulus of the spring. This is due to the fact that delayed elastic deformations are becoming smaller and smaller during the experiment, giving a high value for the secant modulus according to equation 2.5.1. This effect becomes even worse with decrease of ratio T / λ , which affect the slope of the stress-strain curve. In this ratio T is a duration of a cycle. To be honest the estimation of a secant modulus of elasticity of non-elastic system might seems to be a strange idea and of course the values obtained for the secant system's modulus has nothing to do with the real case. However, this analysis will help when it comes for analysis of Burgers model.

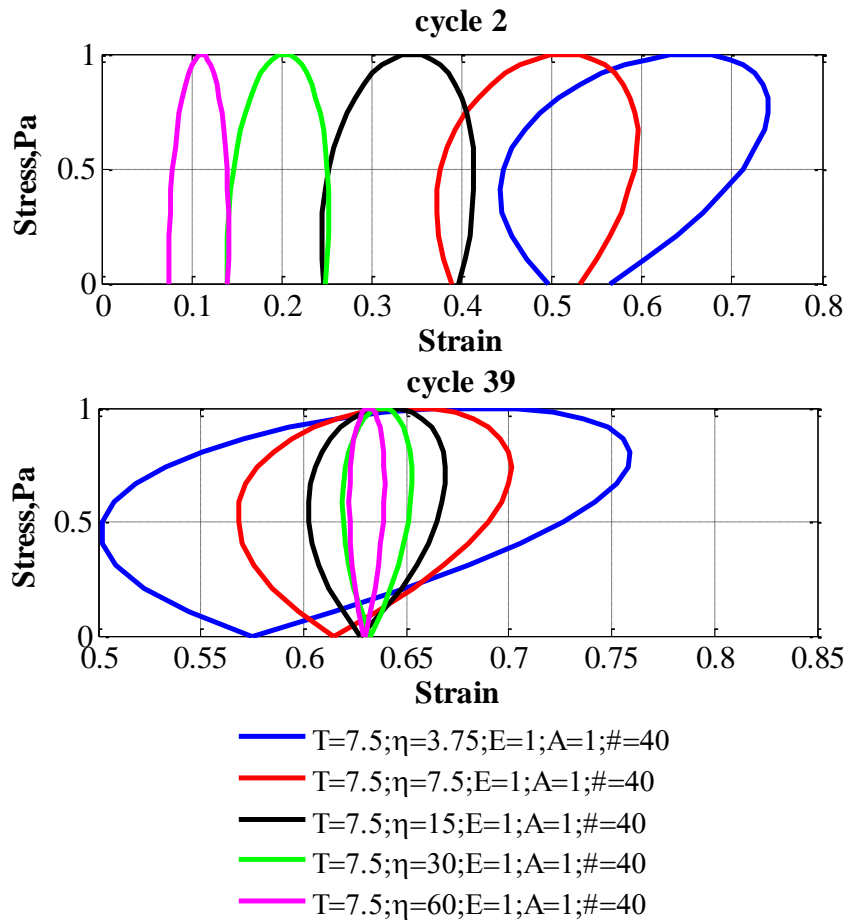


Figure 4.2.1.4. Stress-strain curves for cycles 2 and 39 in case 2.

4.2.2. Maxwell model

The numerical tests indicated that there is no change in secant system's modulus of elasticity of material represent by Maxwell mechanical model in a cyclic loading test (Figure 3.2.2.1.b.-3.2.2.3.b.). This is due to the fact that there is no change in a shape of a stress-strain curves during the test. For instance, when the period of cyclic loading changes from cycle to cycle we observe the different amount of viscous deformations, different shape of stress-strain curve within each cycle and therefore different values for secant system's modulus. The secant system's modulus can be seen as $1/(\alpha_0 - \alpha_{\sigma_0})$, where α_0 is the value of creep function at initial time of stress application and α_{σ_0} is the value of creep function at the time when stress reach it's maximal value. Therefore for Maxwell model the following conclusion can be drawn. Higher the value of the ratio $T/(2\lambda)$ lower is the value of secant system's modulus. The inclination of the stress-strain curve is governed by the same principle.

The is no change in tangent system's modulus of elasticity when the material is represented by Maxwell model, because the inclination and shape of stress-strain curve stays the same during the test.

4.2.3. Burgers model

From all of the figures presented in section 3.2.3. the following conclusions can be drawn. Once the delayed-elastic deformations are fully developed the shape of the strain-stress curve is governed by the ratio T/λ_1 , where T is a period of cyclic loading and λ_1 is a characteristic of the Maxwell element. Before that time the shape of this curve is changing and therefore the value of secant system's modulus. When λ_2 is large, more time is required for development of delayed-elastic deformations. However, as the time passes the influence of the damper in Maxwell unit becomes stronger and stronger, more viscous deformations develop. As a result the shape of the strain-stress curve is governed by Maxwell unit and almost no change in secant system's modulus occurs. Its value tends to the value of tangent system's modulus, that equal to the value of Young's modulus of a spring of Maxwell model. Lower the value of ratio λ_2/λ_1 more change in the secant system's modulus occurs during the creep test.

4.3. Calibration of the model.

Sinha (1978) performed his creep tests for fresh columnar-grained ice. This type of ice and stress condition is common in many field situations, like fresh lakes and rivers. We are of course more interested in sea ice. The reason for calibration with these creep tests was that Sinha's non-linear viscoelastic model describes them well. The linear viscoelastic Burgers model was not only calibrated with creep tests but also compared with a non-linear model.

From figures it clear that the main difference between the strain responses of linear and non-linear viscoelastic model are in the region corresponding to delayed elastic deformations. And in turn this will affect on the rate of change of the secant system's modulus in case of application of cyclic loading to the model. However, this rate of change will be also controlled by the period of this cyclic loading. Even though the final value of the secant system's modulus should be the same for both linear and non-linear model in case when the total duration of the stress application in the test is not less than 200s for ice at -10°C and 300s for ice at -20°C . The strain response in a creep test of linear and non-linear viscoelastic model for ice at -10°C has a little discrepancy.

By analyzing the obtained input parameters for linear viscoelastic model it is clear that the value of viscosity η_1 and η_2 are higher for colder ice. This means that colder ice is more solid and its behavior is more elastic than of the warmer ice. This can also be seen from corresponding strain diagrams. Warmer ice experience more of viscous/creep deformations than the colder one.

It should be mentioned that obtained input parameters are valid only for the corresponding ice temperatures, extent of applied stress and the total duration of stress application less than 800s. However, the duration of stress application can be increased for the case with ice temperature equal to -10°C , due to the fact that the strain response curves of linear and non-linear are in a good correlation after time equal to 200s.

4.4. Numerical simulation of cyclic uniaxial compression test.

From figure 3.4.2 it follows that the peaks of the numerically simulated strain curve are in correspondence with the peaks of the strain curve obtained in test up to a

certain point. Further the fracture occurs in the ice test sample. The linear viscoelastic Burgers model is not taking fracture into account. The main difference between the numerically simulated strain diagram and the one from the test are in the region where the irreversible deformations take place. In figure 3.4.2. this areas can be easily detected.

The main feature of viscoelastic model is that deformations are time-dependent. In other words, viscous and delayed-elastic deformations require some time to develop. The period of a loading cycle is relatively small in the experiment. Each loading cycle is followed by relatively long pause of 15 seconds during which the stress is 0. Therefore, there is not enough time for sufficient irreversible deformations to develop. Whereas delayed elastic deformations have enough time to recover. The irreversible deformations of linear viscoelastic Burgers model are constant only after sufficient time has passed (figure 2.1.2.5.). Whereas in cyclic uniaxial compression test these deformations are constant in time immediately after the stress is removed. Therefore the irreversible deformations that occur in the cyclic uniaxial compression test cannot be described by means of linear viscoelastic model. These deformations can be due to surface flattening or due to plastic behavior of ice in the experiment.

If the surface flattening is the case, the irreversible deformations can be seen as accumulated strain. In other words, the edge of the ice sample may not be flat and perfectly parallel during the test. This result in uneven contact area and therefore in uneven stress distribution over the contact area. This means, that some time is needed to develop a perfectly flat contact area at the beginning of each cycle. The irreversible deformations can be then explained by reduction in the length of the ice sample due to surface flattening effect. Our main goal is to see whether this surface flattening effect may affect the change in Young's modulus of ice. From figure 2.4.4 it follows that the effect of surface flattening was excluded in the estimations of the Young's modulus of tested ice sample. The initial curvature of stress-strain diagram was not taken into account.

The irreversible deformations of ice in cyclic uniaxial compression test can be also described by the theory of plasticity. According to this theory, material experiences plastic deformations once applied stress exceeds the yield stress. In this theory the duration of application of the stress is not important. From figure 3.4.2. it seems that ice is hardening from time equal to 400s. When time equal to 700s ice cannot resist

the stresses anymore. After that time either thickening of the ice sample takes place or fracture in the ice sample occurs.

Figure 4.4.1. (Irgens, 2008) illustrates elastic-plastic material response, where ϵ^p is plastic deformation, f_y is yield stress.

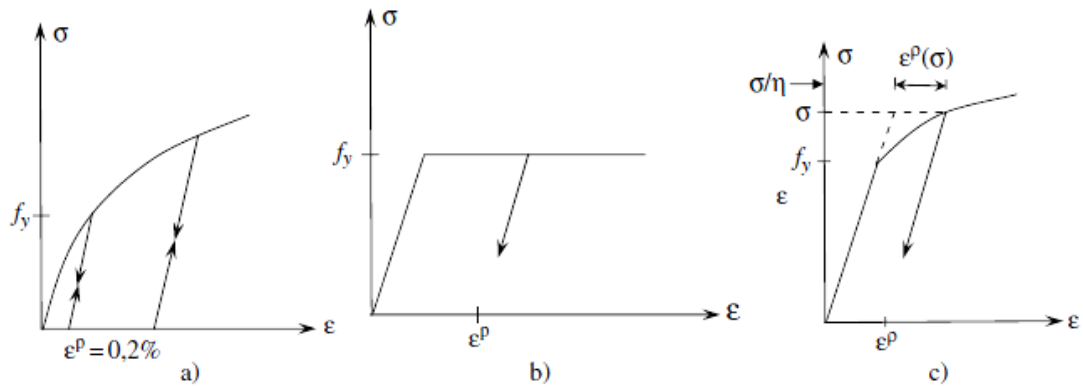


Figure 4.4.1. Elastic-plastic material response. a) General response b) Linearly elastic-perfectly plastic material c) Linearly elastic-plastic hardening material (Irgens, 2008).

After analyzing the stress-strain curves (figure 2.4.4.) and strain-time curves (figure 3.4.2.) and keeping in mind the cyclic stress history (figure 3.4.1.) , it seems that ice behaves as a linearly elastic-perfectly plastic material in the cyclic uniaxial compression test performed at UNIS. This means that the ice experience elastic deformation until the stress exceeds the yield stress. Then plastic deformation takes place. When it comes to rheological model, the ideal plastic unit can be used in order to capture the irreversible deformations of the ice in the test. The unit and its response is shown in figure 4.4.2.

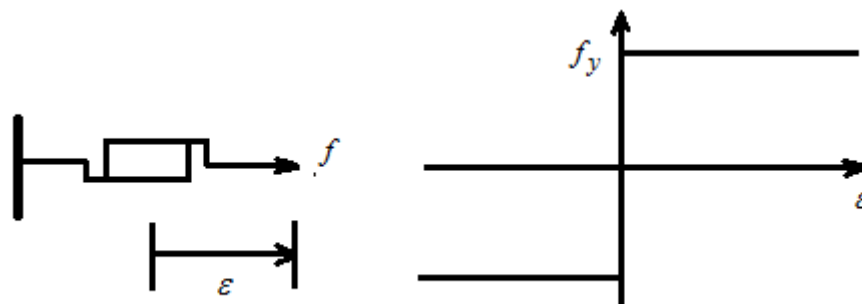


Figure 4.4.2. Ideal plastic unit.

In order to determine the yield stress the Tresca criteria can be used.

The numerical simulation of the cyclic uniaxial compression test showed that the linear viscoelastic model can't capture the effect of increasing Young's modulus to the same extent as in the test.

4.5. Summary

The goal of this work was to simulate the behaviour of ice under cyclic loading. The linear viscoelastic Kelvin, Maxwell and Burgers models were implemented in Matlab by means of The Boltzman superposition principle. This method was verified using cases which could be represented by analytical solutions. During the extensive sensitivity analysis carried out, it was determined that the ratio $n/(f\lambda)$ influences the shape of the strain response curve in a creep test for all of the models considered in this study. With the knowledge of parameter $n/(f\lambda)$, preliminary conclusion on the result of the test can be drawn.

The change of the second modulus is defined by the Kelvin unit which determines the delayed elastic deformations. The time required for these deformations to fully developed is given by $5\lambda_2$. The changes in the value of the second modulus occurs only before this value is attained. However in linear viscoelastic Burgers model, this change is relatively small. This is because the Maxwell unit in the Burger model has a major influence on the shape of the stress-strain curves.

Available literature was used to obtain the input parameters for Burgers model for ice. They were obtained by calibration of the model data with the experimental data presented therein by producing a best fit curve. Since this study utilized a non-linear model to replicate the experimental data, it was also used to compare the results of a linear model with a non-linear model. The region conforming to the delayed elastic deformation was not represented accurately by the linear model.

Uniaxial cyclic compression test performed at UNIS was modeled using the linear viscoelastic Burgers model using the scaled down input parameters obtained through calibration with fresh ice creep test to enable their application to this case. The viscoelastic model was unable to completely agree with the findings from the test carried out at UNIS.

5.CONCLUSIONS

5.1. Conclusions

From the extensive sensitivity analysis carried out, it was concluded that the ratio $n/\dot{\epsilon}$ is the most important parameter that influences the shape of the stress strain curve in a creep test for all of the models used in this study. This parameter can be used to draw preliminary conclusions on the result of the test.

The change in the second modulus is defined by the Kelvin unit which determines the delayed elastic deformations. The time required for these deformations to fully developed is given by $5\lambda_2$.

It is found that linear viscoelastic Burgers model explains the change in the secant system's modulus though the change is not to the as much as seen in the test. Thus, it can be concluded that this model can not yet fully explain the phenomena observed in the experiment.

5.2. Recommendations for future work

In order to better represent the behaviour of ice, a model which incorporates more non-linear behaviour can be developed. This could be achieved by including large number of Maxwell units in parallel. A combination of Maxwell, Kelvin and Burger units in parallel can also be examined for this purpose.

The uniaxial cyclic compression test of sea ice conducted at UNIS was numerically simulated in this study by linear viscoelastic Burger's model. It would be interesting to study the performance of the model by including plastic deformations.

Also, to further improve the numerical simulation, it is recommended to include dilatancy and fracture characteristics, residual deformation and the residual strength of the specimen could be included.

More exhaustive uniaxial cyclic compression testing of sea ice including larger range of periods and more variety of loading and their combinations could be done to ascertain the suitability of the viscoelastic theory. It is also recommended to include creep and relaxation tests on samples similar to the ones used for the cyclic test to obtain better input parameters for the numerical model.

REFERENCES

Blenkarn K.A., (1970): Measurement and analysis of ice forces on Cook Inlet structures. In Proceedings of 2nd Offshore Technology Conference, Houston, TX, USA, OTC 1261, Vol. 2, pp. 365–378.

Engelbrektsen A. (1977): Dynamic ice loads on lighthouse structures. In Proceedings of 4th International Conference on Port and Ocean Engineering under Arctic Conditions (POAC), St. John's, Canada, Vol. 2, pp. 654–864.

Irgens F. (2008): Continuum Mechanics, Berlin, 661 p.

Jordaan I. J. (2001): Mechanics of ice-structure interaction. Engineering Fracture Mechanics, Vol. 68, pp. 1923-1960.

ISO 19906 (2010): Petroleum and natural gas industries - Arctic offshore structures.

Kärnä T. (2007): Research problems related to time-varying ice actions. In Proceedings of the 19th International Conference on Port and Ocean Engineering under Arctic Conditions (POAC), Dalian, China.

Løset S., Shkhinek, K. N., Gudmestad, O. T. and Høyland, K. V. (2006): Actions from Ice on Arctic Offshore and Coastal Structures. St. Petersburg, 271 p.

Määttänen M. (1978): On conditions for the rise of self-excited ice induced autonomous oscillations in slender marine pile structures.. Phd thesis, University of Oulu, Department of Mechanical Engineering, p.98

Peyton H. R. (1968): Sea ice forces. Ice pressures against structures. Technical Memorandum, 92. National Research Council of Canada, Ottawa, Canada, pp. 117–123.

Sanderson, T. J. O. (1988): Ice Mechanics. Risk to Offshore Structures. Graham and Troutman, London, 253 p.

Sæbø A. O. (2007): Ice physics and the strength of sea ice at low porosities. Project, Department of Physics, NTNU, 62 p.

Sinha N. K. (1978): Rheology of columnar-grained ice. *Experimental Mechanics*, Vol. 18, pp. 464-470.

Sinha N. K. (1982): Creep model of ice for monotonically increasing stress. *Cold Regions Science and Technology*, Vol. 1, pp. 25-33.

Sinha N. K. (1984): Delayed-elastic model for initiation and accumulation of creep cavitation at high temperatures. In *Proceedings of the 6th. International Conference on Fracture (ICF6)*, New Delhi, India, pp. 2295-2302.

Sinha N. K. (1989): Elasticity of natural types of polycrystalline ice. *Cold Regions Science and Technology*, Vol. 17, pp. 127-135

Sodhi D. S. (2001): Crushing failure during ice-structure interaction. *Engineering Fracture Mechanics*, Vol. 68, pp. 1889-1921.

Sodhi D. S. (1988): Ice induced vibrations of structures. *IAHR'88, Ice Symposium*, pp. 625–657.

Yue Q., Zhang X., Bi X., Shi Z. (2001): Measurements and analysis of ice induced steady state vibration. In *Proceedings of 16th International Conference on Port and Ocean Engineering under Arctic Conditions (POAC)*, Ottawa, Canada.

http://en.wikipedia.org/wiki/Petroleum_exploration_in_the_Arctic

APPENDIX

A. Matlab code for linear viscoelastic models

A-1. Linear viscoelastic Kelvin model. Creep test.

```
% Matlab script for linear viscoelastic Kelvin model. Creep test
with any type of loading(constant/cyclic)
clear all;
format long;
Input=load('file name.txt'); %File with stress history, if available
time=enter either from the input file or manually via some script;

%Stress:
sigma= enter either from the input file or manually via some script;

eta=1;%Youngs modulus [Pa]
eta_prime=50;% viscosity [Pa*s]
lambda=eta_prime/eta; %Relaxation time [s]

% estimation of stress difference within a time step
for i=1:length(sigma)-1
    d_sigma(i,1)=(sigma(i+1)-sigma(i));
end
%estimation of strain( eq. 2.2.7.)
e(1,1)=0;
for i=2:length(sigma)-1
    e(i,1)=0;
    for k=1:i-1
        alpha(i,1)=1/eta*(1-exp(-((time(i,1)-time(k,1))/lambda)));
%creep function of Kelvin model(eq. 2.1.2.7).
        e(i,1)=e(i,1)+d_sigma(k,1)*alpha(i,1); %strain
    end
end
end
```

A-2. Linear viscoelastic Maxwell model. Creep test.

```
% Matlab script for linear viscoelastic Maxwell model. Creep test
with any type of loading(constant/cyclic)
clear all;
format long;
```

```

Input=load('file name.txt'); %File with stress history, if available
time=enter either from the input file or manually via some script;

%Stress:
sigma= enter either from the input file or manually via some script;

eta_prime= enter parameter value;% Viscosity [Pa*s]
eta= enter parameter value;%Young's modulus [Pa]
lambda=eta_prime/eta; %Relaxation time [s]

% estimation of stress difference within a time step
for i=1:length(sigma)-1
    d_sigma(i,1)=(sigma(i+1)-sigma(i));
end

%estimation of strain( eq. 2.2.7.)
e(1,1)=0;

for i=2:length(sigma)-1
    e(i,1)=0;
    for k=1:i-1
        alpha(i,1)=1/eta*(1+(time(i,1)-time(k,1))/lambda); %creep
function of Maxwell model(eq. 2.1.2.7)
        e(i,1)=e(i,1)+d_sigma(k,1)*alpha(i,1); %strain
    end
end
end

```

A-3. Linear viscoelastic Burgers model. Creep test.

```

%Matlab script for linear viscoelastic Burgers model. Creep test
with any type of loading(constant/cyclic)
clear all;
format long;
Input=load('file name.txt'); %File with stress history, if available

time=enter either from the input file or manually via some script;
%Stress:
sigma= enter either from the input file or manually via some script;

eta_1=enter parameter value; %Youngs modulus of Maxwell unit [Pa]
eta_prime_1=enter parameter value; %Viscosity of Maxwell unit[Pa*s]

eta_2= enter parameter value; %Youngs modulus of Kelvin unit

```



```

eta_prime_2= enter parameter value; %Viscosity of Kelvin unit

lambda_1=(eta_prime_1)/(eta_1); %Relaxation time of Maxwell unit [s]
lambda_2=(eta_prime_2)/(eta_2); %Relaxation time of Kelvin unit [s]

% estimation of stress difference within a time step
for i=1:length(sigma)-1
    d_sigma(i,1)=(sigma(i+1)-sigma(i));
end

%estimation of strain( eq. 2.2.7.):
e(1,1)=0;
for i=2:length(sigma)-1
    e(i,1)=0;
    for k=1:i-1
        alpha(i,1)=1/eta_1*(1+(time(i,1)-
time(k,1))/lambda_1)+1/eta_2*(1-exp(-(time(i,1)-
time(k,1))/lambda_2)); %creep function of Burgers mode(eq. 2.1.2.14)
        e(i,1)=e(i,1)+d_sigma(k,1)*alpha(i,1); strain
    end
end
end

```

B. Results of the numerically simulated creep tests for Kelvin model

The property of Kelvin model is characterized by the following property. If $\Delta t / \lambda = 5$, the strain reaches its maximal value equal to σ_0 / E at time t_1 . time $\Delta t = t_1 - t_0$, where t_0 is time when constant stress σ_0 is applied and t_1 is time when stress is removed, λ is relaxation time, E is Young's modulus. This property of Kelvin model is supported by the following result of numerical simulation of creep tests.

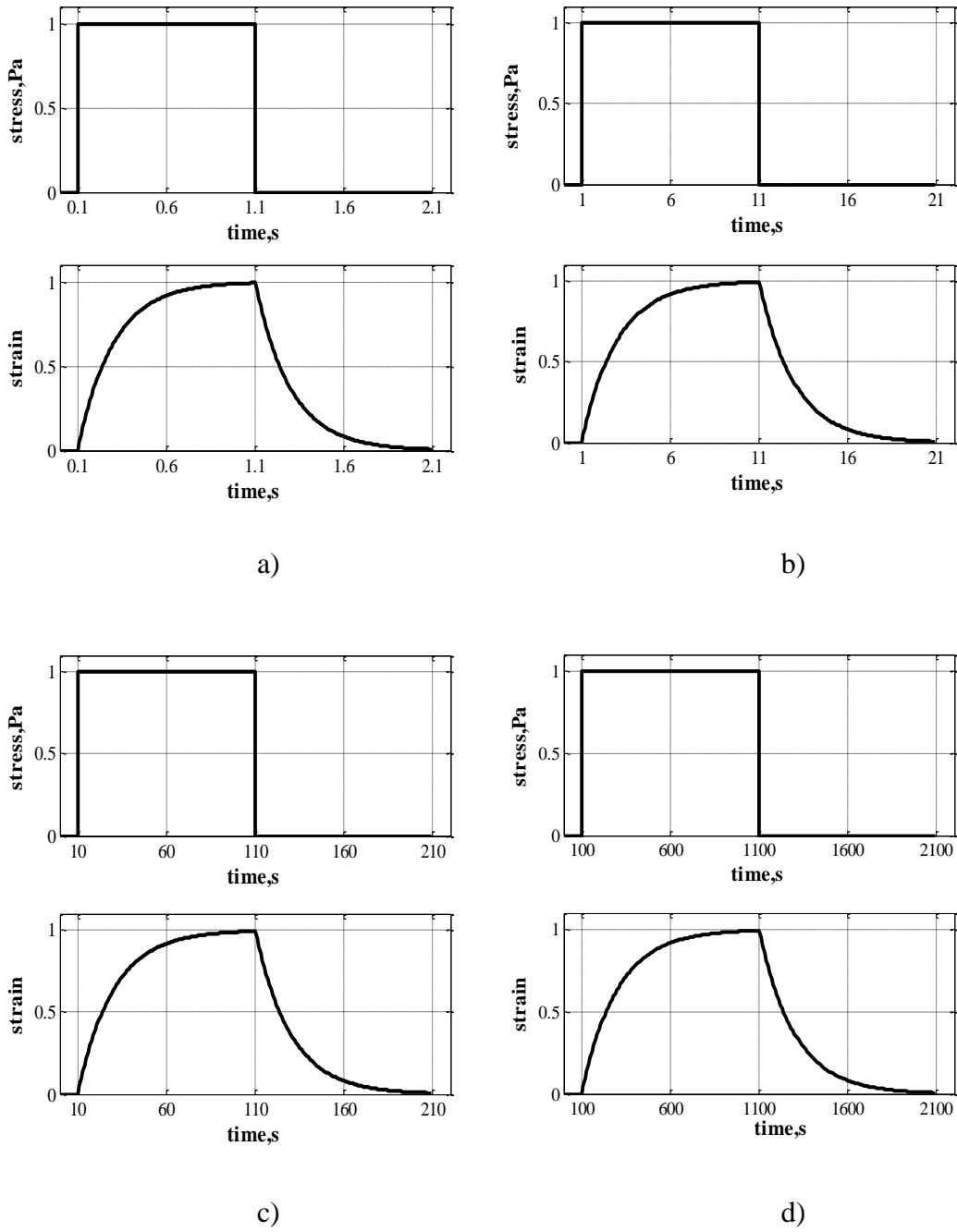


Figure B.1. Stress history and strain response for creep tests of Kelvin model. The value $\Delta t / \lambda$ were kept equal to 5. The following input parameters were selected for the tests:

- a) $\Delta t = 1s$; $\sigma_0 = 1 Pa$; $E = 1 Pa$; $\eta = 0.2 Pa \cdot s$
- b) $\Delta t = 10s$; $\sigma_0 = 1 Pa$; $E = 1 Pa$; $\eta = 2 Pa \cdot s$
- c) $\Delta t = 100s$; $\sigma_0 = 1 Pa$; $E = 1 Pa$; $\eta = 20 Pa \cdot s$
- d) $\Delta t = 1000s$; $\sigma_0 = 1 Pa$; $E = 1 Pa$; $\eta = 200 Pa \cdot s$

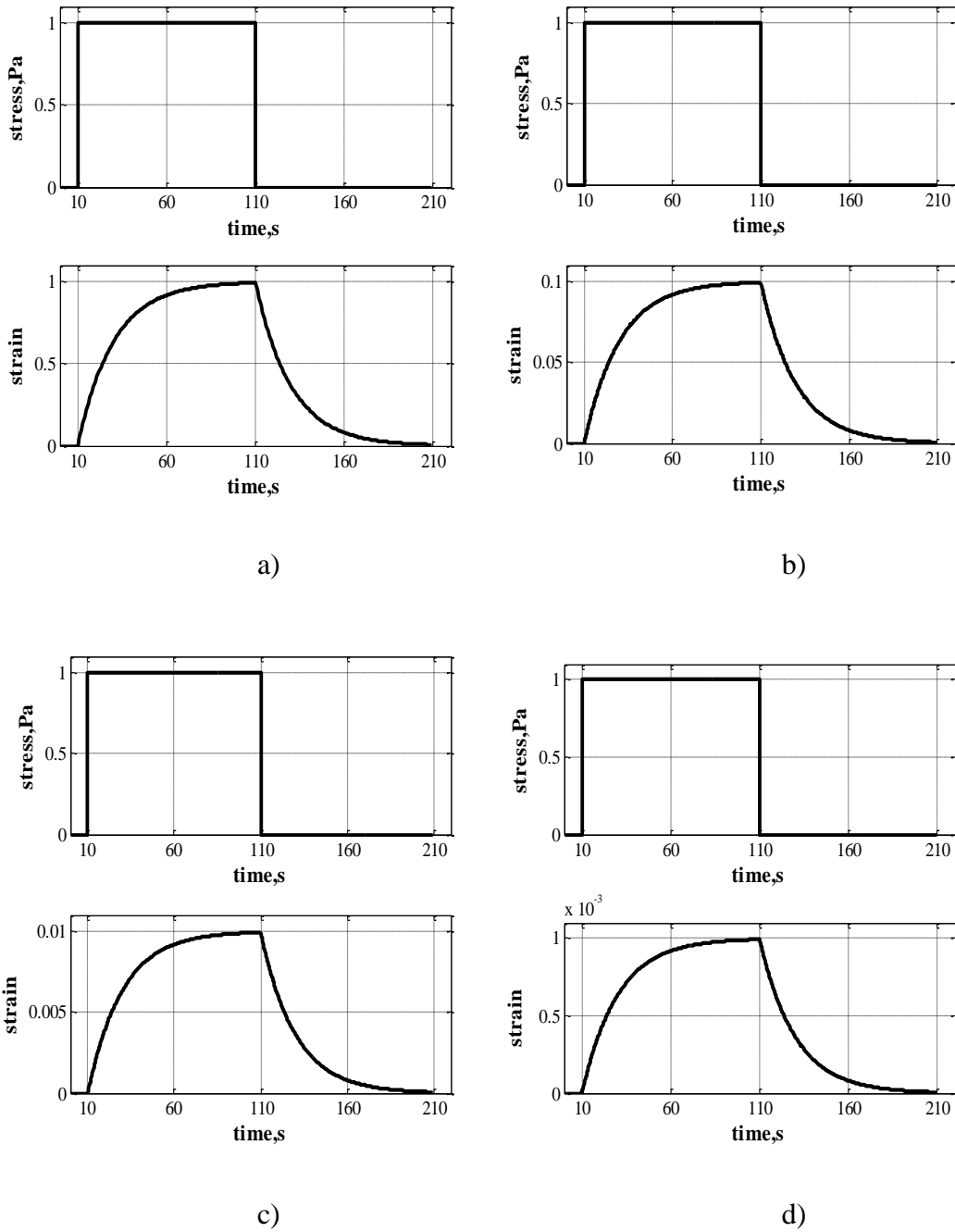


Figure B.2. Stress history and strain response for creep tests of Kelvin model. The value $\Delta t / \lambda$ were kept equal to 5. The following input parameters were selected for the tests:

- a) $\Delta t = 100s$; $\sigma_0 = 1 Pa$; $E = 1 Pa$; $\eta = 20 Pa \cdot s$
- b) $\Delta t = 100s$; $\sigma_0 = 1 Pa$; $E = 10 Pa$; $\eta = 200 Pa \cdot s$
- c) $\Delta t = 100s$; $\sigma_0 = 1 Pa$; $E = 100 Pa$; $\eta = 2000 Pa \cdot s$
- d) $\Delta t = 100s$; $\sigma_0 = 1 Pa$; $E = 1000 Pa$; $\eta = 20000 Pa \cdot s$

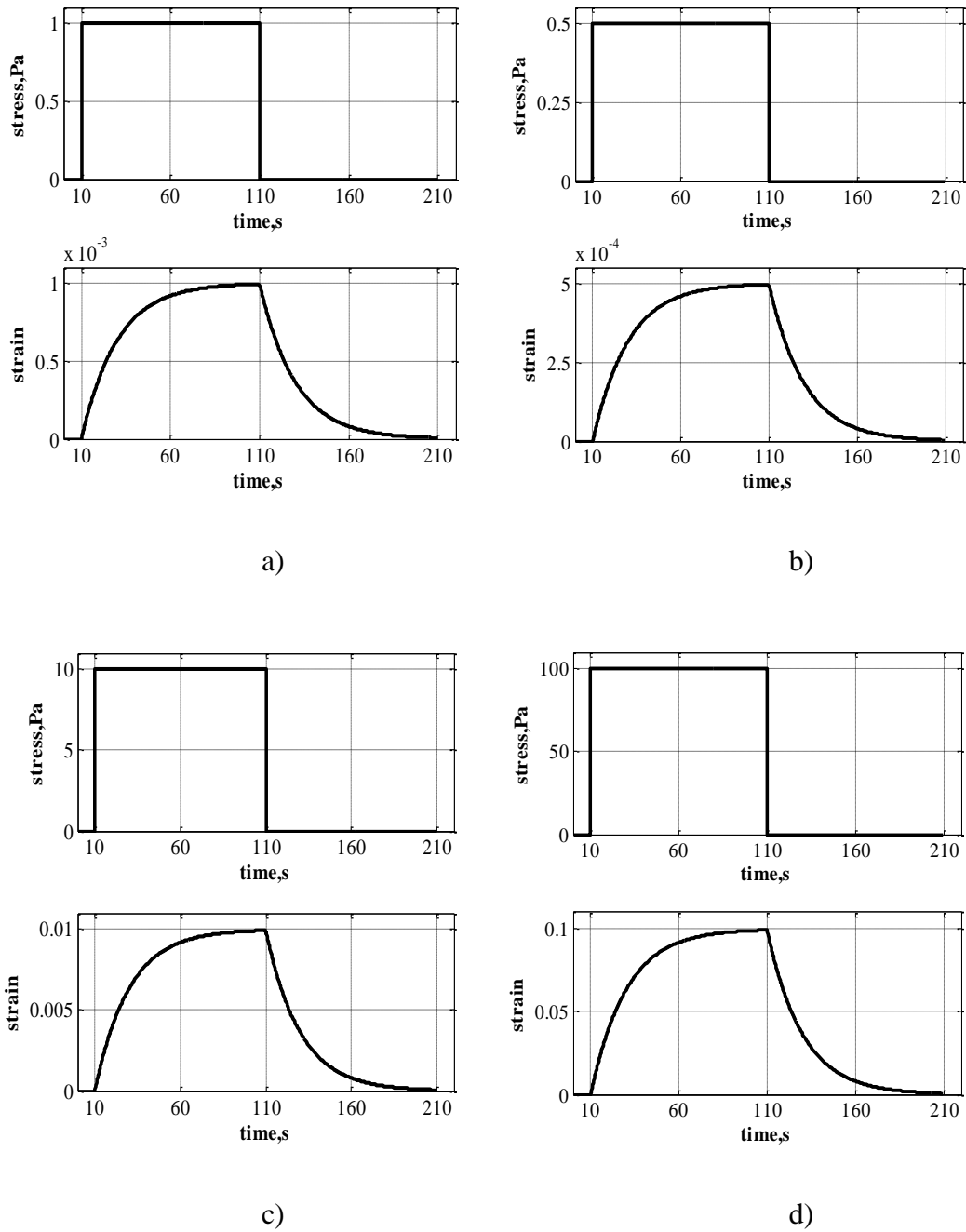


Figure B.3. Stress history and strain response for creep tests of Kelvin model. The value $\Delta t / \lambda$ were kept equal to 5. The following input parameters were selected for the tests:

- a) $\Delta t = 100s$; $\sigma_0 = 1 Pa$; $E = 1000Pa$; $\eta = 20000 Pa \cdot s$
- b) $\Delta t = 100s$; $\sigma_0 = 0.1 Pa$; $E = 1000Pa$; $\eta = 20000 Pa \cdot s$
- c) $\Delta t = 100s$; $\sigma_0 = 10 Pa$; $E = 1000Pa$; $\eta = 20000 Pa \cdot s$
- d) $\Delta t = 100s$; $\sigma_0 = 100 Pa$; $E = 1000Pa$; $\eta = 20000 Pa \cdot s$

C. Matlab code for non-linear viscoelastic model

```
%non-linear viscoelastic model of Sinha. creep test
clear all;
format long;

time=0:.800s;
sigma=constant stress=1MPa; % stress [Pa]

eta_1=9.3 GPa;%Youngs modulus [Pa]
c=3; %constant (Sinha, 1978)
b=0.34; %constant (Sinha, 1978)
n=3; %constant (Sinha, 1978)
s=1; %constant (Sinha, 1978)
a=0.000250; % inverse relaxation time (Sinha 1978)
ep=0.000000176; %viscous strain (Sinha, 1978)
m=mean(sigma); %mean value of stress (Sinha, 1978)
% estimation of stress difference within a time step:
for i=1:length(sigma)-1
    d_sigma(i,1)=(sigma(i+1)-sigma(i));
end

e(1,1)=0;
%estimation of strain( eq. 2.2.7.):
for i=2:length(sigma)-1
    e(i,1)=0;
    for k=1:i-1
        e(i,1)=e(i,1)+d_sigma(k,1)/eta_1+c*(d_sigma(k,1)/eta_1)*(1-
exp(-(a*(time(i,1)-
time(k,1)))^b))+ep*((d_sigma(k,1)/m)^3)*(time(i,1)-time(k,1));
%equation 2.6.2. (Sinha,1978)
    end
end
end
```